UQAC
Université du Québec
à Chicoutimi

Fabrication and characterization of a regenerative superhydrophobic silicone-based coating for electrical insulators

By

Helya Khademsameni

Under supervision of Prof. Reza Jafari and co-supervision of Prof. Gelareh Momen

Dissertation presented to the Université du Québec à Chicoutimi as a partial requirement of the master's degree in engineering (3708)

Board of examiners:

Doctor Agnese Bregnocchi, Derby Building Products Inc., External Member of the Board

Doctor Ehsan Bakhshandeh, Department of Applied Sciences at UQAC, Internal Member of the Board

Professor Gelareh Momen, Department of Applied Sciences at UQAC, Internal Member of the Board

Professor Reza Jafari, Department of Applied Sciences at UQAC, Internal Member of the Board

Québec, Canada

RÉSUMÉ

L'équipement électrique et plus spécifiquement les isolateurs sont plus vulnérables de perdre leur efficacité dans des conditions météorologiques sévères. L'accumulation de glace ou de pollution peut endommager les isolateurs électriques. Une couche de polluants peut mener à l'accumulation d'une pellicule conductrice sur les isolants. Les isolateurs haut tension contaminés, dans des conditions humides peuvent mener à une fuite de courant électrique qui se répandra sur la surface de l'isolateur. Cette couche de matériaux conducteurs accumulée sur l'isolateur peut mener à contournement électrique qui peut résulter en une perte totale de l'isolateur. Par conséquent, les revêtements anti-givrage et auto-nettoyants pourraient profiter aux isolateurs électriques.

Les revêtements superhydrophobes ont le potentiel d'être utilisés pour leurs propriétés anti-givrantes et auto-nettoyantes. Plusieurs chercheurs ont mené des travaux sur la superhydrophobicité. Malgré cela, la plupart des recherches menée dans ce domaine manque à montrer la durabilité des revêtements qui ont une courte durée de vie en conditions environnementales difficiles.

Les revêtements superhydrophobes régénératifs peuvent résoudre ce problème. Ces revêtements récupèrent leur superhydrophobicité après avoir été endommagés ou dégradés. Cette recherche a pour but de concevoir des revêtements superhydrophobes régénératifs à base de silicone et d'étudier leur durabilité et, par conséquence, leur potentielle utilité pour les isolateurs électriques.

Cela dit, un revêtement superhydrophobe contenant des microparticules et des nanoparticules dans une matrice à base de PDMS contenant du trifluoropropyl POSS (F-POSS) et de l'huile de silicone en tant qu'agents de régénération de la superhydrophobicité a été fabriqué par méthode de revêtement par centrifugation. Le revêtement fabriqué présentait un angle de contact de 169,5° et une hystérésis d'angle de contact de 6°.

La capacité autonettoyante du revêtement développé a été testée et étudiée par un test de contamination sèche. La régénération de la superhydrophobicité du revêtement développé a également été mise à l'épreuve par la détérioration du plasma et l'immersion à solution divers de pH. Le revêtement superhydrophobe régénératif développé a montré des performances prometteuses dans les deux tests par rapport aux échantillons de référence. Les revêtements régénératifs développés ont duré plus longtemps dans divers environnements de pH avant de perdre leur superhydrophobicité et de retrouver leur superhydrophobicité après la perte. Ces échantillons ont pu retrouver leur superhydrophobicité après la perte de superhydrophobicité due à la détérioration du plasma, ce qui n'était pas le cas pour les échantillons de référence. La topographie de surface et la composition chimique du revêtement ont été observées par profilométrie, microscopie électronique à balayage (MEB), spectroscopie infrarouge à transformée de Fourier (FTIR) et spectroscopie photoélectronique à rayons X (XPS). De plus, le revêtement présentait des propriétés glaçiophobes. La mesure d'adhésion à la glace du revêtement développé a été examinée par le test de poussée de glace et le test de centrifugation et évaluée en

répétant le test par cycles pour démontrer la capacité de régénération du revêtement développé. Un résumé graphique du principal du travail effectué dans cette recherche est présenté dans (Figure 1).

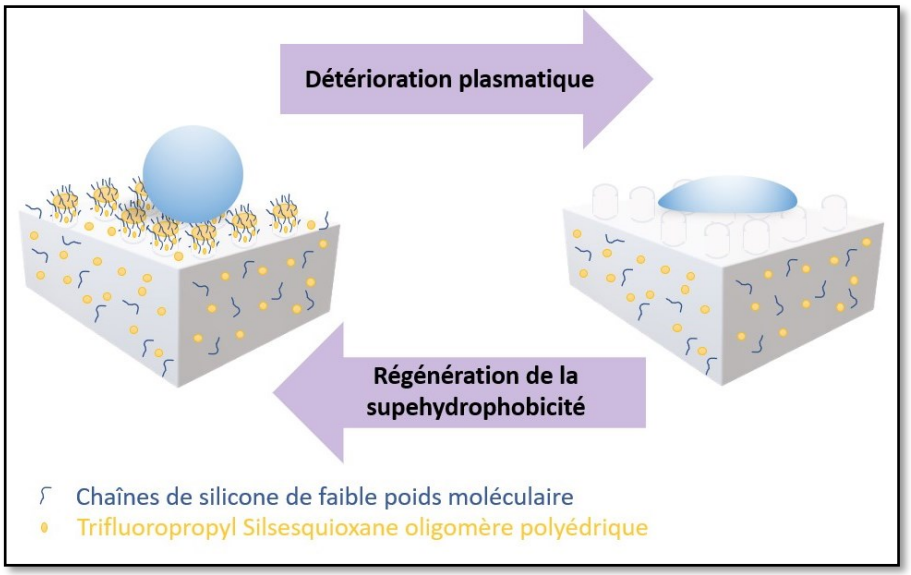

Figure 1. Résumé graphique des principes de cette recherche. © Helya Khademsameni, 2023

Mots clés: Revêtement superhydrophobe ; Hydrofuge; Autonettoyant; La régénération de la supehydrophobicité; Glaciophobie; Polydiméthylsiloxane; Revêtements en silicone; Isolateurs en porcelaine.

ABSTRACT

Electrical power systems, and more specifically electrical insulators are vulnerable to losing their functionality in severe meteorological conditions. Accumulation of ice or pollution can harm the electrical insulators. A layer of pollution can lead to accumulation of a conductive layer on top of the insulator. The contaminated high-voltage insulator in wet conditions could lead into a leakage current which flows through the surface of the insulator. This layer of conductive material on the insulator can lead to flashover which could result in the breakdown of the insulator. Therefore, anti-icing and self-cleaning coatings could be of great interest for electrical insulators.

Superhydrophobic coatings have the potential to be used for anti-icing and self-cleaning properties. A lot of researchers have been focused on superhydrophobicity, yet most of the research carried out in this domain lack durability studies and the developed coatings have small life spans under harsh environmental conditions.

Regenerative superhydrophobic coatings could solve this problem. These coatings will regain their superhydrophobicity after being ruptured or degraded. This research aims to fabricate silicone-based regenerative superhydrophobic coatings and study their durability and consequently their potential applications in electrical insulators. With that said, a superhydrophobic coating containing hydrophobic aerogel microparticles and polydimethylsiloxane modified silica nanoparticles within a PDMS based matrix containing Trifluoropropyl POSS (F-POSS) and Xiamater PMX-series silicone oil as superhydrophobicity regenerating agents were fabricated by spin-coating method. The fabricated coating showed a contact angle of 169.5° and a contact angle hysteresis of 6°.

The self-cleaning ability of the developed coating was attested and studied by dry contamination test. The superhydrophobicity regeneration of the developed coating was also put at the test by plasma deterioration and various pH immersions. The developed regenerative superhydrophobic coating showed promising performance in both tests compared to the reference samples. The developed regenerative coatings lasted longer in various pH environments before losing their superhydrophobicity and regained their superhydrophobicity after the loss. These samples were able to regain their superhydrophobicity after the loss of superhydrophobicity due to plasma deterioration, which was not the case for the reference samples. The surface topography and chemical composition of the coating were observed via Profilometry, scanning electron microscopy (SEM), Fourier transform infrared spectroscopy (FTIR), and X-ray photoelectron spectroscopy (XPS). Additionally, the coating presented icephobic properties. The ice adhesion measurement of the developed coating was examined by ice push-off test and centrifuge test and evaluated by repeating the test in cycles to demonstrate the regeneration ability of the developed coating. A graphical abstract of the principle of the current research is presented in (Figure 2).

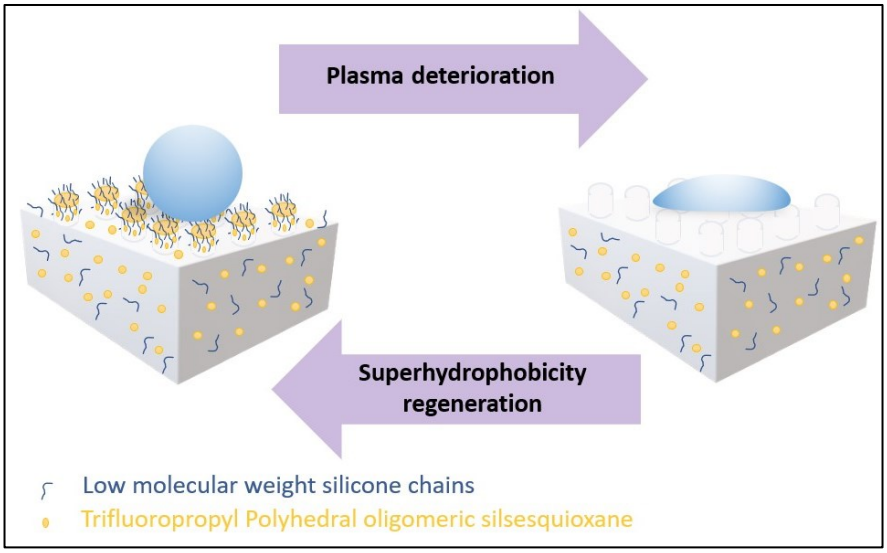

Figure 2. Graphical abstract of the principles of the current research work. © Helya Khademsameni, 2023

Keywords: Superhydrophobic coating; Water-repellency; Self-cleaning; Regenerative Superhydrophobicity; Icephobicity; Polydimethylsiloxane; Silicone coatings; Porcelain insulators.

TABLE OF CONTENT

LIST OF FIGURES

LIST OF TABLES

LIST OF EQUATIONS

LIST OF ABBREVIATIONS

AA	Aerosol-Assisted
ACNTB	Aligned Carbon Nanotube Bundles
ADF	Acid dew And Fog Test
AFM	Atomic Force Microscopy
Ag	Silver
Al	Aluminum
AMIL	Anti-Icing Materials International Laboratory
ATR	Attenuated Total Reflection
CA	Contact Angle
CAH	Contact Angle Hysteresis
CAT	Centrifuge Adhesion Test
CB	Cassie-Baxter
CNT	Carbon Nanotube
CVD	Chemical Vapor Deposition
FAS	Fluorinated Alkyl Silane
FAS-12	Dodecafluoroheptyl-Propyl-Trimetoxysilane
FAS-17	Heptadecafluoro-1,1,2,2-Tetradecyl Trimethoxy Silane
FD-POSS	Fluorinated Decylpolyhedral Oligomeric Silsesquioxane
F-POSS	Trifluoropropyl POSS
FMS	Fluorinated SiO_2 Nanoparticles
FS-NP	Fluoroalkyl Surface-modified Silica Nanoparticles
FTIR	Fourier-Transform Infrared Spectrometry
HDI	Hexamethylene Diisocyanate
HDTMS	Hexadecyltrimethoxysilane
LBL	Layer-By-Layer Deposition
LIPS	Liquid-infused Porous Surfaces
LMWS	Low Molecular Weight Siloxane
MCNTs	Multiwalled Carbon Nanotubes
NPs	Nanoparticles
NWs	Nanowires
ODA	Octadecylamine
OH	Hydroxyl
PAA	Poly (Acrylic Acid)
PAH	Poly (Allylamine Hydrochloride)

PCL	Polycaprolactone
PDMS	Polydimethylsiloxane
PFDT	1H,1H,2H,2H-perfluorodecanethiol
PFOS	Perfluorooctanesulfonic
PMMA	Poly (methyl methacrylate)
PMSF	α,ω-bis(hydroxypropyl)-terminatedpoly(2,2,3,3,4,4,4-heptafluoro butylmethylsiloxane)
POS	Polysiloxane
POSS	Polyhedral Oligomeric Silsesquioxane
POTS	1H,1H,2H,2H-perfluorooctyltriethoxysilane
PS	Polystyrene
PTFE	Polytetrafluoroethylene
PVA	Poly (Vinyl Alcohol)
PVD	Physical Vapor Deposition
PVDF	Polyvinylidene Fluoride
RH	Relative Humidity
RMS	Root Mean Square
SA	Sliding Angle
SEM	Scanning Electron Microscopy
SHP	Superhydrophobic
SiO_2	Silicon Oxide
SMPs	Shape Memory Polymers
SPEEK	Sulfonated Poly (ether ether ketone)
TiO_2	Titanium Oxide
UQAC	Université du Québec à Chicoutimi
UV	Ultraviolet
WCA	Water Contact Angle
WSA	Water Sliding Angle
XPS	X-ray Photoelectron Spectroscopy

LIST OF SYMBOLS

cSt	Centistokes
eV	electron volt
F	Centrifugal Force
f_{SL}	Fraction of Solid- Liquid Interface
m	Detached Ice Mass
γ_{LV}	Interfacial Energy per Unit Area of the Liquid-Vapour Interface
γ_{SV}	Interfacial Energy per Unit Area of the Solid-Vapour Interface
γ_{SL}	Interfacial Energy per Unit Area of the Solid-Liquid Interface
r	Roughness Factor
r	Beam radius
rpm	Revolutions per minute
Sa	Arithmetic Mean Height of Area Roughness
Sp	Maximum Peak Height
Sv	Maximum Pit Height
Sq	Root-Mean-Square Height of Area Roughness
Ssk	Skewness
Sz	Maximum height
T_g	Glass transition temperature
τ	Adhesion Shear Stress
ω	Centrifuge speed at which detachment occurred
θ	Contact Angle
θ_w	Wenzel apparent contact angle

DEDICATION

To my mom, Shideh Dishidi, who is my heroine.
To my loving family who supported me every step of the way.
À mon amour, Nicolas Cusson, qui rend la vie magnifique pour les autres autour de lui.
To Iranian women, who their braveness leaves me speechless.

ACKNOWLEDGMENT

I would like to express my gratitude for my supervisor Prof. Reza Jafari for his support and guidance throughout my studies.

This endeavour would have not been possible without the constant support and kindness of my co-supervisor, Prof. Gelareh Momen.

I am extremely grateful to the former PhD student and my colleague, Dr. Anahita Allahdini Hesarouyeeh, who was my source of positivity throughout the most stressful moments of my graduate studies.

I would like to thank M. Luc Chatigny, technician of CENGIVRE for his assistance in my project.

I would like to extend my sincere thanks to the professionals and technicians of Anti-Icing Materials International Laboratory (AMIL) for their collaboration.

I would like to thank all my friends and colleagues at LARGIS, especially Saba Goharshenasmoghadam, Samaneh Heydarian Dolatabadi, and Mohammadreza Shamshiri for their unlimited support and guidance.

Last but certainly not least, I would like to thank my friends and family for believing in me and supporting me throughout my studies.

FIRST CHAPTER
INTRODUCTION

1.1 Problem Definition

In many regions of the world, accumulation of ice is a cause of great concern for electrical power systems. Catastrophic incidents in the past, particularly in Northern America and Canada, e.g. the ice storm of January of 1998 in Quebec and Ontario [1] or the freezing rain, snowstorms in April of 2019 in southwestern Quebec [2] and even more recently the storm in Quebec in December 2022 [3], lead to undesirable consequences affecting the electrical power systems such as electrical insulators, power grids, transformer lines, etc. Among the electrical power systems, electrical insulators which provide safe connection of power lines to transmission towers are of great importance.

In general, insulating materials should withstand a certain electrical field without losing their insulating properties under applied voltage. However, in reality, that is not always the case. Often, due to the environmental and meteorological conditions the insulators are exposed to, their functionality tends to be interrupted [4], [5].

A layer of ice or pollution accumulated on the insulators is a tremendous hazard to their functionality. Pollution can contain minerals, electronic-conductive metal oxides, soluble salts, and water which can form a conductive layer on the insulators. In the same manner, due to freezing process, corona discharge products, and presence of other contaminating substances, a layer of ice on the insulators can lead to an increase in their conductivity [6], [7]. This can result in leakage currents that can end up in flashover, which is the bypassing of electrical insulation by a breakdown path [8], [9]. Consequently, the material loses its insulation properties. A dielectric breakdown can lead to surface damage, material loss, and eventually breakdown of electrical insulators. On that account, the addition of anti-icing and self-cleaning properties to high-voltage insulators becomes a necessity [10-12].

It is envisioned that superhydrophobic coatings on electrical insulators could lead to enhanced performance and prolonged service life of insulators due to facile water and contamination removal from their surface [13]. Superhydrophobic coatings which are inspired by nature, such as lotus leaf, have been of interest to many researchers [14].

However, the biggest challenge in the application of superhydrophobic coatings is their low durability. The superhydrophobicity property of these coatings can be suppressed in two ways, either by damage to the physical structure of the coating caused by impact or abrasion which would lead to a decrease in the surface roughness or to an increase of contact area between the solid substrate and water. Loss of superhydrophobicity can also be a result of an increase in surface energy which can be caused by contamination, irradiation, or damage to the low surface energy hydrophobic layer [15].

In order to increase the potential applications of superhydrophobic coatings, the low durability of these coatings has to be addressed. In this context, regenerative superhydrophobic coatings are a new technology capable of providing a solution for the mentioned issues. These self-healing superhydrophobic coatings can improve the durability of the coating by their regenerating property in the case of chemical or physical damage [16], [17].

1.2 Objectives

The foremost objective of this research is to fabricate regenerative superhydrophobic coatings for application in electrical insulators. Next chapter (Second Chapter) proposes an exhaustive literature review on the matter. Considering the conducted literature review, development of a silicone-based superhydrophobic coating along with a careful selection of proper chemical compositions will be the focus of this research. The sub-objectives of this research are presented in detail below:

- Selection of the best principle to create regenerative superhydrophobic coatings based on the electrical application.
- Development of a regenerative superhydrophobic coating considering the most suitable fabrication method regarding the chosen material.
- Studying the regenerative superhydrophobicity efficiency of the developed coating through several cycles of superhydrophobicity deterioration and regeneration cycles.
- Coating optimization by implementing changes regarding the selected materials, additives, and synthesis parameters.

1.3 Methodology

The key objective of this research is fabrication of a regenerative superhydrophobic coating for electrical insulators which can heal its superhydrophobicity in case of a loss of this property. Therefore, based on the literature review provided in the following chapter, a coating containing hydrophobic resin with a suitable choice of nano and micro particles and superhydrophobicity healing agents is designed and optimized. The proposed coating has both the required hierarchical topography and the low surface energy that would pave the way toward the main objective.

The first step would be determination of a suitable matrix, micro-nano particles, and superhydrophobic regenerative agents. This choice is made based on various factors such as final application, compatibility, desired properties, price, and etc.

In case of superhydrophobicity loss, the superhydrophobicity healing agents would migrate to the coating surface to decrease the surface energy, thus regenerating the superhydrophobicity. This migration to the surface can be done automatically due to a difference in surface layer energy or can be triggered by external stimuli such as heat or humidity. After extensive research on various superhydrophobicity regenerative agents, a suitable combination was chosen for this research. The

superhydrophobicity regeneration ability of each of the chosen superhydrophobicity regenerative agents will be tested and analyzed in this thesis to find the finest optimization of coating component ratios. The final coating mixture is spin-coated on the substrates and thermally cured. This fabrication method is chosen due to ease of use and scale-up.

The wettability and physicochemical characterization of the coating were measured by water contact angle goniometer, 3D Profilometer, scanning electron microscopy (SEM), Fourier transform infrared spectroscopy (FTIR), and X-ray photoelectron spectroscopy (XPS). Ice push-off test and Centrifuge Adhesion Test (CAT) will reveal the ice adhesion strength of the developed coating as well.

Regarding the main objective of this coating development, which is superhydrophobicity regeneration, this capability will be tested by immersion in solutions with various pH and air plasma deterioration. A summary of the methodology chosen for this work is presented in (Figure 3).

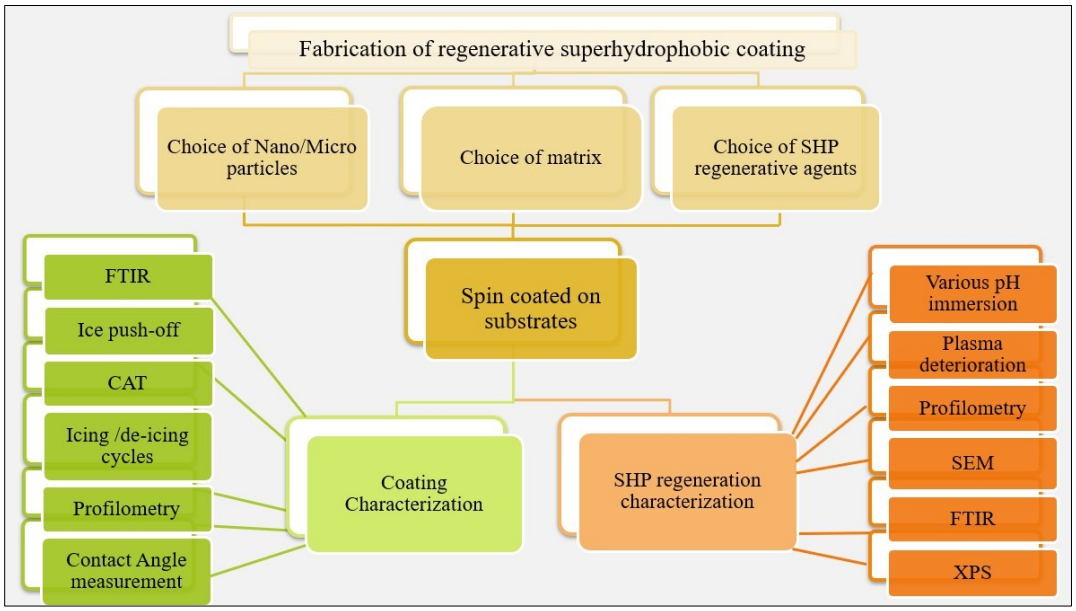

Figure 3. A summary of the methodology used in this research. © Helya Khademsameni, 2023

1.4 Originality statement

This research carries along a comprehensive look at the development of regenerative superhydrophobic coatings, with regard to the final application which is electrical insulators. This final application bounds the coating to withstand specific conditions, which makes this research original in the field of superhydrophobic coatings.

The choice of superhydrophobicity healing agents in the matrix and the associated advantages are the main originality of this work, due to its unicity compared to the other work proposed in this field. Moreover, the study of icephobicity in this work is original compared to the typical literature present in the same field.

This research fills a gap in the research work already done in the domain. Development of a regenerative superhydrophobic coating, which is intended for use on electrical insulators, embedded with the chosen superhydrophobicity agents, benefiting from this simultaneous presence,

and the fabrication and the presented analysis make this research original. The literature review presented in this work is carefully structured, therefore not only it presents a thorough study of other research in the domain, but also follows a logical path and has a high coherence. The presented research explains the literature review and then builds the experimental procedure based on it.

1.5 Memoire Outline

This section provides a summary of the following chapters of this research dissertation. The context of each chapter is complementary to the previous one and they are coherent in the means of context.

Chapter 2.

This chapter is dedicated to familiarizing the readers with the overall idea behind this study. A thorough literature review prepares the reader to understand the basics of this research and provides a coherent bridge to the next chapter. This chapter starts with introducing superhydrophobicity and discusses principal wetting theories. Dynamic water contact angle, contact angle hysteresis, and sliding angle are here explained. Effect of superhydrophobicity on icephobicity and ice adhesion measurement is reviewed. Fabrication methods and materials used for development of superhydrophobic coatings are also elaborated. After presenting various applications of superhydrophobic surfaces, low durability is mentioned as the technological limitation of these surfaces. To find a solution for this drawback, regenerative superhydrophobic coatings are introduced. Coatings with the ability to regain their superhydrophobicity after suffering damage leading to loss of superhydrophobicity are the focus of this chapter. These coatings are categorized based on their healing principles, categories that are explained at length.

Chapter 3.

After providing a complete literature review, the third chapter focuses on the experimental section of this research. It starts with a presentation of the material used in this research and an explanation of the role played by each material used in the coating. Afterward, the process of coating preparation using the mentioned material is discussed. The reader will read the step-by-step procedure the researcher used to develop the coatings in this study. In order to study the effect of superhydrophobicity regeneration agents individually and optimize the coating formulation, the coating preparation is divided into two steps, which are clearly explained in this chapter. This chapter also takes a look at the characterization methods and tests that are used in this research. Tests with the objective of coating characterization, superhydrophobicity regeneration evaluation, and ice adhesion measurement are introduced and discussed in this chapter.

Chapter 4.

The fourth chapter is focused on presenting and discussing the results gained following the previous chapter. It starts by providing data on the prepared coatings as elaborated in the previous chapter. Coating thickness, coating dynamic, and static water contact angles are discussed. During the first phase, with the help of a preliminary plasma deterioration and observing the changes in the water contact angle, effect of the used superhydrophobicity regeneration agents is determined. Using a more complex set of plasma deterioration tests will allow a better optimization as is conducted in the second phase of this chapter. After finalizing the coating formulation based on the conducted optimization, water repellency and self-cleaning ability of the developed coating are measured. The superhydrophobicity regeneration ability of the developed coating and reference ones are demonstrated and compared in this chapter, followed by an ice adhesion study on the mentioned samples. Various characterization tests such as SEM, FT-IR, XPS, and profilometry are also presented in this chapter.

Chapter 5.

The fifth and final chapter provides a complete review of the precedent chapters and provides conclusive remarks and observations. By reading this chapter the reader will understand the path taken from the beginning to the final steps of this research. Conclusions allow to understand where the research meets the main objectives designated for this study. The provided conclusions are followed by recommendations that could be complementary steps to the present research, leading the path to possible future researchers in this field.

SECOND CHAPTER
LITERATURE REVIEW

2.1 Introduction

In recent years, there have been many spotlights put on the development of superhydrophobic materials. These materials are defined by their static water contact angle of more than 150˚ and contact angle hysteresis and sliding angle of less than 10˚, characteristics which are achieved by a combined implementation of low surface energy materials and micro-nano surface roughness [19]. On account of these remarkable characteristics, superhydrophobic materials demonstrate great water repellency and self-cleaning behavior. Properties which have led to vast application of these materials for water-oil separation, anti-corrosion, anti-icing, etc. [15], [20].

Nevertheless, these materials suffer from drawbacks as well. The main drawback of superhydrophobic surfaces is their low durability. Low durability of superhydrophobic materials in real-life conditions could limit and prevent their use in large-scale or industrial applications. Therefore, several research have been shifted into the direction of tackling this issue. A potential solution could be regenerative superhydrophobic materials, materials that after a loss of superhydrophobicity, can regain it [16], [17].

In this chapter, we elaborate on the fundamentals of superhydrophobicity and wetting theories. We continue to distinguish the relation between superhydrophobicity and icephobicity. We take a glance at fabrication methods of superhydrophobic surfaces and take a deeper look into superhydrophobic silicone elastomer coatings. After discussing the possible applications of these technologies, we address the challenges of superhydrophobic coatings. Regenerative superhydrophobic coatings are an area of research that could be an answer to the long-lasting challenge of superhydrophobic coatings, which is low durability. The last section of this chapter discusses in length the principles of these coatings and introduces the characterization methods applied to regenerative superhydrophobic coatings.

2.2 Different wetting regimes and superhydrophobicity

Wettability of a surface is governed by the water droplet contact angle (CA) on a solid surface. Various wetting models attempt to demonstrate wettability of a surface. These models or theories point out the influential factors for wetting phenomena such as surface energy or roughness of the structures (Figure 4) [21]. Young, Wenzel, and Cassie-Baxter are the principal wetting theories explaining the governing rules on the wetting of surfaces. Young's equation focuses on the equilibrium of interaction forces of a drop on a perfectly smooth and chemically homogeneous solid surface (Equation 1, [22]).

$$\cos\theta = \frac{\gamma SV - \gamma SL}{\gamma LV}$$

Equation 1. Young's equation

In the mentioned equation, θ is the contact angle, and Y_{SV}, Y_{SL}, and Y_{LV} are the interfacial tension of the solid-vapor, solid-liquid, and liquid-vapor interfaces. However, most of the surfaces are not perfectly smooth. Researchers such as Wenzel and Cassie-Baxter tried to find a relationship between surface tension, roughness, and contact angle, in order to demonstrate a more realistic model governing surface wettability. Wenzel's model establishes a relation between the surface energy, contact angle, and surface roughness (Equation 2, [23]), however, this model is based on homogeneous wetting state which does not include all the wetting states. Based on this model, by the addition of roughness, a hydrophilic surface could become superhydrophilic and a hydrophobic one could turn into a superhydrophobic surface.

$$\cos\theta_W = \frac{r(\gamma_{SV} - \gamma_{SL})}{\gamma_{LV}} = r\cos\theta$$ *Equation 2. Wenzel's equation*

In this equation θ_w is the apparent contact angle on the rough surface, θ is Young's contact angle on a similar smooth surface, and r is the surface roughness factor which is as follows:

$$r = \frac{A_{real}}{A_{projected}}$$

Meanwhile, the Cassie–Baxter model, also known as the composite or heterogeneous state, is a wetting state where it is considered that the grooves under the droplet are filled with air instead of liquid. This model suggests that low contact angle hysteresis (CAH) and high contact angle (CA) on porous surfaces are a consequence of air entrapment in the pores of the structure which in turn is responsible for diminishing the contact between water droplets and the solid surface (Equation 3, [24]). The trapped air can prevent dust deposition by diminishing the attachment of the deposited dust layers [25].

$$\cos\theta_{CB} = f_{SL}\cos\theta + f_{SL} - 1$$ *Equation 3. Cassie-Baxter equation*

In this equation (Equation 3) θ_{CB} is the Cassie-Baxter contact angle, θ is the Young's contact angle, and f_{SL} is the ratio between the total area of solid-liquid interface and the total area of solid-liquid plus the liquid-air interface of the projected area.

In addition, by including the roughness factor of the wetted surface area, r_f, the Cassie-Baxter equation is modified to the equation mentioned below (Equation 4, [26]): [14], [27-30]

$$\cos\theta_{CB} = r_f f_{SL}\cos\theta + f_{SL} - 1$$ *Equation 4. Cassie-Baxter modified equation*

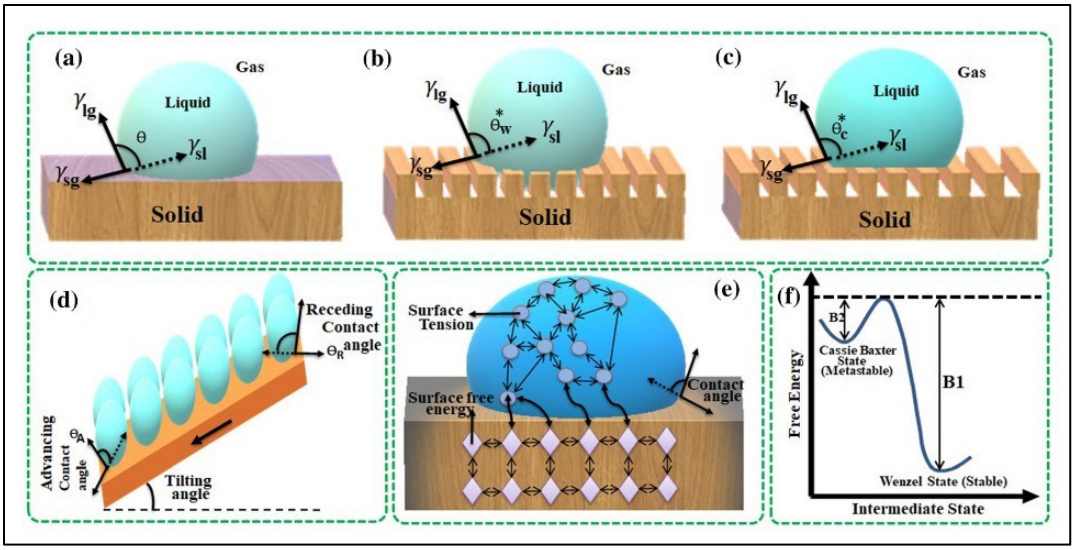

Figure 4. The wetting model of (a) Young, (b) Wenzel, and (c) Cassie- Baxter. (d) Advancing and receding contact angle, (e surface tension and surface free energy, and (f) Free energy schematic plot [21] (Reproduced with permission from Springer Nature).

Koishi et al. [31] showed that the two states of Wenzel and Cassie-Baxter can coexist on a nanopillar surface. Their research on a pillared hydrophobic surface showed that there is a critical pillar height beyond which water droplets on pillared hydrophobic surfaces can be in the bistable Wenzel/Cassie state.

To have a better understanding of superhydrophobicity, we can define it by measuring the water contact angle (WCA) which should be higher than 150°, and the water sliding angle (WSA) which should be less than 10º. In order to design a superhydrophobic surface, two main parameters are essential: (i) low surface energy and (ii) creating micro-and nano-hierarchical roughness on the material surface. By reducing the surface energy and creating micro-nano-level roughness which significantly reduces the contact between the solid surface and water droplets, superhydrophobicity can be achieved. To decrease the surface energy, direct addition of a layer of low-surface energy material on the surface in the form of a coating can be implemented. In another approach, low surface energy materials can be attached to the surface of nanomaterials. These modified nanomaterials can be deposited afterward on the solid surface [32], [33], [15].

Nevertheless, there are more variables crucial in defining a surface superhydrophobic. Of which, sliding angle is the critical angle at which a droplet situated on the surface starts to slide down [34]. A droplet situated on an inclined surface is governed by gravity forcing it to slide down the surface (advancing) and contact angle hysteresis (receding) at the upper side (Figure 4, d and Figure 5). The droplet deforms into an asymmetrical shape and moves only after the deformity reaches a certain point. The contact angle at the lower side is the advancing contact angle (θa), and the contact angle at the upper side is called the receding contact angle (θr). The more the difference between these two measures is, the more the droplet is likely to wet the surface and the less it is, the droplet is likely to repel from the surface [15]. The sliding angle can be determined by the Furmidge equation (Equation 5, [35]):

$$\gamma_{LV}(\cos\theta_r - \cos\theta_a) = \left(\frac{F}{w}\right)\sin\alpha$$ *Equation 5. Furmidge equation*

Where Y_{LV} is the surface tension, F and w are gravitational force and width of the contact area of the liquid droplet respectively (Figure 4, e). The difference between the advancing (θ_a) and receding (θ_r) angles of a droplet, defined as contact angle hysteresis (CAH), correlates with the sliding angle (α) or tilt angle (Figure 5). The advancing and receding contact angle of a surface is dependent on the surface roughness and the chemical heterogeneity of it [36], [37].

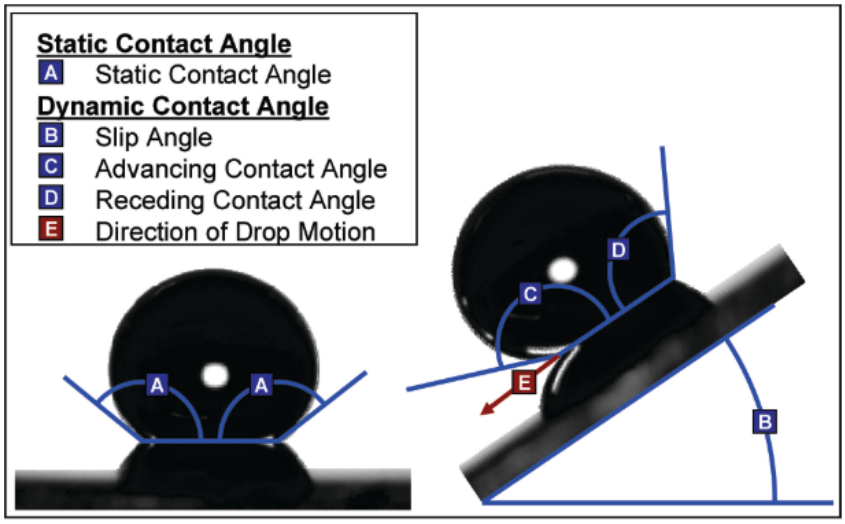

Figure 5. Static and dynamic contact angle schematic [38] (Reproduced with permission from American Chemical Society).

2.3 Superhydrophobicity and icephobicity

Superhydrophobicity can be used as a passive approach to prevent ice accumulation utilizing the mechanism of delay in ice nucleation time (Figure 6). Although there is some research suggesting that not all superhydrophobic surfaces present icephobic properties, an example of which could be observed increase of ice adhesion during condensation at low temperatures due to the possibility of an increased wetting of the surface roughness [39], [40] As the interfacial area between the water droplet and the substrate is smaller, the nucleation points are less. Moreover, the micro/nanostructure topography can lead to a reduction in heat transfer between the substrate and the water droplet. Finally, superhydrophobic surfaces can have less rebounding time for the same water droplet, which could be less than the time required for ice nucleation, leading to a delay or prevention of ice formation [5], [41].

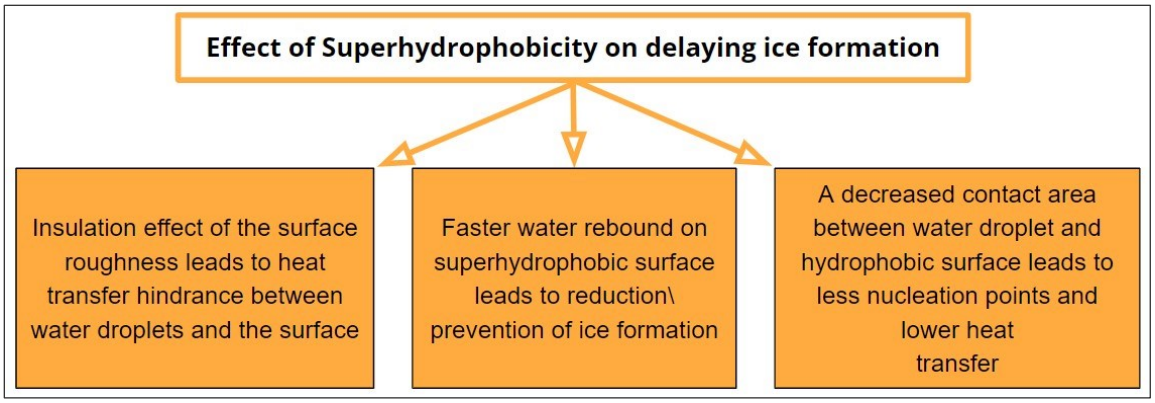

Figure 6. Mechanisms governing ice accumulation and ice nucleation delay on superhydrophobic surfaces [5] (Reproduced with permission from IEEE).

Finally, superhydrophobicity can potentially reduce the ice adhesion strength. Ice adhesion strength can be defined as the maximum force required to remove ice from a surface divided by the interfacial surface area of the ice and the substrate. The simultaneous effect of low-surface energy material and micro and/or nanostructure topography leads to high water contact angle and low contact angle hysteresis, decreasing the ice-surface interfacial area and consequently reducing the ice adhesion strength [42].

2.4 Superhydrophobic surfaces fabrication methods

Superhydrophobicity is the result of an appropriate combination of roughness, surface texture, and low surface energy materials (Figure 7). The fabrication methods of superhydrophobic coatings can be divided into three groups: (1) Top-down approach, (2) Bottom-up approach, and (3) a combination of both. Top-down approaches generally contain material removal of the surface by carving, machining, or using molding methods. For creation of superhydrophobic surfaces using the top-down method, lithography, templating, micromachining, plasma treatments, and etching can be mentioned. Bottom-up approaches contain deposition of materials onto a surface, via methods such as chemical vapor deposition (CVD), electrochemical deposition, layer-by-layer (LbL) deposition, sol−gel, spin coating, and so on [43], [15].

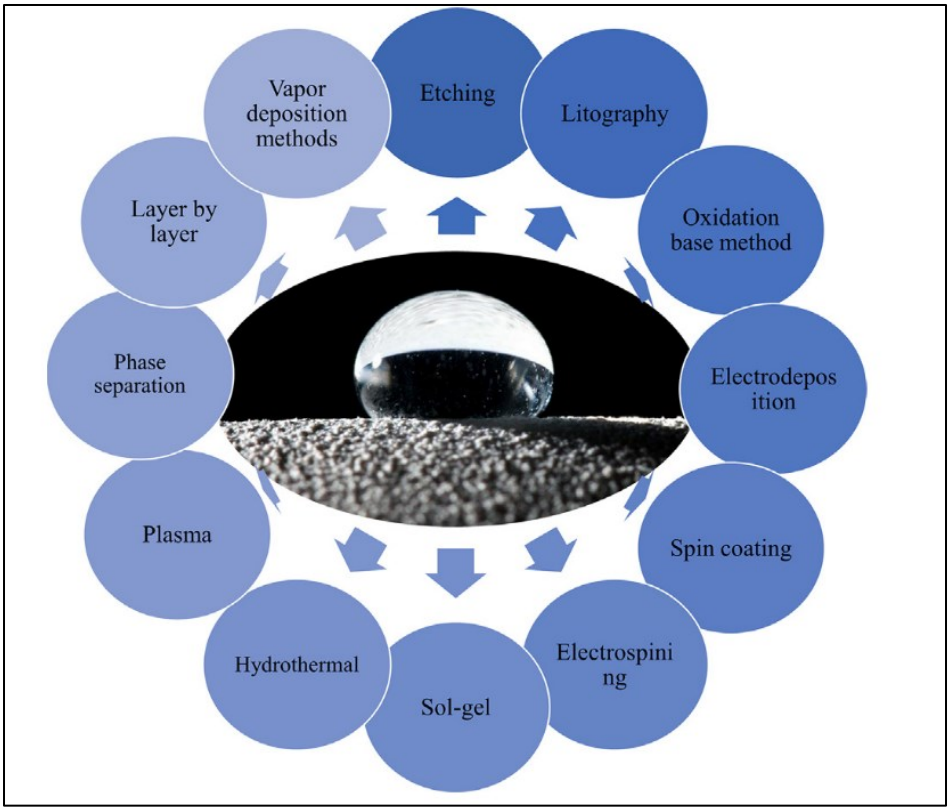

Figure 7. Different superhydrophobic surfaces fabrication methods [44].

Each of the mentioned fabrication methods has its advantages and disadvantages (Table 1). Based on the application of the final coating, the most suitable method can be chosen.

Table 1. Advantages and disadvantages of Superhydrophobic coatings' fabrication methods [33] (Reproduced with permission from Elsevier).

Preparative methods	Advantages	Disadvantages
Sol-Gel	• Complex surfaces • High quality films	• Crackability • Thickness limits • Mechanical stresses
Cold Spray	• Low temperature • Low deterioration • Low oxidation • Low defect	• High energy consumption • Selective substrates • High cost
Chemical vapor deposition (CVD)	• High quality coating • Thickness controllable • Complex surfaces	• High temperature • High cost
Physical vapor deposition (PVD)	• High quality coating • Suitable for almost inorganic compounds • Eco- friendly technique	• Low temperature • High pressure or high vacuums required • Expensive technique
Thermal Spray Method	• Wide variety of coating materials • Wide variety of substrates • Low cost	• Difficult to prepare thick coating • Low adhesion with complex surface • Environmental problems (noisy, fumes…)
In-situ Polymerization	• Contamination free • Suitable for insoluble polymers • High miscibility	• Complex processes • High cost • Small scale
Spin-coating	• High quality coating • Quick dry • Thickness controllable	• Small surface • Smooth surface • Laboratory scale
Dip-coating	• Complex surface • Industrial scale • Materials reusable	• Large amount of solvents • Only for soluble polymers
Electrodeposition	• High quality coating • Low cost • Simple manufacturing process	• Environmental issues • Time consuming • Non-Uniform coatings

One of the bottom-up approaches to the fabrication of superhydrophobic coatings is spin-coating. Spin-coating enables researchers to fabricate uniform and fine coatings. The machine is composed of a vacuum suction and rotation system that keeps in place a substrate. By deposition of a small quantity of the coating mixture on the substrate, the excess mixture is removed from the substrate by the centrifuge force and a fine coating of controlled thickness is placed on the surface (Figure 8). By changes in the speed and time of the spin-coater, the desired thickness of the final coating can be achieved [45].

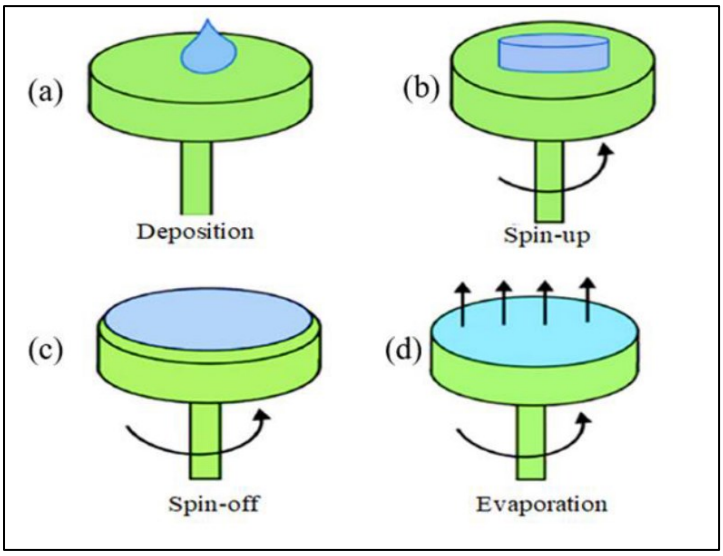

Figure 8. Spin coating process presented in a schematic figure [45].

Due to ease of use and scale-up of this method, spin coating was chosen as the intended fabrication method for this research.

2.5 Superhydrophobic silicone elastomer coatings

The importance of material choice in the fabrication of superhydrophobic coatings should not be underestimated. The matrices used for this purpose are generally low surface energy materials. Of which, Polysiloxanes (−Si–O–Si– groups) [46], fluorocarbons (CF_2/CF_3), and nonpolar materials (containing bulky CH_2/CH_3 groups) are popular choices due to their low surface energy, their nonpolar chemistry, and closely packed stable atomic structures [47]. Among them, silicones, which their classification is rather wide, have gained attention in recent years [48].

As for silicone polymers, polydimethylsiloxanes (PDMS) have been used for protective coatings due to their exceptional properties such as great thermal and chemical stability, biocompatibility, dielectric resistance, abrasion resistance, UV resistance, and low surface energy [49]. Polydimethylsiloxanes consist of stable Si-O bonds and two monovalent organic radicals attached to each silicon atom (Figure 9) [50]. The relatively low T_g of PDMS silicones makes them an excellent choice as a matrix for outdoor insulations, automobile and electronics industries, cookware, and so on [51-53].

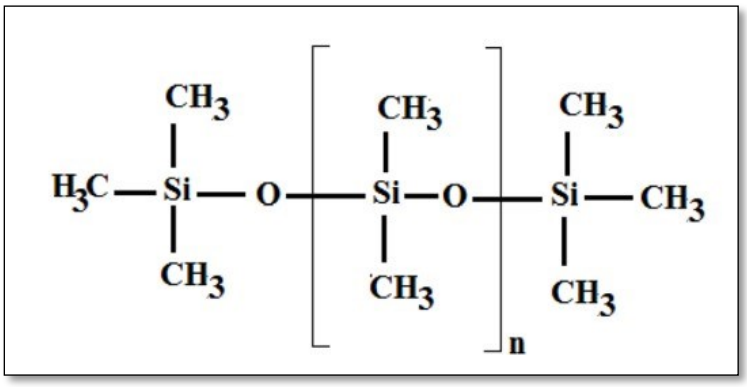

Figure 9. The molecular structures of PDMS [54] (Reproduced with permission from John Wiley and Sons).

PDMS superhydrophobic films containing particles can be coated on various substrates by a wide range of methods such as spray coating, dip coating, and so forth. In addition to other superb properties of silicone rubber, these materials are well known for their hydrophobic recovery properties. Silicone-based materials which lose their initial hydrophobicity, can regain their hydrophobicity [55]; migration of free low molecular weight siloxane (LMWS) in non-crosslinked matrix from the bulk to the surface, reorientation of polar and nonpolar groups in the bulk and surface and condensation of the hydroxyl groups on the surface are among the known mechanisms behind this hydrophobic recovery (Figure 10) [9], [43], [44].

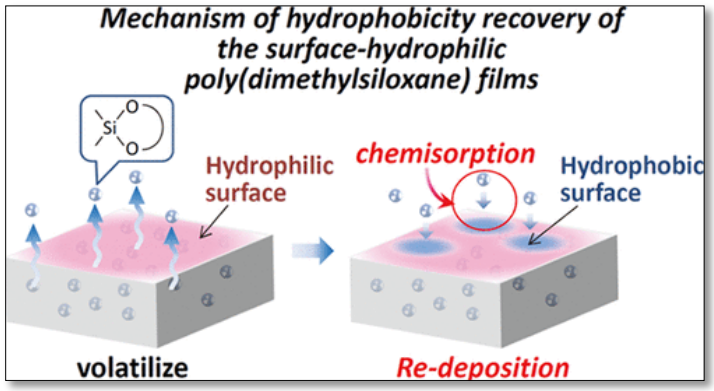

Figure 10. A schematic of the hydrophobicity recovery of poly (dimethyl siloxane) films with hydrophilic surfaces [59] (Reproduced with permission from Langmuir).

Since one of the best ways to fabricate superhydrophobic coatings would be incorporation of micro and nanoparticles due to their role in the creation of hierarchical structure on the surface, the choice of silica particles would be a suitable one owing to their low toxicity and environmental impacts [15]. For example in one work, Li et al. [18] fabricated a robust and flexible bulk superhydrophobic PDMS/silica film by UV curing and solvent evaporation method. This bulk superhydrophobic film is fabricated via thiol-ene photopolymerization. The simultaneous effect of presence of silica particles and porous structure throughout the whole film ended in high robustness of the superhydrophobicity.

Based on the literature review done in this section and with the final application of the coating, which is for electrical insulators, PDMS-based resins are chosen as the matrix of the intended coating. Incorporation of micro and nanoparticles would be an effective way to create the hierarchical topography and lower the surface energy of the coating which are the requirements of superhydrophobicity, which would be the chosen approach for this research as well.

2.6 Applications of superhydrophobic coatings

Superhydrophobic surfaces can play a crucial role in a wide variety of applications (Figure 11) such as self-cleaning, corrosion resistance, anti-icing, water, and oil separation, drag reduction, and so on [60-64]. In addition to the mentioned areas of applications, superhydrophobic coatings, in general, could help with the reduction in the elimination or reduction of manual labor and the cost and time used for cleaning the final products [65].

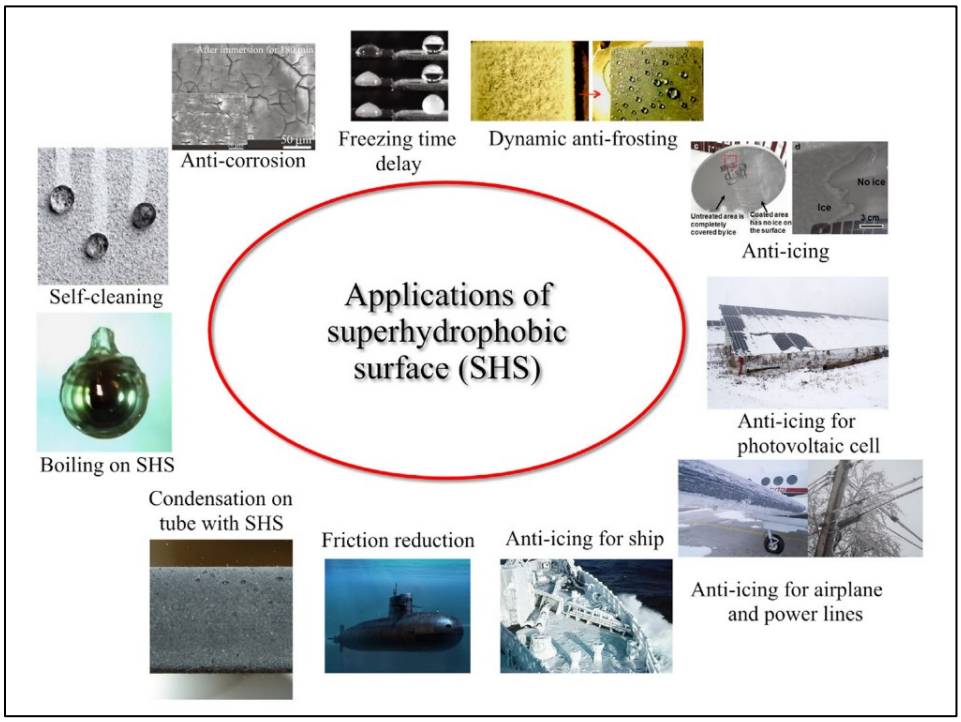

Figure 11. Various applications of superhydrophobic surfaces [30] (Reproduced with permission from Elsevier).

One of the interesting areas of application of superhydrophobic coatings is high voltage insulators. For instance, Li et al.[13] developed a superhydrophobic poly(dimethylsiloxane)/modified nano-silica (PDMS/modified nanosilica) coating to reduce ice accumulation on insulators. These coatings helped the insulators increase the flashover voltage.

In another work, Zuo et al. [66] fabricated superhydrophobic coatings with a contact angle (CA) of 161° and a sliding angle (SA) of 1°. Their coating was a combination of hydrophobic fumed silica nanoparticles, fluorosilicone resin, and epoxy resin and was sprayed on the glass insulators. The fabricated coatings increased the ice flashover voltage from 74 kV to 94 kV.

2.7 Challenges and drawbacks of superhydrophobic coatings

Superhydrophobic coatings could bring along some challenges and drawbacks, either in preparation step or after fabrication. One of the limitations of superhydrophobic coatings implementation in large-scale applications is their low durability. Stability throughout long periods is one of the challenges that superhydrophobic coatings face nowadays.

Surface structures containing micro or nano roughness are more prone to damage caused by mechanical stress compared to regular surfaces. The superhydrophobicity property of these coatings can be suppressed in two ways, either by damage to the physical structure of the coating caused by impact or abrasion which would lead to an increase of contact area between the solid substrate and water, or by an increase in surface energy which can be caused by contamination, irradiation, or any damage to the low surface energy hydrophobic layer.

The durability of superhydrophobic coatings can be categorized into 1) Environmental durability and 2) Durability against mechanical forces. Upon the area of application, the coatings are expected to show durability in various circumstances. The method used for the coating robustness evaluation should be according to the application of the superhydrophobic surface [67]. If the coating is designed to be used outdoors, environmental robustness is crucial. Tests such as UV radiation, ozone durability test, and acid dew and fog test (ADF) could show the environmental durability test [68-70]. Mechanical stability is an area of interest when it comes to superhydrophobic coatings. Various characterization methods for mechanical stability have been suggested, and each of them focuses on a specific aspect of the mechanical properties of the coating. The durability against mechanical forces can be examined via various methods, such as sandpaper abrasion, drop impact durability, and so on.

Mechanical abrasion with the help of sandpaper or a known textile is the most approached method for testing the mechanical durability of superhydrophobic coatings [71]. Wang et al. [72] fabricated a superhydrophobic coating with the mechanical stability of 100 abrasion cycles with sandpaper. The tested coating was a polytetrafluoroethylene/polyvinylidene fluoride (PTFE/PVDF) composite which maintained a high contact angle throughout the test.

Another test to characterize the mechanical properties of a coating is sand abrasion. Sand impact test is done using a funnel full of sand over the sample placed tilted [71]. Ellinas et al. [73] fabricated self-healing superhydrophobic coatings which lasted for 10 abrasion impact tests. The epoxy-based coatings used in this research were spray-coated with a PS/SiO_2 dispersion and a PDMS-based solution. These coatings also regained superhydrophobicity after air plasma treatment.

Li et al. [74] used 120 μm to 260 μm sand grains to test the mechanical durability of their self-healing superhydrophobic coatings. The sprayed coatings of polyelectrolyte complexes of poly (allylamine hydrochloride) sulfonated poly (ether ether ketone) (PAH–SPEEK), poly (acrylic acid) (PAA), healing agents of perfluorooctanesulfonic acid lithium salt (PFOS) and 1H,1H,2H,2H-perfluorooctyltriethoxysilane (POTS) on the surface showed durability after a 1h sand impact test from a height of 30 cm. By increasing the height to 2 m, after only 15 min the SA of the coating rises to 30° (Figure 12). However, after being kept in an environment of 40% RH for 3 h, the SA drops to 2°.

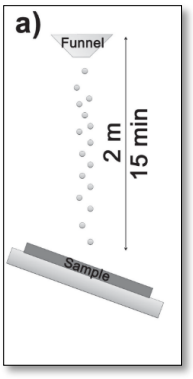

Figure 12. Schematic figure of a sand abrasion test [74] (Reproduced with permission from John Wiley and Sons*).*

Therefore, it can be concluded that fabrication of a robust superhydrophobic coating by modifying the chemical or physical properties is in demand. Designing strategies for a robust superhydrophobic coating can be categorized into passive and active strategies. Passive resistance strategies are the ones helping the surface retain the superhydrophobicity after wear [75]. This can be achieved by strengthening the superhydrophobic properties, with the help of methods such as incorporation of elastic composition to absorb the shocks, increasing the crosslinking sites, increasing the interactions between components, or increasing the adhesion of the coating and substrate [17], [76-80].

Peng et al. [81] made a superhydrophobic fluorinated epoxy-based coating with high robustness based on a passive resistance strategy. Perfluoropolyether (Krytox oil) was added to the fluorinated epoxy to increase the hydrophobicity and mechanical flexibility. Polytetrafluoroethylene (PTFE) nanoparticles were also added to create superhydrophobic coatings. The fabricated coatings showed great mechanical robustness under tape peel (adhesion) test, crosshatch test, and Taber abrasion technique. They benefited from the simultaneous effect of 1) A coating design that experiences failure in a self-similar manner, meaning after being exposed to damage the affected parts of the coating will be the same in texture and functionality as the undamaged layer and 2) once a droplet or jet imposes impact on the coating, the coating would be able to decrease the impact by softening the peak pressure. Peng managed to use a multi-fluorination strategy to achieve the two design strategies mentioned to improve the robustness.

The active method concentrates on superhydrophobicity regeneration after deterioration which can be done by approaches such as self-healing or easy repair strategies [75]. Among those, the former is the focus of this research and will be explained in the following.

2.8 Regenerative superhydrophobic coatings

Regenerative superhydrophobic coatings are a potential solution to address the durability issue associated with superhydrophobic coatings. Regenerative superhydrophobic coatings could be defined as coatings capable of recovering their superhydrophobicity property via self-healing, after losing it due to inevitable deterioration. The concept of self-healing comes from biology, some plants, for example, use this strategy to keep their superhydrophobicity by restoring the epicuticular wax layer [17]. Some plants such as lotus or clover obtain the ability to self-heal the superhydrophobic properties of their leaves. The presence of regenerable epicuticular wax within

the leaves enables these plants to replace the damaged wax layer with a new one. This ability enables these plants to self-heal their superhydrophobicity [82].

2.8.1 Regenerative Superhydrophobicity Principles

Regenerative superhydrophobic coatings can be divided based on their healing principles and the type of damage inflicted on the coating. These coatings can be categorized into three categories (Figure 13). First, the low surface energy material incorporated within the matrix of the coating, migrates to the surface after the low surface energy layer on top of the coating is ruined. This migration to the surface can end up in the regeneration of superhydrophobicity and can be either done with or without any external stimuli such as heat or humidity. The damage to the superhydrophobic layer of these coatings is either due to chemical damage or abrasion.

In the second category, in the situation that the micro/nano structure on the coating is destroyed, the surface topography is healed and therefore the coating becomes superhydrophobic once again. In this case, the coating loses its superhydrophobicity either due to scratch damage or a cut posed upon the coating. Some researchers tend to use a hybrid solution and combine both mentioned principles as the third approach to ensure their regenerative superhydrophobic coatings function accordingly.

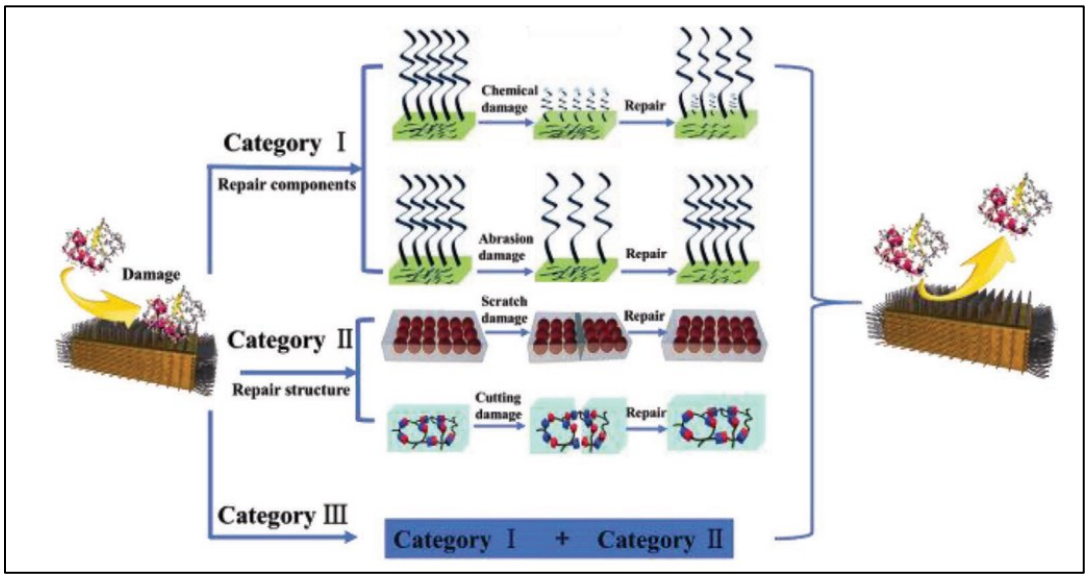

Figure 13. Superhydrophobic coatings possible damages: I) chemical, II) micro-nano structural, and III) combination of the two. The figure also mentions the repair strategies for each category of possible damage [16] (Reproduced with permission from John Wiley and Sons).

In this part, a deeper look into fabrication methods of regenerative superhydrophobic coatings based on healing principles is presented (Figure 14). Each part will discuss the healing methods and provides examples of the research done in that area.

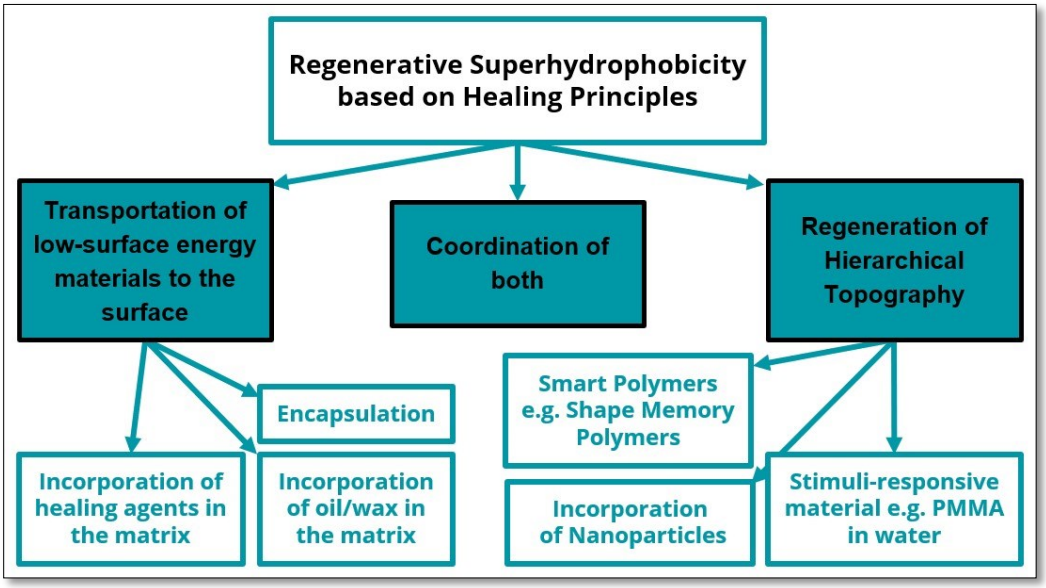

Figure 14. Regenerative superhydrophobic coatings based on their healing principles © Helya Khademsameni, 2023.

2.8.1.1. Transportation of low-surface energy materials to the surface

The first approach toward fabrication of regenerative superhydrophobic surfaces can be done via migration of low-surface energy materials to the surface. This can be achieved by storing hydrophobic material inside the coating which eventually migrates to the surface after deterioration of superhydrophobicity. When the low-surface energy layer is decomposed or degraded, the low-surface energy substances stored in the structures are released automatically or under external stimuli treatment (e.g., humidity [83], UV light [84], temperature [85], etc. [86]). The spontaneous or stimulated transportation of low-surface energy material occurs due to the difference in the surface energy of the stored hydrophobic material and the surface which has higher surface energy. In most cases, spontaneous migration can take more time for healing in comparison to external stimuli healing approaches.

Various approaches have been implemented to benefit from this healing principle which could be summarized in incorporation of healing agents or oil/wax either in the bulk of the coating or in the form of capsules dispersed within the coating.

2.8.1.1.1 Incorporation of healing agents in the matrix

Some researchers focused on the incorporation of functionalized or unfunctionalized nanoparticles within the matrix alongside healing agents. H. Zhou et al. [87] prepared a stable dispersion network of Zonyl321, fluorinated alkyl silane (FAS), and polytetrafluoroethylene (PTFE) nanoparticles in water. The synergetic interaction among Zonyl321, FAS, and PTFE in the solution made it possible to almost make a stable dispersion and created a superhydrophobic coating. After the superhydrophobicity was deteriorated by plasma etching, the samples were heated at 135 °C

for 10 min. The heat was applied to assist the migration of small FAS molecules to the surface and make the surface superhydrophobic again.

Li et al. [74] created regenerative superhydrophobic poly (acrylic acid) (PAA)/ poly (allylamine hydrochloride)-sulfonated poly (ether ether ketone) PAH-SPEEK coatings. On the first try, the author found out spraying a solution containing 1H, 1H, 2H, 2H-perfluorooctyltriethoxysilane (POTS) onto the (PAA)/ PAH-SPEEK) *80 (where 80 is the number of spraying cycles) base coating would not result in fabrication of superhydrophobic coating. Due to the superhydrophilicity of the (PAA/PAH-SPEEK) *80 coatings, the adhesion of the superhydrophobic POTS on the surface would not be a strong one, leading to an unsuccessful attempt of creating superhydrophobic surfaces. This obstacle was overcome by spraying perfluorooctanesulfonic acid lithium salt (PFOS) on the coating prior to spraying a POTS layer. The electrostatic interactions between the sulfonate group of the PFOS molecules and protonated amine groups in the PAH lead to loading of PFOS on these coatings. After loading of PFOS, the surface of the (PAA/PAH–SPEEK) *80 became superhydrophobic, therefore attachment of POTS and diffusion into the inner pores of the coating was facilitated.

The coatings were prone to O_2 plasma treatment. Plasma treatment decomposed the PFOS layer and caused the formation of hydrophilic groups on the surface, meaning a loss in the superhydrophobic properties of the coating. Nevertheless, while left at ambient environment for 4h the PFOS preserved in the structures released and migrated to the surface, causing a decrease in the surface energy of the coating and recreation of superhydrophobicity. The (POTS/PFOS–(PAA/PAH–SPEEK) *80) coatings could regain their superhydrophobicity for 25 cycles of etching/healing.

Another approach could be use of CVD method to make a hydrophilic surface into a regenerative superhydrophobic one, such as the work of the same author in an earlier research [88] which was centered on chemical vapor deposition of POTS on $(PAH–SPEEK/PAA)_{60.5}$, in which 60.5 is the number of deposition cycle (Figure 15). In both aforementioned research, the low-surface material was diffused within the porous matrix, and upon migration of the low-surface energy layer to the top surface regenerative superhydrophobic coatings were obtained.

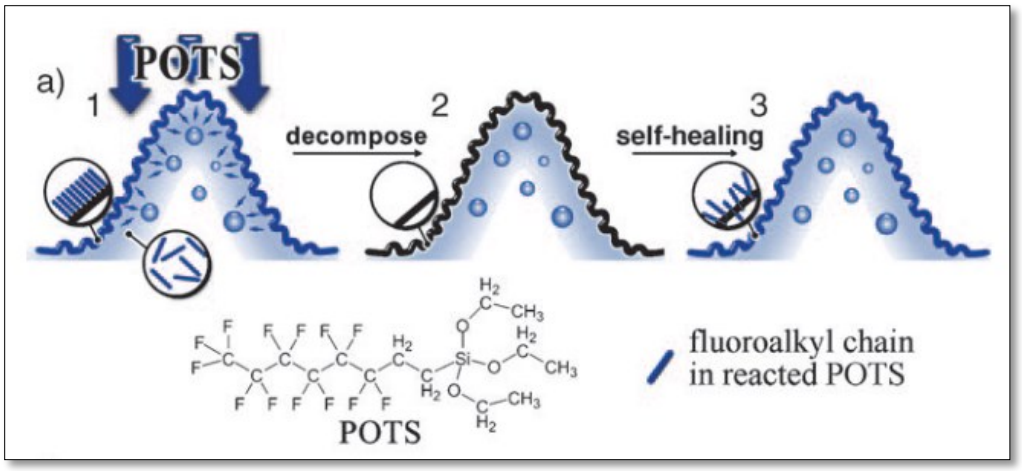

Figure 15. a) A POTS containing self-healing superhydrophobic coating schematic: 1) Pristine; 2) After superhydrophobicity loss due to the top fluoroalkylsilane layer decomposition; 3) Migration of preserved healing agents to the surface and the superhydrophobicity healing process [88] (Reproduced with permission from John Wiley and Sons).

One of the main challenges of using nanoparticles in the coating is their tendency to agglomerate. Therefore, researchers try to achieve a good dispersion of nanoparticles within the coating with various techniques. One of those is Chemical Solution Deposition or Sol-Gel method which is one of the conventional fabrication methods of superhydrophobic coatings as well [89], [14].

Lahiri et al. [90] fabricated H_3BO_3-incorporated SiO_2–alkyl-silane superhydrophobic fabric coatings via sol-gel. Presence of H_3BO_3 in the coating delivers a dual benefit for the coating. Firstly, the reaction of H_3BO_3 and SiO_2 nanoparticles form a nonporous structure which is beneficial for storing the healing agents. Secondly, it creates a strong bond between the SiO_2 and prehydrolyzed hexadecyltrimethoxysilane (HDTMS) in the coating, resulting in high durability due to the high bonding energy between silanol groups and H_3BO_3. After air plasma treatment the loss of superhydrophobicity in the samples was observed. However, after 12 h in ambient temperature, by migration of H_3BO_3–SiO_2–HDTMS/PDMS chains to the surface WCAs increased to even higher than 150° and recovered the superhydrophobicity of the coatings.

2.8.1.1.2 Incorporation of oil/wax in the matrix

To achieve regenerative superhydrophobicity, some researchers store oil or wax within the matrix. In one example, n-Nonadecane wax was stored within the PDMS matrix [82]. Due to the low melting temperature of the wax, after the degradation of the low surface energy layer, the wax easily migrates to the surface, leading to a regenerated superhydrophobic surface. Choice of PDMS as the matrix helped this regeneration as well. The movement of PDMS chains enables the n-Nonadecane molecules to move through this network and reach the surface.

Weng et al. [91] fabricated a photothermal conversion and conductive coating containing beeswax, multiwalled carbon nanotubes (MCNTs), and polydimethylsiloxane (PDMS). Beeswax is a mixture of small molecular compounds with hydrophobic properties such as alkanes, diesters, and fatty acids. In the comparison of samples containing beeswax (BCP7) and reference samples

without beeswax (CP7), BCP7 samples showed regeneration of superhydrophobicity after O_2 plasma treatment (Figure 16). However, the reference samples were incapable of recovering the superhydrophobicity following the plasma treatment, indicating beeswax as the healing agent for the recovery of superhydrophobicity in the BCP7 samples. The difference between the surface energy of the coating and the bulk triggers a surface reorganization and leads the beeswax to the surface and consequently regenerates the superhydrophobicity of the coating.

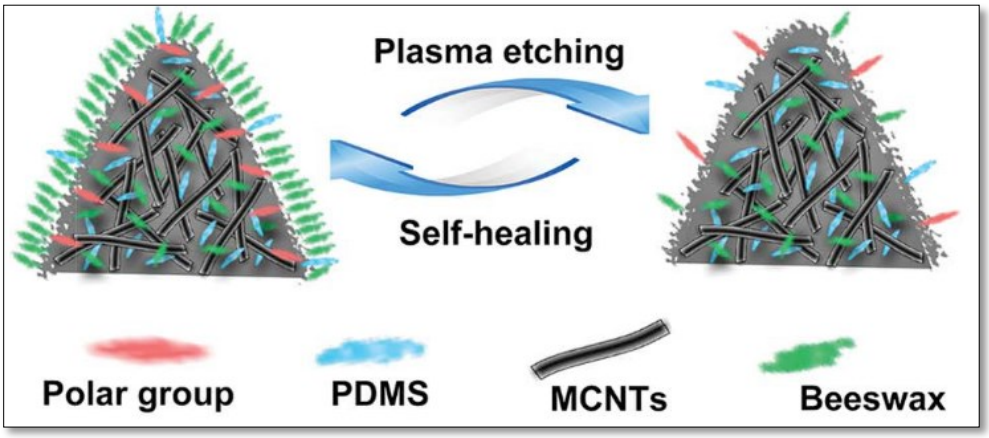

Figure 16. Schematic of the superhydrophobicity regeneration in a regenerative superhydrophobic coating containing beeswax [91] (Reproduced with permission from Royal Society of Chemistry).

A combination of both of the above-mentioned approaches can be of interest for the fabrication of novel regenerative superhydrophobic coatings. However, optimization of various healing agents and oil/wax, their compatibility, and their effect on the properties of the final coating must not be neglected.

2.8.1.1.3 Encapsulation of low surface energy materials

Some approaches focus on the encapsulation of low-surface energy material within a capsule that can be emitted and substitute the low-surface energy layer [92], [93], which is the basis of the research that Rao et al. [94] conducted. Their UV-responsive capsules could release superhydrophobic FAS upon degradation and recreate the superhydrophobicity.

In a similar research, Cong et al. [95] fabricated a regenerative superhydrophobic coating containing microcapsules which carried low-surface energy FAS-12 (dodecafluoroheptyl-propyl-trimetoxysilane). They used Pickering emulsion polymerization of styrene using modified SiO_2 and TiO_2 nanoparticles as Pickering agents in their experiments. The capsules were then mixed with FAS-17 (heptadecafluoro-1,1,2,2-tetradecyl trimethoxy silane)-modified SiO_2 and polysiloxane latex. After exposure to UV, the FAS-12 in the capsules was released due to photo-catalyzed degradation of polystyrene. The released FAS-12 migrated to the surface and recovered the loss of superhydrophobicity.

Although encapsulation method can be of interest in fabrication of self-healing superhydrophobic coatings, various parameters such as compatibility of the core and shell,

durability of the capsules, dispersion of the capsules, on-time response of the capsules to the external stimuli, and several other parameters must be considered [76], [96], [97].

2.8.1.2. Regeneration of hierarchical topography

Regeneration of hierarchical topography is the second principle of creating regenerative superhydrophobic coatings. After the surface roughness is destroyed, the hierarchical topography of the coating is regenerated which can end up showing superhydrophobic properties once again. One of the challenges in this method is to be able to regenerate the former hierarchical structure with different length scales [98]. Several research has been done with a focus on self-regenerating topography of superhydrophobic coatings [99], [100].

First to mention, is the re-arrangement of components in the coating with the aim of regeneration of the hierarchical topography [101], [102]. Nevertheless, this approach is efficient if the loss of superhydrophobicity due to scratches or cuts are too severe. In this case, regeneration of the topography should also include regeneration in the bulk of the coating. In most cases, these regenerations are stimuli driven [98]. Nonetheless, there is some research with a focus on stimuli-free regeneration of self-healing which open a new door in this field of research [103].

2.8.1.2.1 Incorporation of Nanoparticles for surface topography regenerating

The presence of nanoparticles could help with the regeneration of the surface topography by rearrangement of the coating components. Wu et al. [104] prepared a coated film of polycaprolactone (PCL)/poly (vinyl alcohol) (PVA) with a layer of Ag nanoparticles and Ag nanowires (AgNPs-AgNWs) and modified it with 1H,1H,2H,2H-perfluorodecanethiol (PFDT) to reduce the surface energy. The coating was damaged by abrasion using a scalpel or knife and resulted in a loss of superhydrophobicity. Upon the application of a 4 V voltage (0.31 $W.cm^{-2}$) for 1 min the coating retained the superhydrophobic property, confirming a regenerative property. The film converts the electrical energy into thermal energy, making the hydrophilic (PCL/PVA) *7 (where 7 is the number of spin-coating cycles) films soft, and the film material nearby the damaged region is driven by the reduction of its surface tension to flow into the damaged area to fill the gap. Due to the strong adhesion between the PFDT/AgNPs-AgNWs layer and the (PCL/ PVA) *7 films, the flow of the (PCL/PVA) *7 film causes the separated PFDT/AgNPs-AgNWs layers to move toward each other. During this process, the damaged region of the PFDT/ AgNPs-AgNWs/(PCL/PVA) *7 film repairs or is significantly narrowed, and the hydrophilic component is covered by the hydrophobic PFDT/AgNPs-AgNWs layer resulting in surface regeneration of superhydrophobicity (Figure 17).

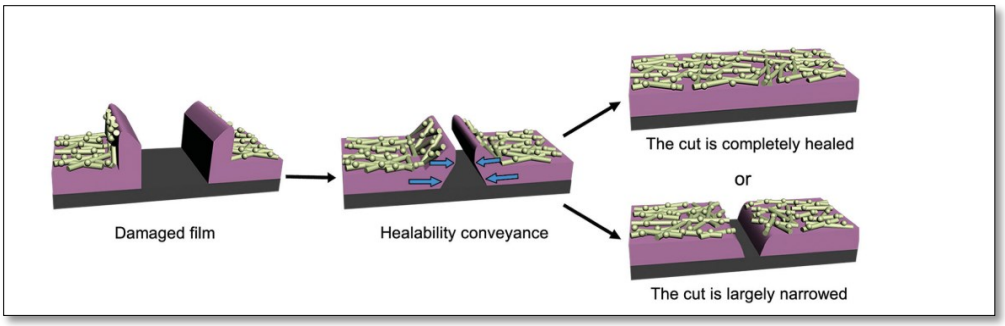

*Figure 17. Superhydrophobicity regeneration schematic in PFDT/AgNPs-AgNWs/(PCL/PVA) *7 film* [104] (Reproduced with permission from John Wiley and Sons).

Some researchers would try to avoid the challenges of achieving a homogenous dispersion by using the Sol-Gel method. Wang et al. [102] synthesized aligned carbon nanotube bundles (ACNTB)-SiO_2-silane coupling agent 3-methacryloxypropyltrimethoxysilan (KH570) hierarchical particles via Sol-Gel and used them to create self-healing superhydrophobic epoxy coatings. The coatings would regain superhydrophobicity after being damaged, by heat treatment of 300 °C for 9 hr. Not only the heat would degrade epoxy and reveal the nanoparticles within the matrix leading to the recreation of hierarchical structure, but it could also weaken the interaction between CNT and SiO_2, which could facilitate the migration of SiO_2 nanoparticles to the surface.

2.8.1.2.2 Smart polymers, such as shape memory polymers

One way to achieve topography regeneration is to rely on shape memory polymers (SMP). SMPs are stimuli-responsive materials that can restore their original morphology after being temporarily deformed under the influence of an external stimulus. They can be used to regenerate the surface roughness and regain superhydrophobicity. In most cases, SMPs can be fabricated by heating the polymer and crosslinking them to a degree which is higher than their melting point which could result in a crosslinking reaction in a mold [105-107].

Although the use of SMPs is an effective method in the case of topography regeneration, the special parameters regarding the fabrication of shape memory polymers could bring along various challenges.

Gua et al. [108] used the same principle to create aerosol-assisted layer-by-layer chemical vapor deposition (AA-LbL-CVD) of epoxy resins and PDMS polymer film. The SMP films which were deteriorated by an external force became superhydrophobic again as they recovered their initial topography when heated at 85 °C for 5 min (Figure 18).

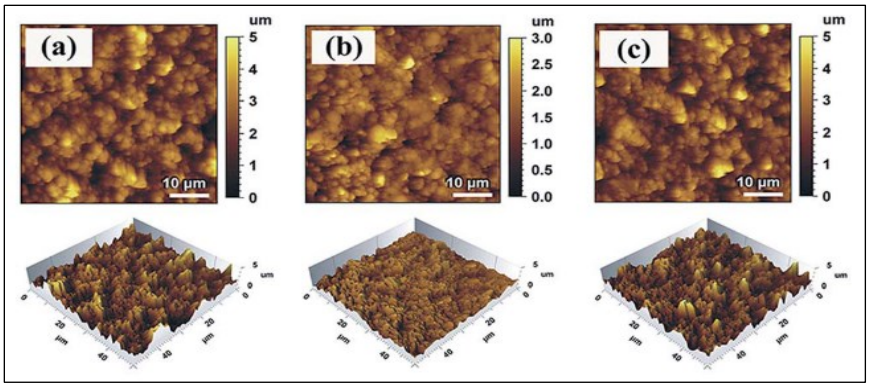

Figure 18. AFM of the surface topography of (a) pristine Epoxy/PDMS coating with Ra=611 nm; (b) crushed Epoxy/PDMS coating with Ra=313 nm; and (c) recovered Epoxy/PDMS with Ra=582 nm [108] (Reproduced with permission from Royal Society of Chemistry).

Wang et al. [109] managed to develop a superhydrophobic SMP surface that repels water and oil droplets. They developed a mushroom liked SMP surface based on thiol-ene/acrylate through a combination of photolithography and reactive ion etching (Figure 19). The aforementioned surface regained its original morphology prior to deformation due to applied pressure. The contact angles of both water and n-hexadecane were studied before and after topography self-healing.

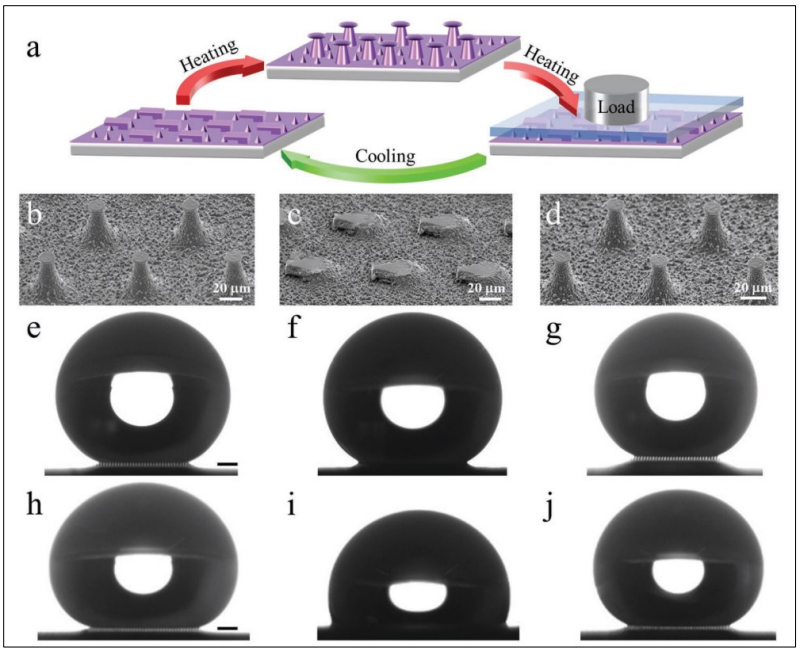

Figure 19. a) Schematic, SEM images, water contact angle and n-hexadecane contact angle on the reversible stages of the fabricated coating: The mushroom-like pillar texture and the collapsed pillar texture [109] (Reproduced with permission from John Wiley and Sons).

2.8.1.2.3 Stimuli-responsive material

One basic approach for surface roughness regeneration is to re-arrange the components in the coating. Therefore, researchers have employed polymers for structure regeneration that rely on

rearrangement aggregation. An example of this could be taking advantage of the swelling behavior of Poly (methyl methacrylate) (PMMA) in water, which can regenerate the surface micro and nanostructures and regain the superhydrophobicity of the surface [110]. As explained, this method is limited to some specific group of materials that can be triggered by some unique stimuli.

2.8.1.3. Low surface energy material migration and hierarchical topography regeneration simultaneous action

Some superhydrophobicity regeneration approaches benefit from a combination of both principles mentioned before. In other words, their superhydrophobicity regeneration is a cause of both migration of low surface energy material to the surface and regeneration of hierarchical topography. These coatings will be able to withstand both physical and chemical damages and recover the superhydrophobicity of the coating [17]. The schematic principle of these superhydrophobicity regeneration approaches is presented in Figure 20. When these coatings are prone to a damage to both the low surface energy layer and the surface topography that ends in loss of superhydrophobicity, their superhydrophobicity regeneration mechanism works by addressing both the occurred damage. This approach appears as a simultaneous act of lowering the surface energy and recreating the surface topography. In the figure, the blue represents the low surface energy substances, and the grey represents the surface structure [98].

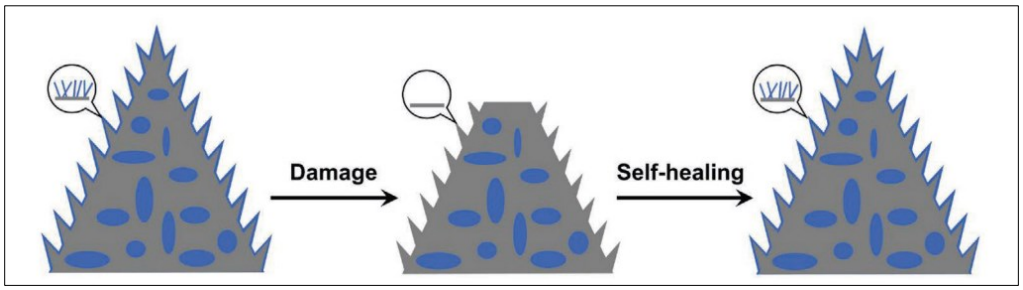

Figure 20. Self-healing principle of superhydrophobic surfaces based on the simultaneous effect of low-surface energy substances transportation and rough topography regeneration [98] (Reproduced with permission from John Wiley and Sons*)*.

Wang et al. [111] fabricated a superamphiophobic coating containing fluoroalkyl surface-modified silica nanoparticles (FS-NP) on a fabric, followed by coating a mixture of tridecafluorooctyl triethoxysilane (FAS) and fluorinated decylpolyhedral oligomeric silsesquioxane (FD-POSS). The superamphiophobic surface lost its amphiophobicity after air plasma exposure and regained it after heating at 140 °C for 5 min. The surface also regained its amphiophobicity after physical damage. 30 min of 140 °C heat allowed the FD-POSS and SiO_2 NPs to reconstruct the surface roughness following a sandpaper abrasion. Therefore, the coating regained its superamphiophobicity.

Chen et al. [112] improved the superhydrophobic coatings they had prepared in their previous research [113] by changing the coating components into a final composition of polystyrene (PS), fluorinated SiO_2 nanoparticles (FMS), α,ω-bis(hydroxypropyl)-terminated poly(2,2,3,3,4,4,4-heptafluoro-butylmethylsiloxane) (PMSF) and TiO_2 nanoparticles. In this

developed coating, FMS nanoparticles and PMSF are the hydrophobic substances and PS is the polymer binder. This superhydrophobic coating loses its superhydrophobicity after abrasion of sandpaper under 20 kPa. When the abraded coating is exposed to UV, the PS is decomposed due to the photocatalysis of TiO_2 nanoparticles. Due to this decomposition, the FMS and TiO_2 nanoparticles in the bulk of the coating are now exposed at the top, reforming the surface structure. Atomic Force Microscopy (AFM) analysis made it apparent that the coating regained the roughness of 534 nm, after a drop to 181 nm due to abrasion, which is similar to the initial roughness (623 nm). Furthermore, PMSF molecules migrated to the surface due to the difference in the surface energy, covering the hydrophilic layer that TiO_2 nanoparticles had created on the surface. At the end, the result was regeneration of the coating superhydrophobicity (Figure 21).

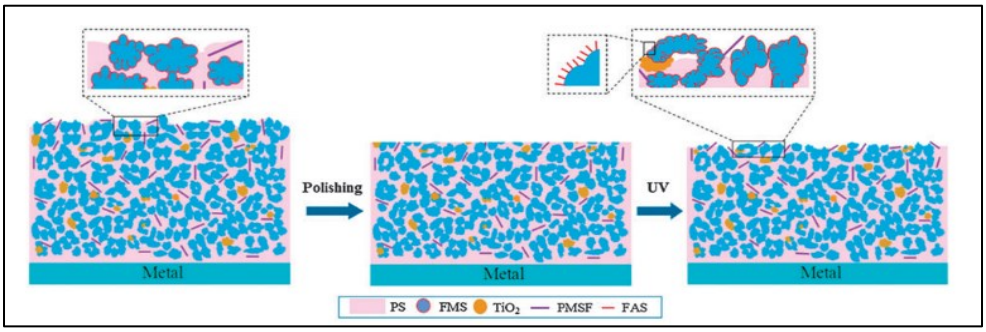

Figure 21. Schematic principle of self-repairing superhydrophobic coatings containing PFMS/TiO_2 [112] (Reproduced with permission from Royal society of chemistry*)*.

2.8.2 Superhydrophobicity healing components

Throughout this literature review, several research work on fabrication of self-healing superhydrophobic coatings was reviewed. Regardless of the self-healing superhydrophobicity principle chosen for each of them, a great amount of consideration must have been devoted to the proper choice of self-healing superhydrophobic components as well, components which are by nature hydrophobic and contribute to the superhydrophobicity regeneration of the coatings by lowering the surface energy, or regeneration of the topography or/and both mentioned. A delicate choice that must be in consideration of various factors such as compatibility with other coating components, the superhydrophobicity healing principle, the application of the final coating, and the expected properties of the coating. Herein, a list of superhydrophobicity healing components chosen by researchers is provided [17], [16], [98]:

Table 2. Superhydrophobicity healing components used in the literature review © Helya Khademsameni, 2023.

Healing agent	Details	References
PFOS/POTS	Perfluorooctanesulfonic /Perfluorooctyltriethoxysilane	[74] , [114]
POSS	Polyhedral oligomeric silsesquioxane	[111], [115]
FAS	Fluorinated alkyl silane	[94], [56], [116]
POTS	Perfluorooctyltriethoxysilane	[117]

POS	Polysiloxane	[118]
Bee wax	-	[91]
HDI	Hexamethylene diisocyanate (HDI)	[76]
n-Nonadecane	-	[82]
n-Octadecane	-	[92]
ODA	Octadecylamine	[119], [120]

Among the superhydrophobicity components mentioned, Polyhedral oligomeric silsesquioxane (POSS) can be a suitable choice, benefiting the final coating for various reasons. POSS is a class of hybrid materials that could not only lower the surface energy of the coating, but also increase the surface roughness and increase the hydrophobicity of the coating [121].

Polyhedral oligomeric silsesquioxanes are quite exceptional due to their cage-like and polyhedral molecular structure and physiochemical properties [122]. Polyhedral oligomeric silsesquioxane has an organic/inorganic structure with a general formula of $R_n(SiO_{1.5})_n$ (Figure 22) [123]. Presence of a silica cage is beneficial to the mechanical and thermal stability of the final coating, while the chemically tunable organic functions of the POSS appoint it as an ideal building block for high-performance applications. The polyhedral structure and the tunable peripheral organic groups on the POSS, make it an ideal choice for increasing the hydrophobicity of a coating, and an interesting choice for a self-healing superhydrophobic coating [111], [115], [124].

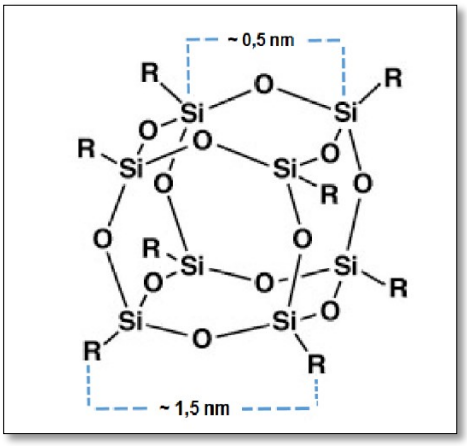

Figure 22. Molecular structure of T8 Polyhedral Oligomeric Silsesquioxanes cage [125].

Another option for superhydrophobicity healing components is silicone oil which could be considered an uncommon choice in this field of research. Silicone oil is a low molecular weight PDMS with the same chemical structure and surface energy [126]. Zhu et al. [127] fabricated silicon-oil-infused polydimethylsiloxane (PDMS) coatings with icephobic properties. Presence of the silicone oil reassured the durability of the liquid-infused porous surfaces (LIPS) approach in his research (Figure 23). A research with a conclusion that the presence of silicone oil with its extremely low surface energy, improves the water-repellency of the coating.

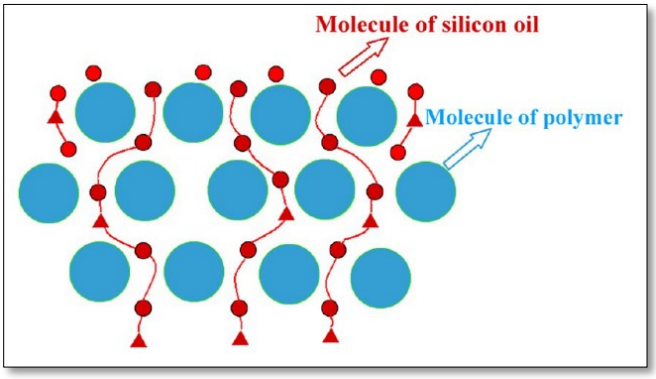

Figure 23. Migration of silicon oil to the surface resulting in regeneration of liquid-infused porous surfaces structure of the silicon oil infused PDMS coating [127] (Reproduced with permission from American Chemical Society).

2.8.3 Characterization of the coating

As discussed in the sections before, the two criteria for superhydrophobicity are i) low surface energy and ii) hierarchical topography. In the case of superhydrophobicity loss, each or both mentioned criteria are affected. In order to characterize the regenerative superhydrophobicity, it is important to establish which of the criteria is being addressed. On that account, for the characterization of regenerative superhydrophobic coatings, the following methods mentioned can be used:

2.8.3.1 Superhydrophobicity Characterization

Static and sliding water contact angles during the process of loss of superhydrophobicity and regeneration of superhydrophobicity are measured to assess the superhydrophobicity of the surfaces. These tests can be done by a fully automated contact angle goniometer with sessile water droplets of different volumes [128-130].

2.8.3.2. Imaging Techniques

Various imaging techniques can be employed to review the surface morphology prior to and after the loss of superhydrophobicity and regeneration of superhydrophobicity. Scanning electron microscopy (SEM), Profilometer and Atomic Force Microscopy (AFM) can be used for this scope. These methods are mainly used to obtain rather qualitative surface information and they could be completed by more quantitative tests [131-133].

2.8.3.3. Surface Chemistry Characterization

Surface chemical and structural composition characterization can be done to obtain more precise information on the chemistry of the surface of the coatings during loss of

superhydrophobicity and the return to superhydrophobicity by Fourier transform infrared spectrometry (FTIR) or X-ray photoelectron spectroscopy (XPS) [134-136].

2.8.4 Characterization of coating durability

Mechanical wear

Mechanical wear not only affects the hierarchical topography of a surface, but also could remove the layer containing low surface energy material. The effect of mechanical wear can be evaluated by sandpaper tests under various pressures [112]. Moreover, sand grains could be dropped on a surface to examine their durability against abrasion. Zhao et al. [137] impacted their polysiloxane robust self-healing superhydrophobic coatings containing POSS-modified SiO_2 nanoparticles with sand grains 300–600 μm diameter from a height of 30 cm and reported the durability of the superhydrophobicity of their coatings even after 30 cycles.

External load on the surface

An external load could be pressed on a surface, aiming to destroy the hierarchical topography of the surface, and resulting in loss of superhydrophobicity. In this method, the chemical composition of the surface is untouched [138]. One of the tests in this category is the sand impact test. An example of which would be force of a thumb on the surface [137].

High and low-temperature stability tests

Verifying the thermal durability of the superhydrophobic coatings, the mentioned coatings could be prone to high or low temperatures for a certain amount of time. Afterward, any possible change in the WCA will be reported [139].

Resistivity against acid and basic solution

To ensure the coatings are durable in case of contact with a solution with high or low pH, the changes of contact angle after immersion of the coating in solutions with various pHs ranging from 2- 12 are observed [17], [44].

2.8.5 Assessment of superhydrophobic self-healing ability

In order to evaluate the superhydrophobicity regeneration ability of the fabricated coating, various tests could be performed. Any test that could chemically or physically damage the coating and affect the superhydrophobicity of the coating, can be of use. After the loss of superhydrophobicity, the recovery ability of the coating needs to be evaluated. Therefore, all the tests mentioned in the previous section can be of use if they lead to loss of superhydrophobicity. On top of that, there are some more specific testing techniques that researchers working on self-healing superhydrophobic coatings tend to use which will be explained below.

Plasma treatment

Surface treatment can be done by various methods, one of which is the use of plasma systems. Plasma systems can be divided into low-pressure and atmospheric plasma depending on the pressure inside the chamber. Plasma, which is the fourth state of matter (others would be gas, liquid, and solid), is an ionized gas. Plasma consists of ions, free electrons, and neutral species. In the condition that a stream of gas is subjected to electrical energy, it will get ionized and forms a high-speed stream of glowing discharge which is known as plasma [140].

The traditional sources of atmospheric-pressure plasma systems are transferred arcs, plasma torches, corona discharges, and dielectric barrier discharges [141]. Based on the plasma parameters, the plasma treatment can influence both the surface roughness and surface chemical composition; Parameters such as the generation power, treatment time, distance between nozzle and substrate, gas flow, and the plasma gas can be determinants while using an atmospheric-pressure plasma jet [142]. Certain atoms or phases on the substrate could react with plasma particles.

High-energy particles of the plasma colliding with the surface could break chemical bonds or form new ones, ending in a change in the chemistry of the surface. Two free radicals during the plasma treatment can combine or form branches or cross-links [143].

One of the means of surface modification with the help of plasma, could be interfering with the surface tension and therefore changing a superhydrophobic surface into a hydrophile one. Hence, plasma treatment with O_2 or air which could increase the oxygen-containing functional groups on the surface, modifying the chemistry of the surface and resulting in loss of superhydrophobicity is used as a means of testing the regeneration of superhydrophobicity [17], [16], [98], [144].

Scratch or cut test

Implementing a scratch or cut on a superhydrophobic coating could lead to loss of superhydrophobicity if the crack area would be a domain with different wettability characteristics which could compromise the consistency of the non-wettable surface. Hence the ability of the coating to recover the loss of superhydrophobicity could be of value [145], [111].

2.9 Conclusion

In this chapter, an essential literature review was provided. At first, superhydrophobicity and various wetting theories were discussed. Afterward the relation between icephobicity and superhydrophobicity was studied, followed by a description of superhydrophobicity fabrication methods. Due to the importance of the chosen material for coating fabrication, a glance at the material used for superhydrophobic coatings was provided and silicone elastomer was presented. After familiarizing with superhydrophobic coating, the applications of them were discussed. The intended application of a superhydrophobic surface is of great importance since it influences the choice of material, fabrication method, and prospective properties. Next, the challenges and drawbacks of superhydrophobic coatings were discussed and low durability was introduced as the

main challenge these coatings are facing. Various potential approaches to tackle this problem were presented, of which regenerative superhydrophobic coatings were introduced and presented thoroughly. Regenerative superhydrophobic coatings, which are coatings with the ability to regenerate the superhydrophobicity after a loss or damage to the coating, are the focus of this research. Regenerative superhydrophobic coatings were categorized based on their healing principles, and each category was fully discussed. By reading this chapter, the reader will have a clear idea of superhydrophobicity and the focus of this research. The following chapters will concentrate more on the experimental section, nevertheless, the content of the current chapter is an essential start to understanding the line of thought of the author in the following chapters.

THIRD CHAPTER
EXPERIMENTAL PROCEDURE

3.1 Introduction

Based on the literature review presented in the previous chapter, this chapter focuses on a step-by-step description of coating preparation, characterization, and assessment. Materials and methods chosen for this research will be discussed and justified based on their properties, compatibility, and the part they play in the final application and desired properties of the coating. Moreover, the devices and test methods used for coating characterization in this research are introduced.

3.2 Materials

In order to prepare a regenerative superhydrophobic coating, a silicone resin is chosen as a base matrix for the other components to be dispersed in. PDMS resin is an eminent choice for this research due to its low glass transition temperature and large free volume. This would enable storage of regenerative superhydrophobic agents which is a necessity for this research. Moreover, due to its low surface energy and good chemical and weathering resistance, PDMS is an excellent choice for dielectric and insulating properties required for a coating fabricated for an electrical insulator. Therefore, Sylgard 184 obtained from Dow Corning was chosen as the base resin for this coating. This polydimethylsiloxane elastomer is used with a proper curing agent included in the kit with a ratio of 10:1 [146].

Micro and nanoparticles are used in the coating to ensure the formation of the essential topography of superhydrophobic coatings on the surface. Hydrophobic-modified nanoparticles AEROSIL® R 202 from Evonik Co. were chosen for this research. These nanoparticles are in fact fumed silica after-treated with polydimethylsiloxane with an average primary particle size of 14 nm. This specific nanoparticle offers electrical insulating properties which would be of great benefit for this work, with a final intended application for electrical insulators. Moreover, this hydrophobic nanoparticle has good flowability, which is highly beneficial in the coating preparation step [147]. Hydrophobic silica aerogel microparticles, Aerogel Enova IC3 100, from Cabot Aerogel with a particle size range of 2-40 μm, and particle density of 120-150 Kg/m were also chosen for this research. This specific microparticle has high process stability and is known for its ease of dispersion. Also, this material is tested to preserve its hydrophobicity in temperatures as low as -196°C making it an ideal choice for a coating intended to be used in cold climates [148]. The simultaneous use of these microparticles alongside the mentioned hydrophobic nanoparticles will provide the surface topography required for achieving superhydrophobicity.

Based on the literature review presented in the previous chapter, considering the application of the regenerative superhydrophobic coatings aimed to fabricate which are electrical insulators, incorporation of both Polyhedral oligomeric silsesquioxanes and low molecular weight silicones as superhydrophobicity regenerative agents can be advantageous toward achieving the main objective of this research which is the fabrication of regenerative superhydrophobic coatings.

The integrated use of those two different methods leads to fewer challenges due to compatibility with the matrix and will be more likely to be suitable choices for the final applications of the coating. FL0578 Trifluoropropyl POSS (F-POSS) from hybrid plastics and Xiamater PMX-200 50 cSt silicone oil from Dow Corning were selected as superhydrophobicity regeneration agents. FL0578 Trifluoropropyl POSS (F-POSS) is a hybrid inorganic silsesquioxane with attached trifluoropropyl groups on the cage corners (Figure 24). This particular low surface energy trifluoropropyl POSS could be accounted for an increase in coating porosity [149].

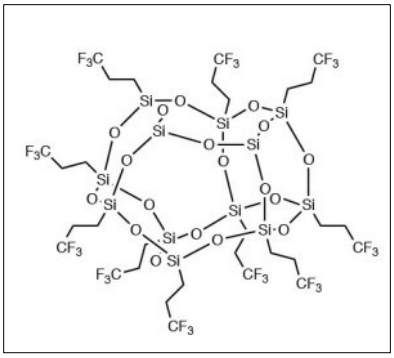

Figure 24. Molecular structure of the FL0578 Trifluoropropyl POSS (F-POSS) used in this research [149] (Reproduced with permission from Hybrid Plastics, Inc.).

Silicone oil, which is a straight-chained polydimethylsiloxane fluid, was chosen based on its electrical insulating properties, high oxidation resistance, and high compatibility with the base resin. Silicone oils with a hydrophobic nature are monomeric compounds containing silicon-oxygen bonds. The particular XIAMETER™ PMX-200 Silicone Fluid 50 cSt chosen for this research has the chemical composition of $(CH_3)_3SiO$ $[SiO(CH_3)_2]nSi(CH_3)_3$. It has a specific gravity of 0.960 at 25°C and a melting point of -41 °C. This crystal-clear silicone fluid is inherently water-repellent. Properties that make this material an excellent choice for this research [150].

All the materials used in this research and their function are summarized in Table 3.

Table 3. Materials used in this research and their function.

Material Name	**Function**	**Company**
SYLGARD™184 Silicone Elastomer	Matrix	Dow Corning
AEROSIL® R 202	Nanoparticles	Evonik Co
Aerogel Enova IC3 100	Microparticles	Cabot Aerogel
Hexane	Solvent	Fisher scientific
XIAMETER™ PMX-200 Silicone Fluid 50	Superhydrophobicity self-healing agent	Dow Corning

FL0578 Trifluoropropyl POSS	Superhydrophobicity self-healing agent	Hybrid plastics

3.3 Coating preparation

Coating preparation starts with the dispersion of nanoparticles in Hexane with the help of a Fisherbrand™ 505/705 Sonic dismembrator for 15 min. The ultrasonicator was used at an amplitude of 25 with a 5s pulse-on time and a 3s pulse-off period. A water bath was also used to prevent a temperature rise. This duration was determined after series of trial & errors to achieve the minimum duration of sonication required for achieving a homogenous dispersion of nanoparticles in the solvent.

Afterward, the microparticles, the base resin, and the curing agent were added and mixed with the help of a mechanical overhead mixer for 10 min. For the coatings containing superhydrophobicity self-healing agents, the chosen agent is also added to the mixture at this step.

The uniform mixture is then spin-coated on the substrates with the help of a K4-WA Setcas LLC spin coater with the spinning parameters of 150 rpm for 10s. Prior to the spinning, the substrates are fixed with the help of a vacuum system. The solution is then poured on the substrate, which uniformly covers the whole substrate throughout the spinning, resulting in a uniform coating formation. The samples are afterward cured in the 125°C oven for 20 min (Figure 25).

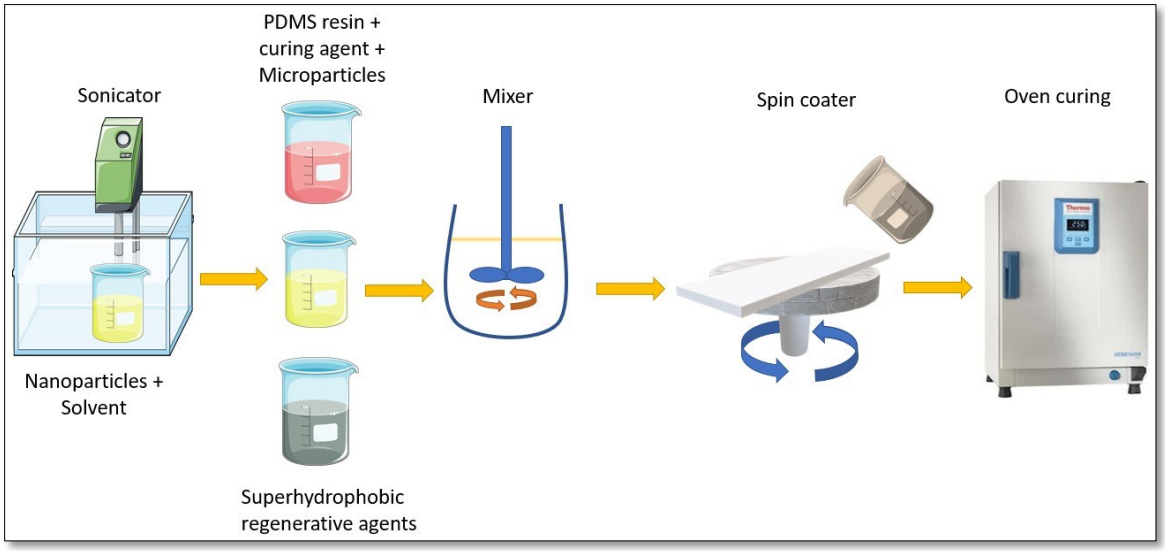

Figure 25. Schematic of the coating preparation steps in this research © Helya Khademsameni, 2023.

3.3.1 Preparation of reference samples

For fabrication of reference Sylgard coating, the polydimethylsiloxane resin was mixed with the curing agent (with a ratio of 10:1) and Hexane. In case of presence of bubbles, the composite is then vacuum filtered. Then, it was spin-coated on the substrates and cured in the 125° C oven for 20 minutes. These samples are coded as "Sylgard" throughout this research.

For fabrication of the reference superhydrophobic coating the base resin and curing agent were used with a 10:1 ratio as it is recommended by the manufactory. The mixture of micro and nanoparticles was optimized keeping in mind cost, efficiency, and performance. The final optimized ratio was found to be at a solid ratio of 25 wt.% of nanoparticles and 15 wt.% microparticles. The logic behind this optimization is described below.

Due to the cost of the chosen micro and nano particles and their probable negative effect on the mechanical properties of the coating in case of overuse, the coating optimization started with the lowest possible weight percentage of micro and nanoparticles. Table 4 demonstrates the coating formulations trial and error.

Table 4. Component ratio examination for fabrication of the reference superhydrophobic coating.

Sample	Nanoparticle (%)	Microparticle (%)
1	10	5
2	15	5
3	20	5
4	25	5
5	10	10
6	15	10
7	20	10
8	25	10
9	15	15
10	20	15
11	25	15

At other ratios other than the last one, either the coating was not formed or in the case of coating formation the coating did not present superhydrophobic properties. Therefore, the formulation of 25% nanoparticle and 15% microparticle was chosen as the formulation at which with the least possible amount of micro and nanoparticle a uniform superhydrophobic coating was

formed. At this optimized ratio, fine coatings can be spin-coated on the substrates and afterward cured in the oven (125° C oven for 20 minutes). These samples are coded as "SHP Ref" herein.

Table 5 demonstrates the component ratios of the fabricated reference Sylgard and reference superhydrophobic coating.

Table 5. Component ratio of the prepared reference coatings.

Material (%)	Sample	
	Sylgard	SHP Ref
Resin+Curing agent	100:10	60
Microparticle	0	15
Nanoparticle	0	25

3.3.2 Preparation of regenerative superhydrophobic coatings

For the fabrication of regenerative superhydrophobic coating, two steps were put in place (Figure 26). The first step is the investigation of each superhydrophobicity self-healing agent's effect on the regeneration of superhydrophobicity and the second one is coating ratio optimization.

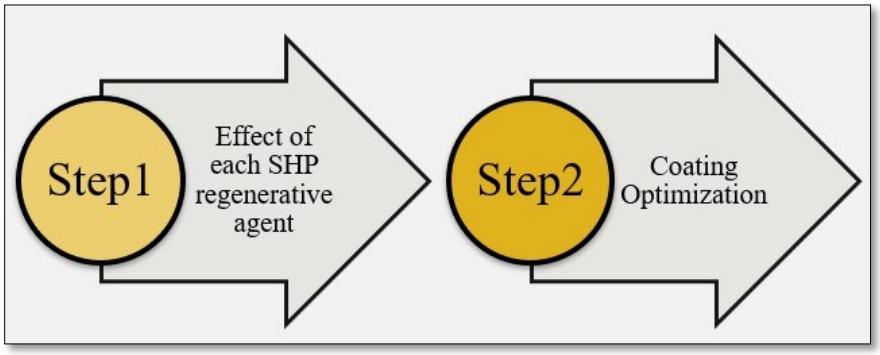

Figure 26. Coating preparation steps for fabrication of superhydrophobic regenerative coating © Helya Khademsameni, 2023.

3.3.2.1 First step: Superhydrophobicity healing agents investigation

For this step, a coating formulation similar to the "SHP Ref" samples was used and the chosen superhydrophobicity regeneration agent was added to the mixture prior to the spin coating step. Therefore, three sets of samples were fabricated, all containing base resin and curing agent with a 10:1 ratio and a solid ratio of 24 wt.% of nanoparticles and 14 wt.% microparticles.

0.8 wt.% F-POSS compared to the solid ratio of the coating mixture was added to the mixture, mixed, and then spin-coated on the substrates, creating samples coded "F Reg". Second

set of samples contained 0.8 wt.% of the solid ratio of silicon oil, coded as “SO Reg”. The last set of samples contained 0.4 wt.% of the solid ratio F-POSS and 0.4 wt.% of the solid ratio of silicone oil. These samples were coded as “FSO Reg”. On one hand, due to the relatively high price of F-POSS and silicone oil, it is preferable to use the least possible amount of these additives. On the other hand, since the aim of this study is to have a coating that can regenerate the superhydrophobicity, the more superhydrophobicity regeneration agents preserved in the coating the more beneficial it would be. Therefore, the amount of superhydrophobicity regeneration agents to be added to the coating was optimized with great care.

Moreover, during the coating formulation at this step, the focus was to have the almost same weight percent of the micro and nano particles in the coating as the “SHP Ref” so that comparison between these samples would be easier. Also considering a threshold of the base resin required for a fine coating formation, the most precise amount for the superhydrophobicity regeneration agents in the coating was optimized at 8 wt.%. For the “FSO Reg”, this amount was divided in two so that 4 wt.% of each superhydrophobicity regeneration agent was added to the coating mixture.

Table 6 illustrates the material ratio in the fabrication of the coatings in this step. Following the spin coating step, all samples are cured in the 125°C oven for 20 minutes.

Table 6. Component ratio of the prepared coatings in the first step.

Material (%)	**SHP Reg Sample**		
	F Reg	SO Reg	FSO Reg
Resin+Curing agent	54	54	54
Microparticle	14	14	14
Nanoparticle	24	24	24
F-POSS	8	0	4
Silicone Oil	0	8	4

To better investigate the effect of each superhydrophobicity regenerative agent, the three sets of samples of “F Reg”, “SO Reg” and “FSO Reg” underwent a preliminary plasma deterioration test. Each sample withstood 5s of plasma discharge (plasma conditions explained in 3.5.1 Regeneration of Superhydrophobicity), after which the “FSO Reg” samples were able to retain superhydrophobicity which will be discussed in the next chapter. Based on this experiment which is thoroughly explained in the next chapter, the samples containing both F-POSS and Silicone oil were chosen as the basis of the Regenerative superhydrophobic coating intended for this research. Now that coatings containing both F-POSS and silicone oil were chosen, an optimization is necessary in order to determine the best ratio of them in the coating to achieve the best regenerative superhydrophobic coating. The next step is allocated to this aim.

3.3.2.2 Second step: Coating optimization based on the superhydrophobicity regeneration agents ratio

Once all the coating components are chosen, a ratio optimization is necessary. In this step three sets of coatings are fabricated: all containing both superhydrophobicity healing agents however with different ratios. Also, all the samples contain base resin and curing agent with a 10:1 ratio and a solid ratio of 20 wt.% of nanoparticles and 12 wt.% microparticles.

Based on the optimization of 8 wt.% done in the previous step, the minimum threshold for one superhydrophobicity regeneration agent is determined to be at 8 wt.%. Since the focus is to have the highest similarity of micro-nano particles with the "SHP Ref" sample and assigning a high weight percentage of the coating to the base resin to ensure a fine coating formation, 10 wt.% is the highest amount of superhydrophobicity agents chosen to be added in the coating mixture. Therefore the threshold for superhydrophobicity agents in the coating mixture is increased to 10 wt.% to be able to see a 2 wt.% for the second agent as well.

Since in the previous step coatings containing 8 wt.% F-POSS and 8 wt.% Silicone oil were developed and a preliminary plasma deterioration was conducted on them which is presented in the next chapter, the optimization of the coating formulation benefits from this step in a way that 8 wt.% is chosen for the weight percentage of one of the superhydrophobicity regeneration agents, providing us to benefit from the previous steps formulation as well. Since the desired combination for the superhydrophobicity regeneration agents is chosen to be 10 wt.% it leaves us with a 2 wt.% for the second regenerative agents. Therefore three sets of samples are formulated as follows: The first set of the samples also contained 8 wt.% F-POSS and 2 wt.% Silicone oil of the solid, a 4:1 ratio. These samples were coded as "SHP Reg 4:1". The second batch contained 2 wt.% F-POSS and 8 wt.% Silicone oil were labeled as "SHP Reg 1:4". The last set of samples contained 5 wt.% F-POSS and 5 wt.% Silicone oil, labeled as "SHP Reg 1:1". Table 7 illustrates the material ratio in the fabrication of the coatings in the second step. Then, these samples were prone to plasma deterioration and their ability to regenerate the superhydrophobicity was studied, which is explained in detail in the next chapter.

Table 7. Component ratio of the prepared coatings in the second step

Material (%)	**SHP Reg Sample**		
	SHP Reg 4:1	SHP Reg 1:4	SHP Reg 1:1
Resin+Curing agent	56	56	56
Microparticle	12	12	12
Nanoparticle	22	22	22
F-POSS	8	2	5
Silicone Oil	2	8	5

3.4 Coating characterization

3.4.1 Contact angle measurement

The wetting behavior of the samples was studied with a Kruss™ DSA100 contact angle goniometer. With this instrument, both static and dynamic contact angles were measured. Sessile droplet measurements require a droplet size large enough to overcome the effect of evaporation and larger than surface features [151]. In this study, a 4µL water droplet was placed on the surface to measure the static contact angle. The test is repeated at least 5 times at different spots of the sample and an average of the results is provided.

Moreover, the sliding angle is measured with the help of an adjustable tilting plate, able to tilt even up to 90°. By tilting the plate till the droplet starts to slide off, the sliding angle will be measured.

3.4.2 Scanning electron microscopy (SEM)

Scanning electron microscopy (SEM) is used to study surface morphology and composition. In this study a JSM-6480 LV SEM, JEOL Japan scanning electron microscopy is used to compare the surface morphology and composition of samples prior to plasma deterioration, plasma deteriorated samples, and the samples with regenerated superhydrophobicity.

3.4.3 Fourier transform infrared spectroscopy (FTIR)

The chemical composition of the surface is studied with Fourier-transform infrared spectroscope, which is a vibrational spectroscopy, to review the formation of chemical bonds and components of the coating. The FT-IR analysis for this research is carried out using Cary 360 FT-IR spectrophotometer (Agilent, USA) in ATR (Attenuated Total Reflection) mode. ATR is a common method for investigating coatings in which an IR beam is directed into a crystal of a relatively higher refractive index. The beam reflects from the crystal and creates an evanescent wave which projects onto the sample. Some of the wave energy is absorbed by the sample and the reflected radiation is gathered by the detector. The usual depth of penetration of ATR FT-IR is from 0.5 microns up to about 5 microns depending upon the experimental conditions [152]. Another use of the FT-IR test is to show the homogeneity of the surface, which could be demonstrated by comparing various FT-IR test results from different points of the same sample [153].

3.4.4 X-ray photoelectron spectroscopy (XPS)

The surface chemical composition of the coating, prior to plasma treatment, after plasma treatment, and the regenerated superhydrophobic coating can be reviewed with the help of X-ray photoelectron spectroscopy. An X-ray photoelectron spectrometer jointly produced by Plasmionique (Canada) and Staib Instruments (Germany), equipped with a non-monochromatic Al

(max energy 1486.6 eV) source was used. XPS is known for its precision, compared to FT-IR, and is a study of projected X-rays on the surface. In this test, a photoelectron spectrum with its peaks is recorded which can be correlated to characteristic energies and identify the surface elements. The penetration range of XPS is from 1-10 nm, however, the precision of the analysis depth is a variable of the anode type and material, sample conductivity, etc [154]. The parameters used for survey acquisition and high-resolution acquisition are presented in Table 8.

Table 8. Survey and high-resolution acquisition parameters for XPS spectra.

	Starting Energy	**Ending Energy**	**Step width**	**dE**	**Dwell time**	**Beam power**
Survey	0 eV (Al anode)	1300 eV	1 eV	4 eV	100 ms	150 Watts
High-resolution	A small range covering the observed peak		0.1 eV	0.3 eV	300 ms	300 Watts

In order to analyze the XPS data, CasaXPS software was used. With the help of this software, spectrum calibration, peak identification, elemental and component quantification, and several other functions can be deployed on the acquired data. For the quantification of elemental peaks in the high-resolution deconvolution section, the Shirley background type was used.

3.4.5 Profilometry

To review the surface topography of the coatings, profilometry is used. With 3D Profilometer: Profilm3D® various topographic data such as roughness average, average maximum height, maximum height of the surface, and depth of valley is reported.

3.5 Durability

3.5.1 Regeneration of Superhydrophobicity

Various tests can be applied to verify the superhydrophobicity regeneration ability of the prepared coating. In one approach, the prepared coatings are treated by air plasma to the point of loss of superhydrophobicity. In this research Plasma Jet AS400" (Plasmatreat GmbH, Germany) atmospheric-pressure plasma system with a reference voltage of 70%, plasma voltage of 250 V, plasma current of 16 A (Power of 2.8 kW), distance of 30 mm from the plasma nozzle to the sample surface, and speed of 2m/min was used. After the deterioration by plasma, the samples were kept in various conditions so their superhydrophobicity regeneration progress is observed. At each step, the water contact angle is measured to verify the superhydrophobicity regeneration.

Another test to verify the self-healing superhydrophobic coating is immersion in acid or bases which could lead to loss of superhydrophobicity, in that case, the ability of superhydrophobicity regeneration can be at stake.

3.5.2 Superhydrophobicity regeneration assessment

The assessment of superhydrophobicity regeneration can be proceeded by characterization assessments of the coating or can be demonstrated by repeating the superhydrophobicity regeneration for several cycles. The key method used for proof of regained superhydrophobicity is the water contact angle measurement which shows the contact angle of the water droplet and the surface at each step: pristine coating, the coating which has lost its superhydrophobicity and the coating which regained its superhydrophobicity. Other superhydrophobicity regeneration characterization assessments could be done by observation of the composition and structure of the healed superhydrophobic coating and a comparison of it to the pristine samples with the help of FT-IR, SEM, XPS, and profilometry assessments.

3.6 Icephobicity evaluation

3.6.1 Push-off test

The final regenerative superhydrophobic developed samples, superhydrophobic reference samples "SHP Ref", and PDMS reference samples, "Sylgard" were put in a cold room at -15°C for 5 hours. After reaching the cold room temperature, a cylindrical mold is placed on each coating and is filled with deionized water. The samples are left in the cold room for ice formation for 24 hr. With the help of an ice push-off set-up, the cylinder is pushed off the surface and the force used for this movement is noted. The maximum force recorded divided by the area of the ice cylinder in touch with the substrate would determine the ice adhesion strength (Figure 27Figure 27. Push-off test apparatus) [155].

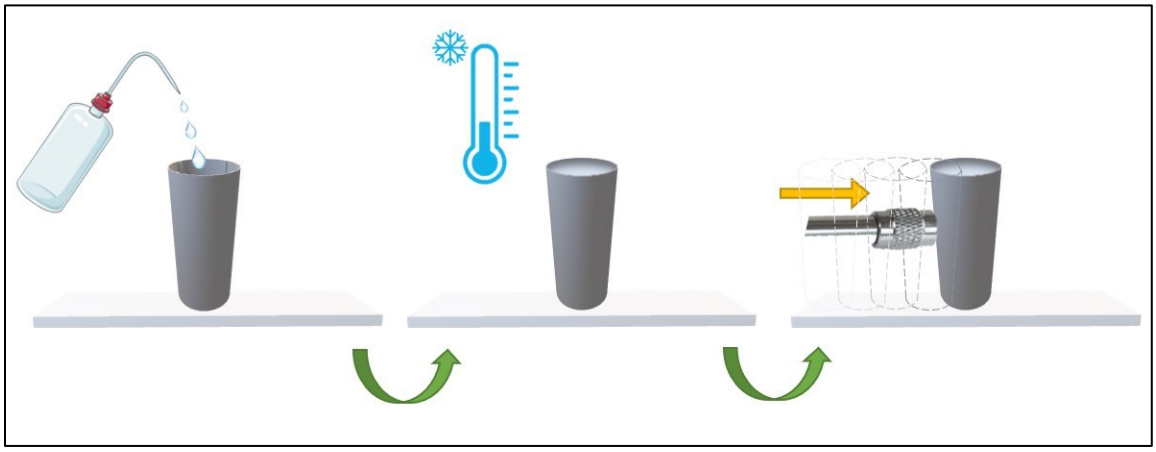

Figure 27. Push-off test apparatus schematics © Helya Khademsameni, 2023.

3.6.2 Centrifuge Adhesion Test

Ice adhesion on the surface can be determined with Centrifuge Adhesion Test (CAT). Firstly, samples are iced in a cold chamber usually with the help of glaze ice. Another approach

could be the use of a wind tunnel that stimulates various atmospheric icing by a variety of parameters such as temperature, humidity, or wind velocity on some samples. This method would demonstrate a better evaluation of coating performance in natural winter conditions. After ice formation via either one of the methods mentioned, the samples are tested via a centrifugal instrument. The applied force is measured and divided by the icing area leading to a determination of ice adhesion.

In order to measure the ice adhesion via centrifuge adhesion test, three sets of coating on 2.5 cm × 3.5 cm Aluminum substrates were prepared: 1) The final regenerative superhydrophobic developed samples, 2) superhydrophobic reference samples "SHP Ref", and 3) PDMS reference samples "Sylgard". All the samples were sprayed with supercooled water microdroplets, stimulating freezing drizzle conditions, which lead to a layer of 5.9 ± 0.02 g ice covering the samples. This step was performed in a climatic chamber with a temperature down to -8°C. 1 hour later, the samples were moved to a cold room with a temperature of -10°C ± 0.2°C containing a centrifugal instrument. Each sample was put on the end of a beam and was rotated at a controlled frequency. The force applied at the breaking point of each sample was recorded. This centrifuge force (F) is calculated as:

$$F = mr\omega^2 \qquad \textit{Equation 6}$$

Where m is the mass of detached ice, r is the beam radius and ω is the speed at the time of ice detachment.

By dividing this force by the icing area, the adhesion stress is then calculated. The adhesion reduction factor (ARF) is defined as the following:

$$ARF = \frac{\tau_{\text{Pristine}}}{\tau_{\text{Coating}}} \qquad \textit{Equation 7}$$

Where τ_{Pristine} is the shear stress of ice removal on the pristine sample or the aluminum reference sample, and τ_{Coating} is the shear stress of ice detachment on the coating sample. In order to review the effect of regeneration on the developed samples, this test was repeated once more. For each sample, the two test results will be discussed in the next chapter. These tests were done at Anti-icing Materials International Laboratory (AMIL).

3.7 Conclusions

Based on the regenerative superhydrophobic coating principles mentioned in the previous chapter, the incorporation of low molecular weight silicone and polyhedral oligomeric silsesquioxanes as regenerative superhydrophobicity components in a PDMS-based coatings containing micro, and nanoparticles was the strategy chosen for this research. Based on this approach, the experimental chapter focused on finding the most optimized coating preparation steps which would result in the best possible superhydrophobicity regeneration properties. The current chapter discussed the coating material, fabrication, and characterization methods used for this

research. The next chapter which is highly coordinated with the current chapter focuses on the results of coating evaluation, characterization, and durability test results.

FOURTH CHAPTER
RESULTS AND DISCUSSION

4.1 Introduction

This research aimed to fabricate silicone-based regenerative superhydrophobic coatings and study their durability and consequently their potential applications in electrical insulators. A superhydrophobic coating containing hydrophobic aerogel microparticles and polydimethylsiloxane-modified silica nanoparticles within a PDMS-based matrix containing Trifluoropropyl POSS (F-POSS) and Xiamater PMX-series silicone oil as superhydrophobicity regenerating agents were fabricated by spin-coating method. The fabricated coating showed a contact angle of 169.5° and a contact angle hysteresis of 6°. Compared to reference samples, regenerative testing showed that the coating was able to regain its superhydrophobicity after various pH immersion and plasma deterioration tests. The performance of the developed coating as icephobic material was also studied by various ice adhesion measurement tests is also observed. The experimental process and the overall rationale of this research were explained in the previous chapter. In this chapter, the samples developed in the previous chapter are characterized and evaluated. Afterward, each test result is demonstrated and thoroughly discussed. Characterization and test assessment are the main focus of this chapter. Based on the test results and observation, the conclusion of this research is then provided.

4.2 Wettability assessment

The fabricated "Sylgard" reference samples showed a CA of 110.3°±1.5, SA of >30°, and CAH of 12°±0.5. The CA, SA, and CAH for the "SHP Ref" samples were 162.2°±0.8, 3° and 5°±0.1 respectively.

4.2.1 Evaluation of the effect of each superhydrophobicity self-healing agent's incorporation

In order to develop a regenerative superhydrophobic coating, self-healing superhydrophobic agents are to be added to the coating mixture. To see the effect of each self-healing agent individually and obtain the best ratio, a series of experiments were conducted. The main goal was the addition of either F-POSS or silicone oil or the simultaneous addition of both. To ensure the achievement of the best possible results, with the same formulation (PDMS resin containing hydrophobic Aerogel microparticles and fumed silica nanoparticles), three sets of samples were fabricated: One containing only F-POSS as regenerative superhydrophobic agent "F Reg", one with only silicone oil "SO Reg" and the last set containing both F-POSS and silicone oil, "FSO Reg".

Table 9 provides the CA, CAH, and SA of all the prepared coatings (regenerative and non-regenerative). For the developed superhydrophobic coatings, the combination of surface topography and low surface energy material on the surface has led to a Cassie-Baxter state explaining the superhydrophobic behavior [156]. However, it is observed that the samples

containing only silicone oil as a superhydrophobic self-healing agent ("SO Reg") demonstrate not efficient CAH and SA angles required for superhydrophobic properties. This could be due to surface roughness covered by oil, to a sense that the same micro-nano roughness as other developed coatings was not achieved in this coating. This finding demonstrated that during the coating design, it has to be kept in mind that if the aim is to have a regenerative superhydrophobic coating with the same amount of silicone oil in the coating in comparison to the sample containing F-POSS, more micro/nanoparticles must be implemented in the coating mixture to acquire a low CAH. Since the addition of micro/nanoparticles could affect the mechanical properties and price, this action is in general not preferred.

Table 9. CA, CAH, and SA of water droplet on the developed coatings.

Sample code	CA (°)	CAH (°)	SA (°)
Sylgard	110.3±1.5	12±0.5	>30
SHP Ref	162.2±0.8	5±0.1	3
F Reg	169.3±0.6	2±0.3	6
FSO Reg	167±0.9	6±0.6	3
SO Reg	159.6±1.2	55±1.2	40

In the next step, to establish the most effective coating mixture, the self-recovery ability of the fabricated coatings was tested. Hence, to distinguish the best sample with regenerative superhydrophobicity properties an initial plasma deterioration as described in the previous chapter (3.3.2.1) was implemented on the developed coatings which are candidates for superhydrophobicity regeneration: a) "F Reg", b) "SO Reg", and c) "FSO Reg". The point of treatment on each sample was prone upon 30s of plasma deterioration.

As shown in Table 10, all three sets of samples endured a loss of CA after plasma deterioration. However, after being kept at room temperature for 24 hr, the water contact angle for samples "F Reg" and "FSO Reg" increased back to higher than 150°, which was not the case for the "SO Reg" samples. The highest increase in CA after plasma deterioration was for samples containing both F-POSS and silicone oil as superhydrophobicity regeneration agents which were able to have a CA almost as high as the original before plasma deterioration. Therefore, the "FSO Reg" samples appear to be better candidates for this research, due to high water contact angle retention after 24 hr at room temperature after a loss of superhydrophobicity due to plasma deterioration. This result is coherent with the literature review presented in the second chapter. The presence of oil in the coating is proven to be beneficial toward a self-healing process of coatings [157-159], and fluorine-containing particles such as F-POSS or FAS have improved the superhydrophobicity regeneration ability of coatings as well [83], [137]. The "FSO Reg" samples are benefiting from the mutual presence of F-POSS and silicone oil in the coating, which would justify the results obtained at this step. The point of focus from now on would be to find the best ratio of the superhydrophobicity regeneration components to optimize the developed coating in order to achieve the best possible superhydrophobicity regeneration results.

Table 10. CA, CAH, SA of water droplets on developed coatings prior to any treatment, after air plasma deterioration, and after being kept 24hr in room temperature.

Sample	Initial CA (°)	CA (°) after plasma	CAH (°) after plasma	SA (°) after plasma	CA (°) after 24 hr at RT	CAH (°) after 24 hr at RT	SA (°) after 24 hr at RT
Sylgard	110.3±1.5	95.2±0.7	62±1.5	>80	96.5±0.8	58±2.1	>80
SHP Ref	162.2±0.8	140.2±1.2	43±2.6	>80	141.7±0.7	38±0.8	78±2.1
F Reg	169.3±1.4	141.7±0.6	28±1.1	57±2.3	151.2±1.3	22±0.7	48±1.9
FSO Reg	167±0.9	147±0.8	31±0.9	50±1.3	162.7±0.6	25±0.9	36±1.2
SO Reg	159.6±0.2	139.2±0.9	39±1.8	>80	140±0.4	64±1.7	69±2.3

4.2.2 Evaluation of the superhydrophobicity self-healing agent's incorporation ratio

Knowing the samples containing both F-POSS and silicone oil are the best candidates for this research (due to findings of the experiments presented in Table 10), in order to achieve the best coating formulation for a regenerative superhydrophobic surface, the most suitable ratio of F-POSS and silicone oil in the coating mixture has to be determined.

Therefore, three sets of superhydrophobic samples all containing both F-POSS and silicone oil were prepared: the first one with a higher amount of F-POSS compared to silicone oil ("SHP Reg 4:1"), the second one with a higher ratio of silicone oil to F-POSS ("SHP Reg 1:4".) and the third one with equal amount of silicone oil and F-POSS ("SHP Reg 1:1") were prepared. The samples were treated by air plasma to verify the self-healing superhydrophobicity ability and the results are presented in Table 11.

All three sets of samples faced an almost equal loss of CA after plasma deterioration. However, after being kept at room temperature for 24 hr, the only set of samples that were able to regenerate superhydrophobicity and regain a CA higher than 150° were the "SHP Reg 4:1" samples. For the samples "SHP Reg 1:4" it could be interpreted that the higher ratio of silicone oil than F-POSS could lead to entrapment of F-POSS into the silicone oil, prohibiting the F-POSS to lower the surface energy, therefore showing less favorable results in the means of superhydrophobicity regeneration. The point of treatment on each sample was prone upon 45s of plasma deterioration.

Table 11. CA, CAH, and SA of water droplets on superhydrophobic coatings containing both silicone oil and F-POSS as superhydrophobic regenerative agents with various ratios, prior to any treatment, after air plasma deterioration, and after being kept for 24 hr at room temperature.

Sample	Initial CA (°)	Initial CAH (°)	Initial SA (°)	CA (°) after plasma	CAH (°) after plasma	SA (°) after plasma	CA (°) after 24 hr at RT	CAH (°) after 24 hr at RT	SA (°) after 24 hr at RT
SHP Reg 1:4	166.9 ±0.8	9±0.4	2±0.1	133.1 ±0.7	56±0.7	56±0.9	145.2 ±0.6	39 ±0.8	30±0.4
SHP Reg 1:1	168 ±1.4	3±0.1	3±0.1	135.4 ±1.6	59±0.8	54±1.1	148.1 ±1.1	39 ±1.2	42±0.9
SHP Reg 4:1	169.5 ±0.6	6±0.7	4±0.2	135.3 ±0.4	60±1.4	40±0.7	168.2 ±0.9	21 ±0.3	20±0.2

To conclude, based on the experiments conducted in this step, superhydrophobic coatings containing both F-POSS and silicone oil, with a higher ratio of F-POSS to silicone oil are developed and optimized in this research. These samples are coded as "SHP Reg" herein.

4.2.3 Wettability assessment of the final developed coating

The thickness of the semi-transparent "SHP Reg" coating was measured with ElektroPhysik 80-125-0900 MiniTest 70E-FN Coating Thickness Gauge and was reported to be around 100-150 micrometers. The developed coating can be applied on various substrates such as glass, aluminum, and fabric.

As shown in (Figure 28), the developed "SHP Reg" coating was applied on the fabric (Figure 28, a), while on the other side (Figure 28, b), the fabric is intact. Colored water droplets were deposited on both sides of the fabric, and as can be seen in the figure, on the side without any coating the droplets got absorbed within the fabric. On the coated side of the fabric, the fabric has a superhydrophobic layer on top leading to a high-water contact angle, prohibiting the water droplets to penetrate the fabric.

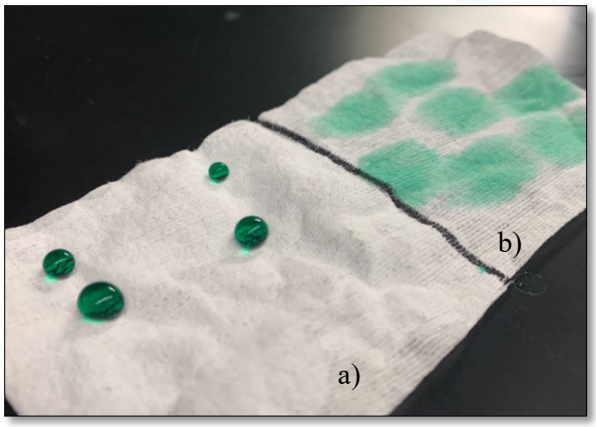

Figure 28. a) Demonstration of the developed superhydrophobic coating applied on fabric b) pristine fabric without any coating © Helya Khademsameni, 2023.

The water-repellent nature of the developed regenerative superhydrophobic coating is shown in (Figure 29). The developed coating was spin-coated on a filter paper, showing superhydrophobic characteristics. Once the paper is pushed into the colored water, it effortlessly floats to the surface.

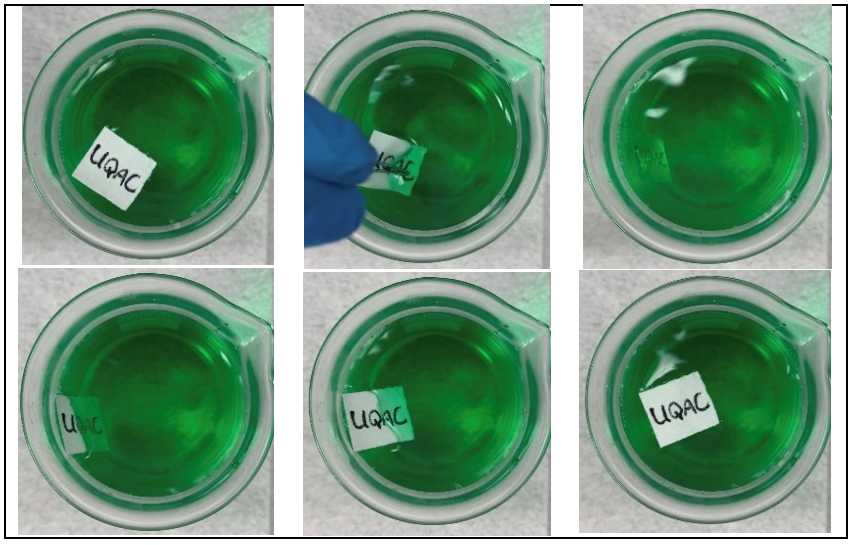

Figure 29. The water-repellency of the developed superhydrophobic regenerative coating resulting in floatation on water surface © Helya Khademsameni, 2023.

Superhydrophobic coatings can benefit from their self-cleaning property in some applications. Self-cleaning which can be seen in lotus plants in nature, is defined as a property in which the slide of water droplets off the surface is along with moving the dirt particles and resulting in a clean surface [160], [161].

To demonstrate the self-cleaning behavior of the fabricated coating, samples on filter paper (Figure 30) and glass slides (Figure 31) were chosen. With the help of carbon black particles, simulating pollution on the surface, the self-healing ability of the coating was investigated. Water

droplets easily remove the dirt from the superhydrophobic coating, resulting in a clear surface (Figure 30).

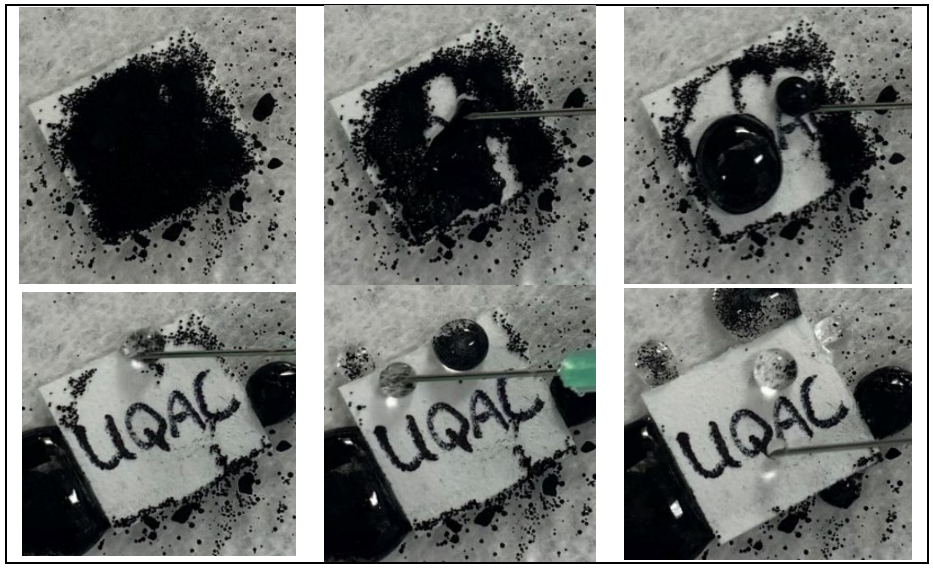

Figure 30. Self-cleaning evaluation of the developed superhydrophobic regenerative coating. © Helya Khademsameni, 2023

To better illustrate, the letters UQAC were covered prior to the coating application on the slide (Figure 31). The covers were taken off afterward, and therefore the UQAC word was not covered with any coating. The other parts of the glass slide surrounding the UQAC letters were coated with the developed "SHP Reg" coating mixture, showing superhydrophobic properties. Carbon black was sprinkled on all parts of the slide and was attempted to be rolled off the surface with the help of water droplets. Interestingly, the water droplets on the pristine area (UQAC letters) were stuck to the surface, meaning a higher adhesion between the water droplet and the contaminated area compared to the water droplet on the superhydrophobic areas which were easily rolled off the surface.

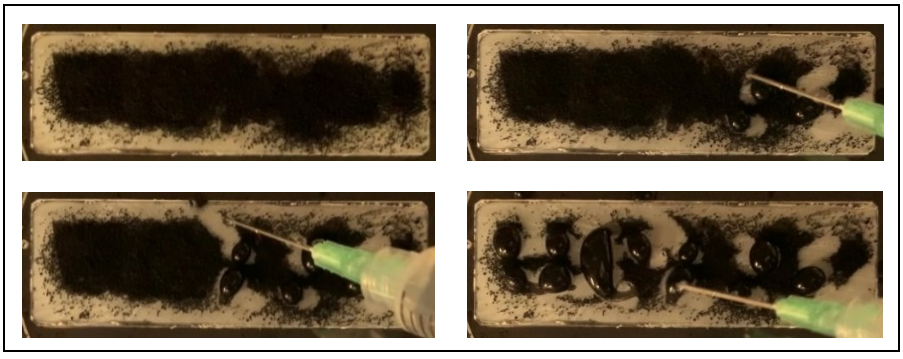

Figure 31. Contamination stuck to the pristine areas, in comparison with superhydrophobic areas which is washed off with water droplets © Helya Khademsameni, 2023.

4.3 Self-healing Superhydrophobicity Characterization

To demonstrate the durability of the developed regenerative superhydrophobic coating, three sets of samples a) "Sylgard", b) "SHP Ref", and c) "SHP Reg" on glass substrates were immersed in solutions with pH as low as 2 and as high as 10 (Table 12). At any time that one of the samples losses its superhydrophobicity, the time is noted and the WCA on all the samples is reported at that time.

In the first 2 hours of the test, the changes in the water contact angle of the coatings were examined every 15 minutes. After 2 hours, the first sample ("SHP ref" in pH=10) lost its superhydrophobicity, therefore the CA on all the samples was recorded at this time as well. After the first two hours of the test, the changes in the water contact angle of the samples where observed every hour to determine the point where the "SHP Reg" samples would lose their superhydrophobicity as well. Finally after 12 hr since the start of the experiment, all samples including the "SHP Reg" ones lost their superhydrophobicity, showing CA of less than 150°.

Nevertheless, the developed "SHP Reg" regained its superhydrophobicity after 12 hr at ambient temperature which was not the case for the "SHP Ref" samples. The loss of superhydrophobicity can be mainly due to an increase in the surface energy of the sample. During storage at ambient temperature, the superhydrophobic regeneration agents start to migrate to the surface, lowering the surface energy which results in superhydrophobicity regeneration. After 12 hr at room temperature, a minor increase in the water contact angle on the "Sylgard" and "SHP Ref" samples can be seen as well, which could be due to the hydrophobic recovery property of PDMS-based coatings [59].

Table 12. Effect of immersion in solutions with various pH on the developed coatings.

Sample	pH	Initial CA (°)	CA (°) after 2 hr immersion	CA (°) after 12 hr immersion	CA (°) after 12 hr in RT
Sylgard	10	110.3±1.5	105.7±0.8	97.8±0.7	104.5±0.4
	2	110.3±1.5	108.2±0.6	100.3±1.9	107.3±0.7
SHP Ref	10	162.2±0.8	147±1.4	140.1±2.1	147.9±0.6
	2	162.2±0.8	151±1.2	142.8±0.8	148±1.4
SHP Reg	10	169.5±0.6	159±0.6	143.3±1.7	165.9±0.6
	2	169.5±0.6	163±0.4	148.5±0.4	166.4±1.4

In order to further attest to the regeneration of superhydrophobicity, the developed "SHP Reg" samples were treated with air plasma for 8 min. Figure 32 clearly shows the changes in the water contact angle on the deteriorated coating by plasma. The air plasma could produce hydrophilic oxygen-containing groups on the surface [162], [163]. The surface becomes hydrophilic, and the contact angle drops significantly. The transformation from superhydrophobic to hydrophilic surface suggests a chemical modification on the surface by chemical interaction with

oxygen and nitrogen radicals and ions along with the presence of polar groups [164] and/or a modification in surface roughness. However, after being heated to 140°C for 5 min or being kept at the ambient temperature for 12h, the samples become superhydrophobic again.

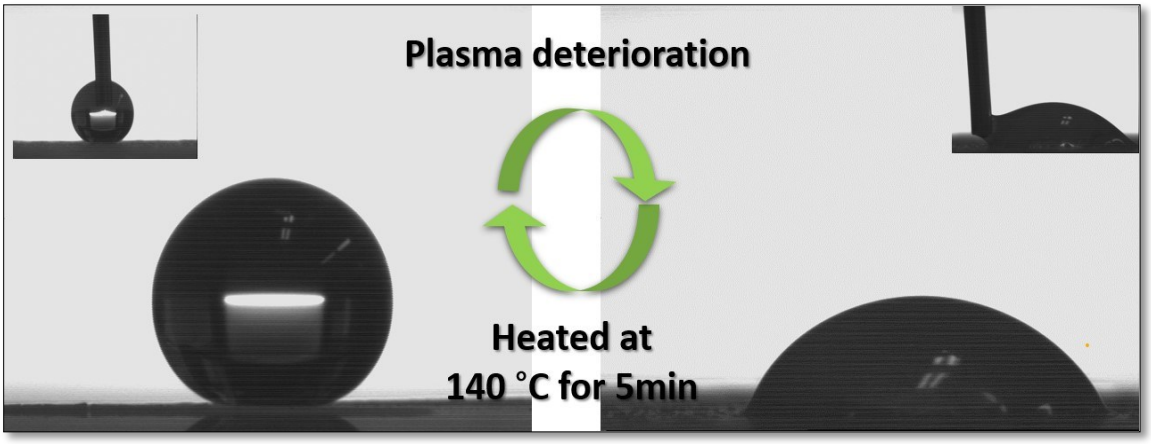

Figure 32. Loss of superhydrophobicity after plasma deterioration and superhydrophobicity regeneration for the developed superhydrophobic regenerative sample © Helya Khademsameni, 2023.

As for the CAH and SA, since these parameters are highly dependent on the surface hierarchical topography, the effect of plasma deterioration on them is more severe. After plasma deterioration, the CAH and SA for the developed coatings could increase up to 34°±2.6° and >30°, respectively, which after 12 h at room temperature or being kept in the oven for 5 min at could drop to 13°±3.2° and >20°. Many studies in the field tend to only report the CA values after imposing the samples to plasma [165], [91], [166]. However, smart coatings which focus on the regeneration of surface topography with the help of smart polymers such as shape memory polymers are able to reach desirable values of CAH and SA. These coatings mostly have difficult or complicated fabrication methods and conditions which can be counted as their drawback. Focus on the full regeneration of the surface chemical and physical properties which can be seen in nature, is where the focus in this field is headed towards.

The self-healing property of the developed coatings was further assessed by repeating the plasma deterioration and healing for several cycles (Figure 33). For a better comparison, both "SHP Ref" and "SHP Reg" samples were deteriorated by plasma for at least 6 cycles. After each plasma deterioration, the CA for both samples dropped. After the first round of plasma deterioration, during the healing phase the CA of the "SHP Ref" only increased to 120°, incapable of regaining the surface superhydrophobicity. It was only the "SHP Reg" sample that was able to recover its superhydrophobicity and demonstrate a CA higher than 150° again after each plasma deterioration.

As shown in Figure 33, the developed "SHP Reg" coating was able to regain its superhydrophobicity for several cycles. After almost six cycles, the coating still showed a CA of 154°. This superhydrophobicity self-healing process of the developed coating can be attributed to the upward movement of the silicone oil and F-POSS in the coating.

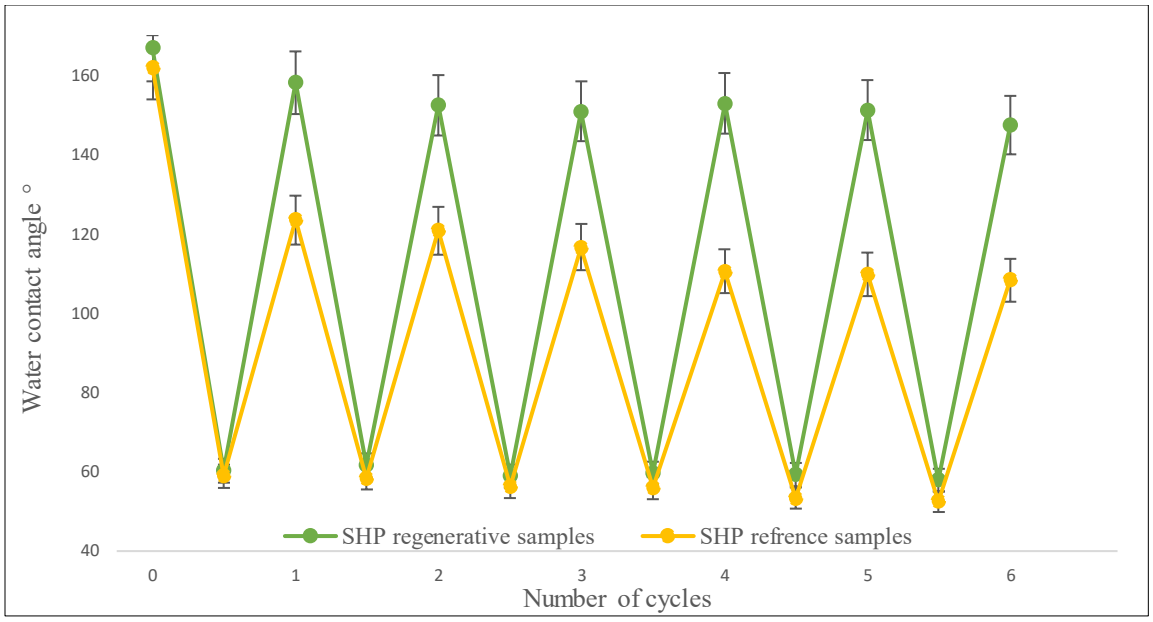

Figure 33. Wettability changes of superhydrophobic self-heal samples and superhydrophobic reference samples after air plasma deterioration and the following self-healing process © Helya Khademsameni, 2023.

Surface morphology is one of the most important factors in a superhydrophobic coating formation [19]. Therefore, to assess the damage that plasma deterioration has brought upon the surface, a surface profilometry of the "SHP Reg" coating a) prior to any damage b) after plasma deterioration with a loss of superhydrophobicity and c) after regeneration of superhydrophobicity by being kept in room temperature for 12h is presented (Figure 34). The roughness values from this analysis are presented in (Table 13).

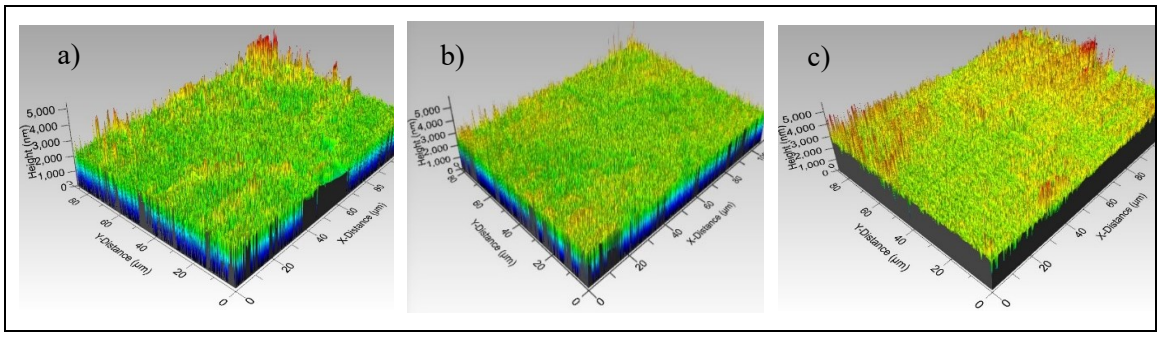

Figure 34. 3D surface profiles in tilted view of the SHP Reg sample a) prior to any damage b) after plasma deterioration which has led to loss of superhydrophobicity c) after regeneration of superhydrophobicity © Helya Khademsameni, 2023.

It is worth mentioning that root mean square (RMS) roughness signifies the standard deviation of the distribution of surface roughness height. The pristine "SHP Reg" coating presents a root mean square (RMS) and arithmetic average (Sa) roughness value of 306.8 nm and 175 nm respectively. This hierarchical structure was not severely affected by the plasma deterioration, since in the plasma-treated sample the RMS and Sa only dropped to 225 nm and 150.3 nm respectively.

The hierarchical micro-nanostructures are helpful in the entrapment of air pockets and leading to the air layer trapped underneath the water droplet leading to the formation of

superhydrophobicity. By the comparison of the 3D profilometry of the superhydrophobic coating and the plasma deteriorated one it can be concluded that the loss of the hierarchical roughness is negligible. Since hierarchical roughness is a requirement for having a superhydrophobic coating, due to this negligible loss after plasma deterioration, the achievability of the superhydrophobicity regeneration in the developed superhydrophobic regenerative coating can be justified.

Skewness (S_{sk}) represents the asymmetry of the distribution of the surface height relative to the mean. Surfaces with a $S_{sk}>0$ are dominated by peaks and surfaces with a $S_{sk}<0$ are dominated by pits or valleys. $S_{sk}=0$ is a height distribution that is symmetrical around the mean plane [167]. S_z shows the maximum height which is the accumulation of the largest peak height value and largest pit depth value [168]. The negative values for the S_{sk} show a domination of the valleys for the samples.

Table 13. Roughness values of the pristine superhydrophobic and plasma treated coating.

Roughness parameter (nm)	**SHP Reg**	**SHP REG PLASMA DETERIORATED**	**PLASMA DETERIORATED SHP REG AFTER 12 HR IN RT**
RMS (s_q)	306.8	225	272.2
Mean roughness (s_a)	175	150.3	155.9
Maximum peak height (s_p)	3110	2241	2532
Maximum pit height (s_v)	2270	2290	2285
Skewness (Ssk)	-0.3594	-0.03001	-0.2708
Maximum height (Sz)	5.86	4.53	5.38

In order to examine the self-healing superhydrophobicity mechanism of the developed superhydrophobic regenerative coatings, various characterization techniques were applied. To further investigate the surface morphology of the samples, a scanning electron microscope (SEM) was used. The developed "SHP Reg" coating was observed with SEM in three stages a) prior to plasma deterioration, b) after plasma deterioration leading to loss of superhydrophobicity, and c) after superhydrophobicity regeneration (Figure 35). The images show a similar structure on the coating surface with no obvious change in comparison to before and after superhydrophobicity regeneration. There is no trace of a huge aggregation of the coating on the samples, which could be accounted for the favorable wetting of the added particles in the base resin.

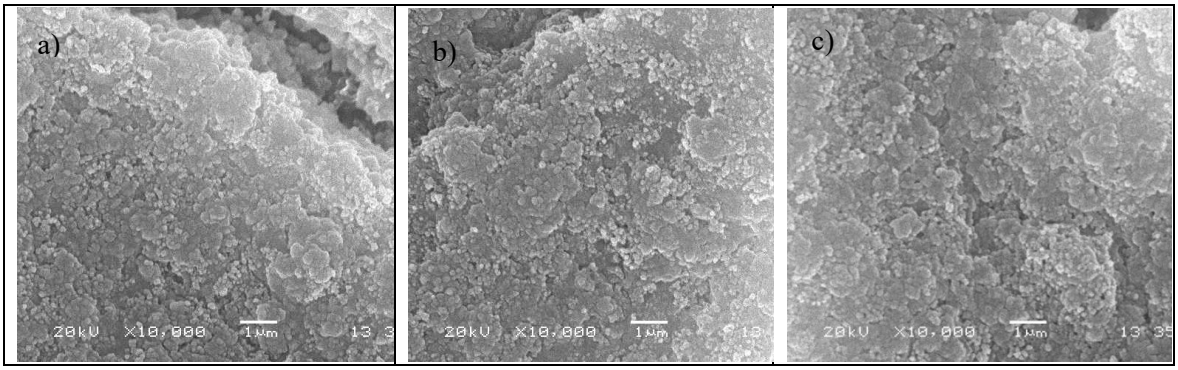

Figure 35. SEM images at magnification of 10kX of a) Pristine "SHP Reg" b) Plasma deteriorated sample with a loss of superhydrophobicity c) after regeneration of superhydrophobicity © Helya Khademsameni, 2023.

The FTIR spectra study for the "SHP Reg" sample a) prior to any damage, b) after plasma deterioration leading to a loss of superhydrophobicity, and c) after superhydrophobicity regeneration is presented below (Figure 36). Peaks at 1259 cm^{-1}, and 795 cm^{-1} represent $Si-CH_3$ and Si-C bonds in the coating and the peak around 2950 cm^{-1} is of asymmetric CH_3 stretching in $Si-CH_3$ [169]. The CH_3 peak is evident in the developed sample prior to any plasma deterioration. However, for the sample deteriorated by plasma, this peak rarely exists. As evident in the figure, the peak can be observed once again in the sample with regenerated superhydrophobicity. This could suggest that the surface chemistry of the samples is prone to changes during plasma deterioration.

By comparing the spectra of the pristine superhydrophobic sample and the regenerated superhydrophobic sample, no significant difference was detected. Presence of negligible difference between the sample prior to plasma and after superhydrophobicity regeneration could indicate that the sample has been able to regain its primitive surface chemistry. Nevertheless, more precise investigation is required to perceive a clear view of the changes the developed coating withstands. Therefore the samples are investigated by X-ray photoelectron spectroscopy as well.

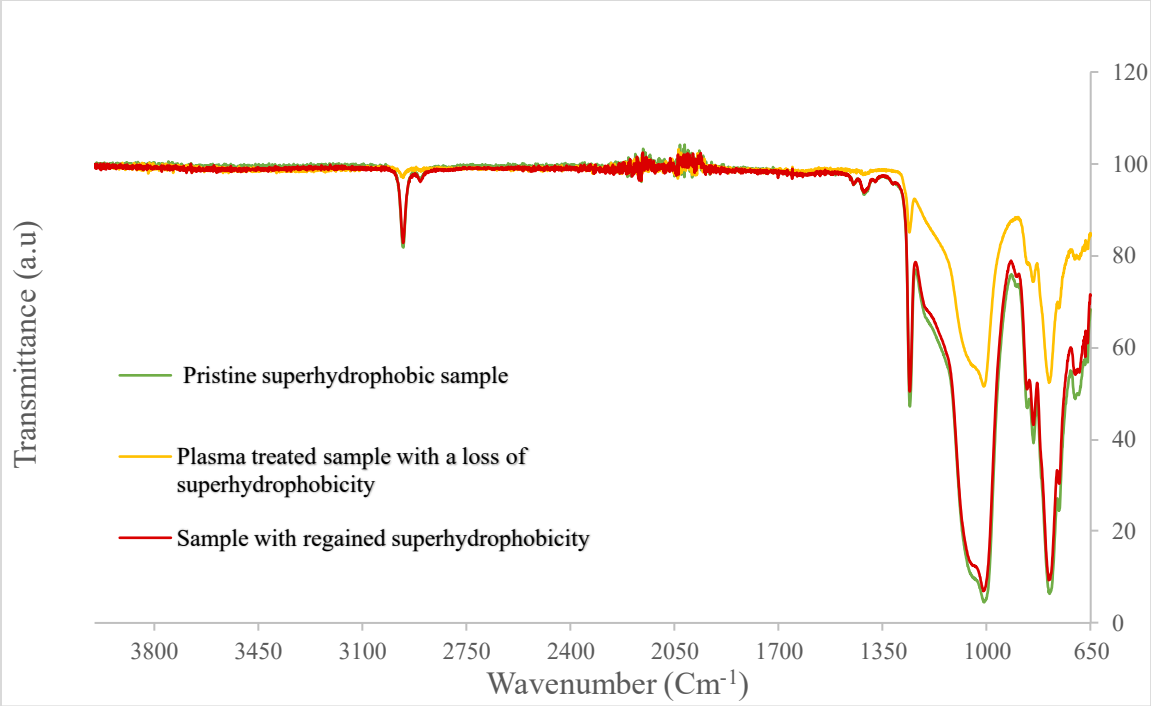

Figure 36. FTIR spectra of the "SHP Reg" prior to any damage, after plasma deterioration leading to a loss of superhydrophobicity, and after superhydrophobicity regeneration © Helya Khademsameni, 2023.

To have more clear understanding of the superhydrophobicity self-healing mechanism governing the coating surface of the developed coating, the coatings were analyzed by XPS. All the binding energy values were calibrated using the reference peak of C1s at 284.8 eV. Figure 37 shows the survey XPS spectrum of the samples "Sylgard", "SHP ref", "SHP Reg" prior to any deterioration, "SHP Reg" after plasma deterioration and "SHP Reg" after superhydrophobicity regeneration. The X-ray photoelectron spectroscopy demonstrates the elemental composition of the coating surfaces. As shown in Figure 37, the "SHP Reg" sample has withstood the increase of O 1s signal for the "SHP Reg" sample after plasma deterioration. Upon plasma treatment, the generation of hydroxyl, groups on the coating surface could cause the changes in O 1s signals [170]. The signal drops in the "SHP Reg" coating after superhydrophobicity regeneration which shows that due to the rearrangement of the coating components the hydroxyl groups get covered [171] and formation of other carbon–oxygen polar groups.

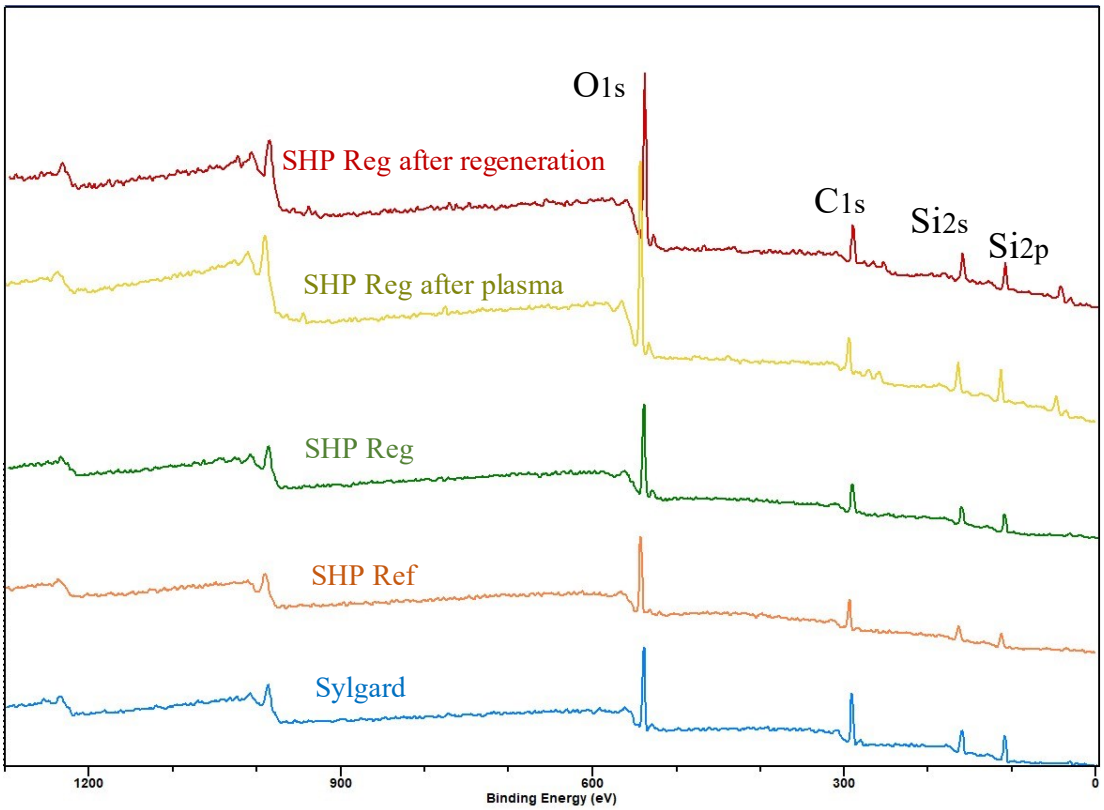

Figure 37. XPS spectra of the samples Sylgard, SHP Ref, SHP Reg prior to any damage, SHP Reg after plasma deterioration, and SHP Reg after superhydrophobicity regeneration © Helya Khademsameni, 2023.

Table 14 provides the elemental composition provided by the XPS for each sample. After plasma deterioration the "SHP Reg" sample turn hydrophilic, which could be attributed to the presence of hydrophilic polar oxygen-containing groups on the surface after air plasma. Afterward, due to the difference in surface energy after plasma deterioration, hydrophobic C-H chains in the matrix migrate to the surface [172]. Generation of hydroxyl groups on the SHP Reg after plasma deterioration causes changes in the C 1s and O 1s.

Table 14. Elemental composition (% atomic) by XPS analysis of the samples Sylgard, "SHP Ref", "SHP Reg" prior to any damage, "SHP Reg" after plasma deterioration, and SHP Reg after superhydrophobicity regeneration

Sample	C 1s	O 1s	Si 2p
Sylgard	44.71	31.55	23.73
SHP Ref	47.40	27.84	24.76
SHP Reg	42.53	23.73	34.09
SHP Reg after plasma	35.36	24.05	40.59
SHP Reg after regeneration	41.35	25.82	32.83

To better elaborate, curve fittings of C1s "SHP Reg" prior to plasma, after plasma deterioration, and after superhydrophobicity regeneration can be found in Figure 38. The spectrum is fitted by a combination of four peaks: the peak at 274 eV corresponding to C-Si, the peak at 284.8 eV which corresponds to C–C and C–H moieties, the peak at 286.4 eV corresponding to C–OH and C–O–C functional groups, and the peak at 286.4 eV which corresponds to C–OH and C–O–C functional groups [173-175]. The ratio of C-OH and C-O-C in the "SHP Reg" sample before the plasma deterioration is around 22.65% which increases to 37.12% after plasma deterioration. However, this ratio drops back to around 23.52% for the sample after superhydrophobicity regeneration. Therefore, the increase of hydrophilic polar oxygen-containing groups on the surface after air plasma could justify the decrease in the water contact angle on these samples.

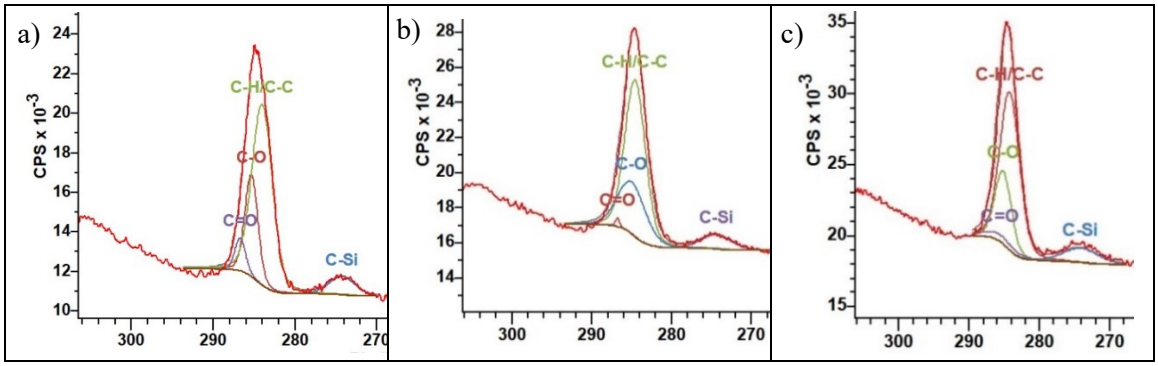

Figure 38. C1s spectra of SHP Reg a) prior to any damage, b) after plasma deterioration, and c) after superhydrophobicity regeneration © Helya Khademsameni, 2023.

4.4 Ice adhesion Measurements

4.4.1 Ice push-off test

A comparison between the ice adhesion strength of the "SHP Reg", "SHP Ref", and "Sylgard" samples is presented in (Figure 39). The "Sylgard" sample presents an ice adhesion strength of 414.1 kPa. However, the ice adhesion strength for the developed "SHP Ref" and the "SHP Reg" samples was measured to be 215.6 kPa and 71.2 kPa respectively. The ice adhesion strength for the aluminum sample was also recorded at 650 kPa. On the condition that there is a transition of Cassie to Wenzel during ice formation on superhydrophobic coatings, the icephobic behavior of the surface could be affected by the air pockets trapped underneath the formed ice, here the ice cylinder. This could lead to a decrease in ice adhesion strength which matches the result presented in (Figure 39) [176], [177]. By comparing the "SHP Ref" and "SHP Reg" samples, a significant drop in the ice adhesion strength is observed, a drop which can be attributed to the presence of F-POSS and oil silicone resulting in an increase in the slipperiness of the surface [178].

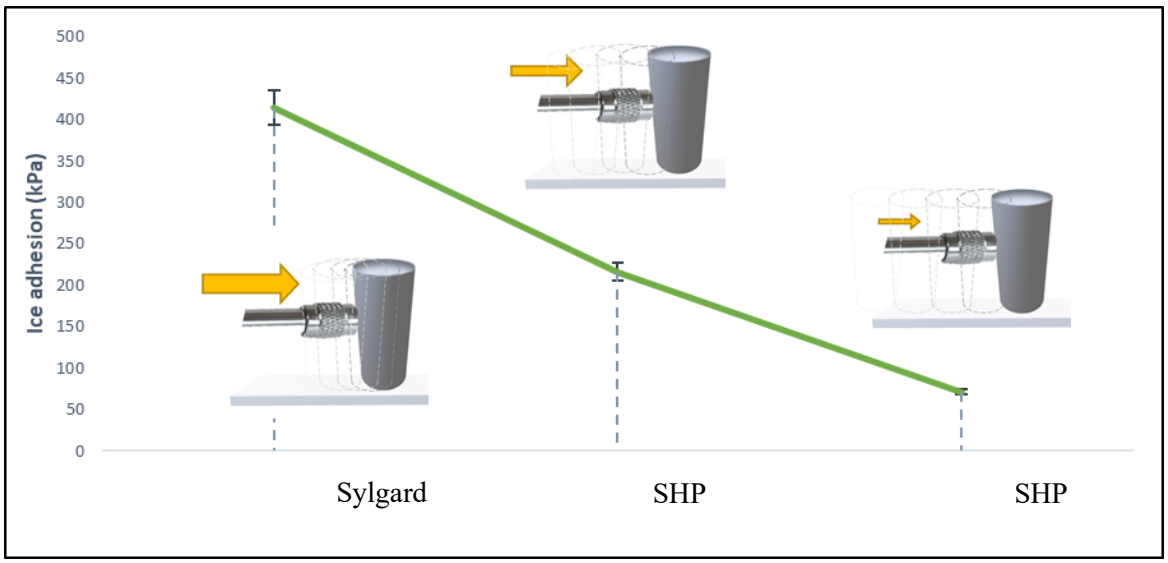

Figure 39. Comparison of ice adhesion strength of "Sylgard", "SHP Ref", and "SHP Reg" © Helya Khademsameni, 2023.

The durability of the ice adhesion test was evaluated by several icing/de-icing cycles of the ice push-off test (Figure 40). Each cycle is followed by an interval of 24 h. For "SHP Reg" samples it could be expected to witness an increase in ice adhesion after each icing/de-icing cycle due to the depletion of the silicone oil present on the surface [178]. However, the contrary is observed and the developed regenerating superhydrophobic coating presents an even lower ice adhesion after each cycle. It could be explained that since in each cycle, the silicone oil present on the surface is depleted the surface energy of the coating increases, leading to an upward movement of the silicone oil and the F-POSS from the matrix to the surface in order to lessen the surface energy, ending up in a low ice adhesion strength of the coating. By following the changes in the ice adhesion of the regenerative superhydrophobic coating, it can be concluded that this coating can be a proper choice for passive ice removal.

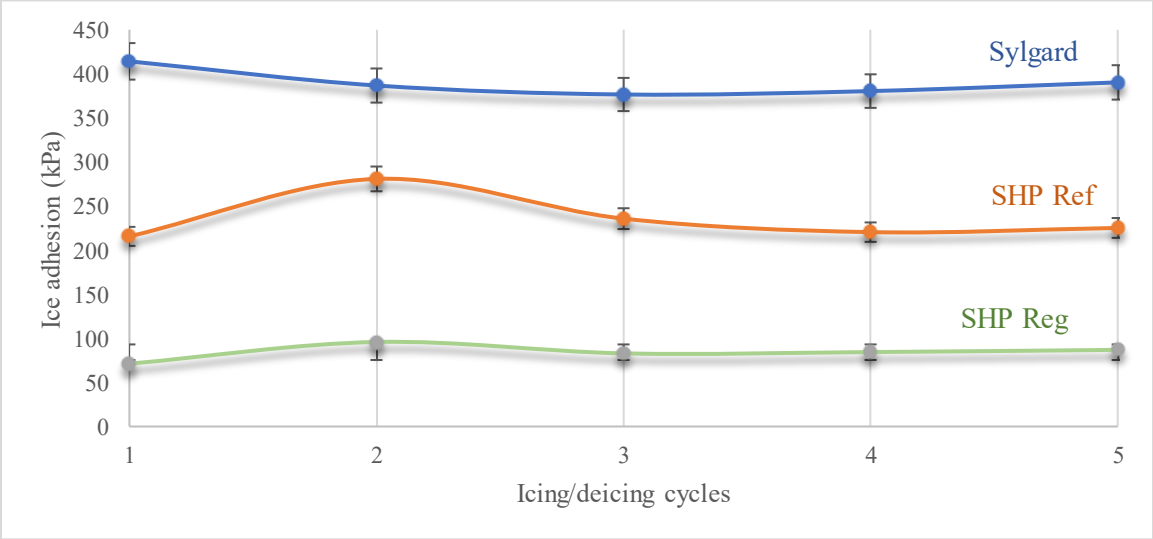

Figure 40. The ice adhesion strength of PDMS reference samples, superhydrophobic samples without the superhydrophobic self-healing agents, and regenerative superhydrophobic samples over five icing/de-icing cycles © Helya Khademsameni, 2023.

4.4.2 Centrifuge Adhesion Test

The second test used in this research to measure the ice adhesion strength on the developed coatings is the centrifuge adhesion test. In the push-off test, the ice adhesion strength of ice bulk was measured, however, in the centrifuge adhesion test, the glaze ice adhesion is of focus. The glaze ice is prone to stimulate harsher icing conditions [179]. The ice adhesion strength of 195.5 and 221 kPa was recorded for the "SHP Ref" and "SHP Reg" samples respectively for the CAT test. The ice adhesion strength for the Aluminum sample and the "Sylgard" sample were 652 and 255.5 kPa respectively. With the help of the equations demonstrated in the 3.6.2 section of this study, the ARF of the "SHP Ref" and "SHP Reg" compared to the Aluminum reference were obtained as 3.33 and 2.95 and in comparison, to the pristine "Sylgard" sample the results were 1.37 and 1.16 respectively.

The same centrifuge adhesion test was repeated once more with a time interval of 24 h. The aim of this repetition was to observe the effect of the probable migration of superhydrophobicity regeneration agents to the surface after a potential depletion of low surface energy material from the coating surface following the first centrifuge adhesion test. This time the ice adhesion strength for the "Sylgard" sample increased to 342 kPa. The ice adhesion strength recorded for the second test for the samples "SHP Ref" and "SHP Reg" was recorded at 246.5 and 233 kPa respectively, leading to an ARF of 2.64 and 2.8 in comparison to the Aluminum reference subsequently. The ARF in the second time in comparison to the Sylgard sample was 1.38 and 1.47 for the "SHP Ref" and "SHP Reg" respectively.

A comparison of the CAT test cycles is provided in Figure 41. The trendline for the "SHP Ref" sample is an increasing trend as expected, meaning the low durability of the ice adhesion in the "SHP Ref" coating is in fact affecting the results, leading to an increase of ice adhesion after each repetition. A trend that can be observed for the "SHP Reg" sample as well. However, this increase for the "SHP Ref" sample is much greater than the "SHP Reg" sample. To the point that even though in the first cycle the ice adhesion strength for the "SHP Ref" sample is reported lower than the "SHP Reg" sample, the contrary can be remarked for the second cycle. The absence of superhydrophobicity regeneration agents in the "SHP Ref" results in low ice adhesion durability after two cycles. Nevertheless, the presence of F-POSS and silicone oil in the "SHP Reg" sample has made a big difference in the ice adhesion durability of this coating, a result that makes this

coating an appropriate choice for real-life applications where the durability of the ice adhesion is of great importance.

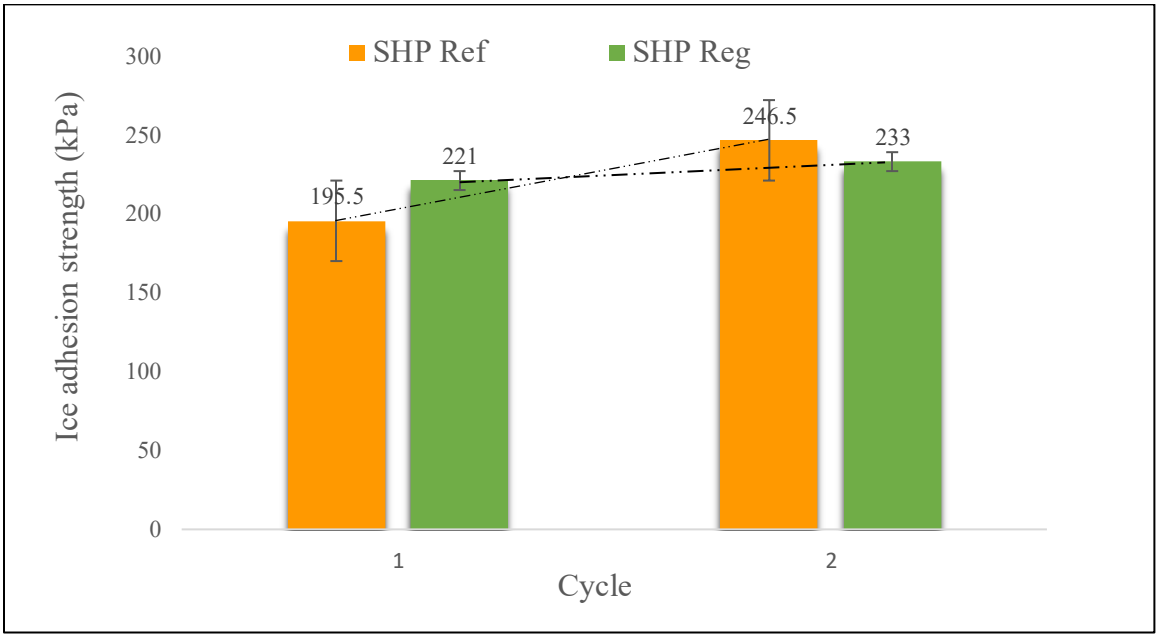

Figure 41. Ice adhesion strength measurements centrifuge tests for two cycles on "SHP Ref" and "SHP Reg" samples
© Helya Khademsameni, 2023.

4.5 Conclusions

Fabrication of regenerative superhydrophobic coatings with the ability to become superhydrophobic again after damage to the superhydrophobicity layer is the focus of this research. According to this objective and based on the provided literature review, fabrication method and the material for the development of the desired coating were chosen. A superhydrophobic regenerative coating containing aerogel microparticles and polydimethylsiloxane nanoparticles is developed and spin-coated on substrates. Of the factors influencing these choices, the final application which is electrical insulators, cost, efficiency, and performance can be mentioned. This coating also contains superhydrophobicity regeneration agents which their efficiency in the coating is put at test by plasma deterioration and pH immersion. Based on their efficiency and compatibility with the coating components, FL0578 Trifluoropropyl POSS and Xiamater PMX-series silicone oil were chosen as these agents for this research. The coating was then optimized to have the best possible superhydrophobicity regeneration agents. After studying the effect of each superhydrophobicity regeneration agent and achieving the best ratio of coating components, the coating was optimized. The final coating showed a contact angle as high as 169.5±0.6°. The coating also showed excellent water repellency and self-cleaning properties after water immersion and dry contamination tests. Two sets of reference samples, one being a superhydrophobic reference sample and the other one a base resin reference sample are developed as well.

This chapter step by step explained the coating fabrication and optimization process of the regenerative superhydrophobic coating. Effects of each self-healing superhydrophobicity agent and

the ratio of their content on different parameters were observed, and the coating formulation was optimized. The superhydrophobicity regeneration of the developed coating was attested by damaging the coating through various pH immersions and plasma deterioration. In comparison to the reference superhydrophobic coating, the developed superhydrophobic regenerative coating showed a contact angle as high as the primary contact angle after both tests, showing a favorable performance for the overall application. After each plasma deterioration, the developed coating was able to recover its contact angle without human intervention. During these evaluations, the CAH and SA were increased. The superhydrophobicity regeneration ability was characterized by water contact angle measurement, Profilometry, XPS, and FTIR analysis. The test results confirmed the superhydrophobicity regeneration of the coating.

To better evaluate the performance of the developed coating for the real-life application ice adhesion measurements of the developed coatings were investigated through two testing approaches of push-off test and centrifuge adhesion test. The push-off test was conducted for several icing/de-icing cycles, proving the ability of the developed coating to maintain the relatively low ice adhesion. The centrifuge adhesion test which normally presents a harsher testing environment proved the durability of the developed coating in the means of ice.

FIFTH CHAPTER
CONCLUSIONS AND FUTURE RECOMMENDATIONS

5.1 Conclusions and contributions of this dissertation

The presence of ice or pollution on the electrical infrastructures such as electrical insulators could be harmful to their functionality. Superhydrophobicity could serve these infrastructures greatly. It could firstly decrease the nucleation points and therefore delay ice formation on the insulators. Secondly, due to the self-cleaning application of superhydrophobic surfaces, it could delay or decrease the chances of a film formation of conductive particles left on the surface of these infrastructures. Hindrance in heat transfer and water rebound on the surface of superhydrophobic surfaces could be beneficial as well. Therefore, the addition of superhydrophobic coatings on the electrical insulators seem to be an appropriate response to the mentioned issue.

There are various fabrication methods for superhydrophobic coatings, and they can be made from various materials. These coatings, however, tend to have low durability, which could be considered as their major drawback. Fabrication of regenerative superhydrophobicity, coatings with the ability to become superhydrophobic again after a loss to the low-surface energy layer or the hierarchical topography, could be the right response to tackle this issue. These coatings obey certain self-healing principles, of which migration of low-surface energy materials to the surface in case of a loss of superhydrophobicity, is the focus of the current work.

A PDMS-based superhydrophobic coating containing hydrophobic aerogel microparticles and fumed silica after-treated with polydimethylsiloxane nanoparticles was fabricated via the spin-coating method. In order to achieve superhydrophobicity regeneration, the addition of self-healing superhydrophobicity agents into the coating is a necessity. Due to the great potential of F-POSS in increasing the coating hydrophobicity and silicone oil in decreasing the surface energy, FL0578 Trifluoropropyl POSS (F-POSS) and Xiamater PMX-series silicone oil were added to the coating mixture. The coating was deposited on substrates with the help of the spin coating fabrication technique. Use of fluorinated particles as superhydrophobicity regeneration agents has been proven before in other works. For silicon oil though, the benefits were more related to icephobicity properties and were used less commonly in the field of superhydrophobicity. This research presents a simultaneous use of both F-POSS and silicone oil as superhydrophobicity regeneration agents and evaluates the role of these agents in the regeneration of superhydrophobicity. The delicacy and novelty of this research is the simultaneous use, optimization of the coating to find the best ratio of them, and the final application of the coating.

In order to determine functionality of the superhydrophobicity regeneration agents, three sets of coatings were fabricated: one containing only F-POSS as a superhydrophobicity regeneration agent, one containing only silicone oil, and the last set containing both F-POSS and silicone oil. The superhydrophobicity regeneration of the samples was tested by plasma deterioration and samples containing both F-POSS and silicone oil showed better superhydrophobicity regeneration results.

After samples with both F-POSS and silicone oil proven to bring the best results during the optimization period, determination of the most suitable ratio of these agents in the coating mixture was the task to be focused on. To tackle this challenge three sets of samples containing both F-POSS and silicone oil with different ratios (4:1,1:4,1:1) were fabricated. The developed samples were attested by plasma deterioration and samples containing more F-POSS than silicone oil showed better superhydrophobicity regeneration results.

The final coating showed excellent superhydrophobic and icephobic properties and the self-cleaning properties of the developed coating were observed through dry contamination tests. The regeneration of superhydrophobicity was attested for six cycles of plasma deterioration, in which the coating was able to recover its superhydrophobicity without human intervention in each cycle. The superhydrophobicity regeneration ability was observed with water contact angle and FTIR measurements. The superhydrophobicity regeneration of the developed coating was also tested by immersion in various pH solutions, which the developed regenerative superhydrophobic samples were the only ones that were able to regain their superhydrophobicity in comparison with PDMS reference sample and superhydrophobic reference sample without any superhydrophobicity healing agents. Moreover, the final developed coating showed low ice adhesion compared to the reference samples which is evidence of the anti-icing capability of the developed coating, a capability that was tested for several cycles.

5.2 Recommendations for future work

Implementing complementary tests

Complementary tests could examine the developed coatings more comprehensively. Severe pressing of water droplets on the coating can be recorded by the initial water contact angle, the water contact angle at the time of pressing, and in the lifting stage. Moreover, dropping a water droplet on the superhydrophobic coatings can demonstrate the droplet behavior at the impact time and the following rebounds.

Optimization of the current coating regarding the mechanical properties

The mechanical durability of the coating should be further explored. The developed coating can be tested by various test methods such as sandpaper abrasion or sand impact to demonstrate mechanical durability. The obtained results can be compared with the reference samples.

Coating fabrication with a wider variety of superhydrophobicity regeneration agents

The current coating was fabricated with FL0578 Trifluoropropyl POSS (F-POSS) and Xiamater PMX-200 50 cSt silicone oil as superhydrophobicity regeneration agents. The next step of this work could be focusing on other superhydrophobicity regeneration agents, such as other silicone oils in the family of PMX-200 series, with different viscosities and special gravity.

Experimenting various environmental conditions for the superhydrophobicity regeneration

After the superhydrophobicity is ruined with methods such as plasma deterioration or various pH immersions, the samples could be held in different environmental conditions so that the effect of temperature and humidity on the healing process can be studied.

Deployment of electrical tests on the fabricated coatings

Since the final application of the developed coatings is to be used on electrical insulators, these coatings can be tested with various electrical tests. Of which, flashover tests in dry and humid environments, would demonstrate the ability of this coating to be used in real-life applications.

Providing complementary icephobicity tests

Additional tests can demonstrate the ability of the developed coating under various icing conditions. Freezing delay time on the developed coating can be measured and compared with the reference samples. Another approach could be manipulating the healing process between each cycle of push-off and centrifuge test. It can be done by putting the sample in an environment with high temperature, low temperature, high humidity, immersed in acidic or basic solutions and etc.

Focus on Hysteresis regeneration

In the literature review chapter, the superhydrophobicity regeneration principles were thoroughly discussed. These principles were categorized into three categories: 1) Transportation of low-surface energy materials to the surface, 2) Regeneration of hierarchical topography, and 3) a combination of the two. This research focused on the first principles and developed coating according to these healing principles. A future step for this research could be the implementation of the second principle as well and having a final coating with more of a focus on hierarchical topography regeneration.

REFERENCES

[1] L. P. Marilla Steuter-Martin, “Looking back on the 1998 ice storm 20 years later.” cbc.ca/news/canada/montreal/ice-storm-1998-1.4469977

[2] Lynn Desjardins, “Ice storm cuts power to over a quarter million homes.” https://www.rcinet.ca/en/2019/04/09/electrical-failures-freezing-rain-canada-quebec/

[3] The Canadian Press, “Late December storm cost Hydro-Quebec $55 million,” *CTV News*, Jan. 19, 2023.

[4] “Polluted insulators: A review of current knowledge,” 2000.

[5] Arshad, G. Momen, M. Farzaneh, and A. Nekahi, “Properties and applications of superhydrophobic coatings in high voltage outdoor insulation: A review,” *IEEE Transactions on Dielectrics and Electrical Insulation*, vol. 24, no. 6, pp. 3630–3646, 2017, doi: 10.1109/TDEI.2017.006725.

[6] T. R. Society, P. Transactions, and E. Sciences, “Ice Accretions on High-Voltage Conductors and Insulators and Related Phenomena Author (s): Masoud Farzaneh Source : Philosophical Transactions : Mathematical , Physical and Engineering Sciences , Vol . 358 , No . 1776 , Ice and Snow Accretion on Structu,” vol. 358, no. 1776, pp. 2971–3005, 2013.

[7] X. Qiao, Z. Zhang, X. Jiang, Y. He, and X. Li, “Application of grey theory in pollution prediction on insulator surface in power systems,” *Eng Fail Anal*, vol. 106, no. August, p. 104153, 2019, doi: 10.1016/j.engfailanal.2019.104153.

[8] M. Farzaneh, “Insulator flashover under icing conditions,” *IEEE Transactions on Dielectrics and Electrical Insulation*, vol. 21, no. 5, pp. 1997–2011, 2014, doi: 10.1109/TDEI.2014.004598.

[9] S. Khatoon, A. A. Khan, and S. Singh, “A review of the flashover performance of high voltage insulators constructed with modern insulating materials,” *Transactions on Electrical and Electronic Materials*, vol. 18, no. 5, pp. 246–249, 2017, doi: 10.4313/TEEM.2017.18.5.246.

[10] A. Allahdini, G. Momen, F. Munger, S. Brettschneider, I. Fofana, and R. Jafari, “Performance of a nanotextured superhydrophobic coating developed for high-voltage outdoor porcelain insulators,” *Colloids Surf A Physicochem Eng Asp*, vol. 649, no. April, 2022, doi: 10.1016/j.colsurfa.2022.129461.

[11] X. Qiao, Z. Zhang, X. Jiang, R. Sundararajan, X. Ma, and X. Li, “AC failure voltage of iced and contaminated composite insulators in different natural environments,” *International Journal of Electrical Power and Energy Systems*, vol. 120, no. October 2019, p. 105993, 2020, doi: 10.1016/j.ijepes.2020.105993.

[12] G. Momen and M. Farzaneh, “Survey of micro/nano filler use to improve silicone rubber for outdoor insulators,” *Reviews on Advanced Materials Science*, vol. 27, no. 1, pp. 1–13, 2011.

[13] J. Li, Y. Zhao, J. Hu, L. Shu, and X. Shi, “Anti-icing performance of a superhydrophobic PDMS/modified nano-silica hybrid coating for insulators,” *J Adhes Sci Technol*, vol. 26, no. 4–5, pp. 665–679, 2012, doi: 10.1163/016942411X574826.

[14] S. L. Sanjay, B. G. Annaso, S. M. Chavan, and S. V. Rajiv, “Recent progress in preparation of superhydrophobic surfaces: a review,” *J Surf Eng Mater Adv Technol*, vol. 2, no. April, pp. 76–94, 2012.

[15] J. Jeevahan, M. Chandrasekaran, G. Britto Joseph, R. B. Durairaj, and G. Mageshwaran, “Superhydrophobic surfaces: a review on fundamentals, applications, and challenges,” *J Coat Technol Res*, vol. 15, no. 2, pp. 231–250, 2018, doi: 10.1007/s11998-017-0011-x.

[16] F. Liu, H. Du, Y. Han, C. Wang, Z. Liu, and H. Wang, “Recent Progress in the Fabrication and Characteristics of Self-Repairing Superhydrophobic Surfaces,” *Adv Mater Interfaces*, vol. 8, no. 17, pp. 1–29, 2021, doi: 10.1002/admi.202100228.

[17] E. Kobina Sam *et al.*, “Recent development in the fabrication of self-healing superhydrophobic surfaces,” *Chemical Engineering Journal*, vol. 373, no. May, pp. 531–546, 2019, doi: 10.1016/j.cej.2019.05.077.

[18] Y. Li *et al.*, “A robust and flexible bulk superhydrophobic material from silicone rubber/silica gel prepared by thiol-ene photopolymerization,” *J Mater Chem A Mater*, vol. 7, no. 12, pp. 7242–7255, 2019, doi: 10.1039/c8ta11111a.

[19] Y. Jiang and C. H. Choi, “Droplet Retention on Superhydrophobic Surfaces: A Critical Review,” *Adv Mater Interfaces*, vol. 8, no. 2, pp. 1–26, 2021, doi: 10.1002/admi.202001205.

[20] R. H. A. Ras and A. Marmur, *Non-wettable Surfaces Theory, Preparation, and Applications*, vol. 7, no. 8. 2017. doi: 10.1182/blood.v7.8.850.850.

[21] D. Deo, S. P. Singh, S. Mohanty, S. Guhathakurata, D. Pal, and S. Mallik, “Biomimicking of phyto-based super-hydrophobic surfaces towards prospective applications: a review,” *J Mater Sci*, vol. 57, no. 19, pp. 8569–8596, 2022, doi: 10.1007/s10853-022-07172-1.

[22] B. Thomas Young and M. D. For Sec, “HI, An Essay on the Cohesion of Fluids.” [Online]. Available: https://royalsocietypublishing.org/

[23] R. N. Wenzel, “Resistance of solid surfaces to wetting by water,” *Industrial & Engineering Chemistry*, vol. 28, no. 8, pp. 988–994, May 2002, doi: 10.1021/ie50320a024.

[24] A. B. D. Cassie and S. Baxter, “Wettability of porous surfaces,” no. 5, pp. 546–551, 1944.

[25] A. Hooda, M. S. Goyat, J. K. Pandey, A. Kumar, and R. Gupta, “A review on fundamentals, constraints and fabrication techniques of superhydrophobic coatings,” *Progress in Organic Coatings*, vol. 142. Elsevier B.V., May 01, 2020. doi: 10.1016/j.porgcoat.2020.105557.

[26] O. Tricinci, T. Terencio, B. Mazzolai, N. M. Pugno, F. Greco, and V. Mattoli, “3D Micropatterned Surface Inspired by Salvinia molesta via Direct Laser Lithography,” *ACS Appl Mater Interfaces*, vol. 7, no. 46, pp. 25560–25567, Nov. 2015, doi: 10.1021/acsami.5b07722.

[27] E. Vazirinasab, R. Jafari, and G. Momen, “Application of superhydrophobic coatings as a corrosion barrier: A review,” *Surf Coat Technol*, vol. 341, no. October 2017, pp. 40–56, 2018, doi: 10.1016/j.surfcoat.2017.11.053.

[28] A. Fihri, E. Bovero, A. Al-Shahrani, A. Al-Ghamdi, and G. Alabedi, “Recent progress in superhydrophobic coatings used for steel protection: A review,” *Colloids Surf A Physicochem Eng Asp*, vol. 520, pp. 378–390, 2017, doi: 10.1016/j.colsurfa.2016.12.057.

[29] S. Das, S. Kumar, S. K. Samal, S. Mohanty, and S. K. Nayak, “A Review on Superhydrophobic Polymer Nanocoatings: Recent Development and Applications,” *Ind Eng Chem Res*, vol. 57, no. 8, pp. 2727–2745, 2018, doi: 10.1021/acs.iecr.7b04887.

[30] P. Zhang and F. Y. Lv, “A review of the recent advances in superhydrophobic surfaces and the emerging energy-related applications,” *Energy*, vol. 82, pp. 1068–1087, 2015, doi: 10.1016/j.energy.2015.01.061.

[31] T. Koishi, K. Yasuoka, S. Fujikawa, T. Ebisuzaki, and C. Z. Xiao, “Coexistence and transition between Cassie and Wenzel state on pillared hydrophobic surface,” *Proc Natl Acad Sci U S A*, vol. 106, no. 21, pp. 8435–8440, 2009, doi: 10.1073/pnas.0902027106.

[32] A. Hooda, M. S. Goyat, J. K. Pandey, A. Kumar, and R. Gupta, “A review on fundamentals, constraints and fabrication techniques of superhydrophobic coatings,” *Prog Org Coat*, vol. 142, no. January, p. 105557, 2020, doi: 10.1016/j.porgcoat.2020.105557.

[33] P. Nguyen-Tri *et al.*, “Recent progress in the preparation, properties and applications of superhydrophobic nano-based coatings and surfaces: A review,” *Prog Org Coat*, vol. 132, no. March, pp. 235–256, 2019, doi: 10.1016/j.porgcoat.2019.03.042.

[34] M. Miwa, A. Nakajima, A. Fujishima, K. Hashimoto, and T. Watanabe, “Effects of the surface roughness on sliding angles of water droplets on superhydrophobic surfaces,” *Langmuir*, vol. 16, no. 13, pp. 5754–5760, Jun. 2000, doi: 10.1021/la991660o.

[35] J. de Coninck, J. C. Fernández-Toledano, F. Dunlop, T. Huillet, and A. Sodji, “Shape of pendent droplets under a tilted surface,” *Physica D*, vol. 415, Jan. 2021, doi: 10.1016/j.physd.2020.132765.

[36] R. E. Johnson and R. H. Dettre, “Contact angle hysteresis. III. Study of an idealized heterogeneous surface,” *Journal of Physical Chemistry*, vol. 68, no. 7, pp. 1744–1750, 1964, doi: 10.1021/j100789a012.

[37] S. Rabbani, E. Bakhshandeh, R. Jafari, and G. Momen, “Progress in Organic Coatings Superhydrophobic and icephobic polyurethane coatings : Fundamentals , progress , challenges and opportunities,” *Prog Org Coat*, vol. 165, no. January, p. 106715, 2022, doi: 10.1016/j.porgcoat.2022.106715.

[38] C. J. Long, J. F. Schumacher, and A. B. Brennan, “Potential for tunable static and dynamic contact angle anisotropy on gradient microscale patterned topographies,” *Langmuir*, vol. 25, no. 22, pp. 12982–12989, 2009, doi: 10.1021/la901836w.

[39] X. Wu, V. v. Silberschmidt, Z. T. Hu, and Z. Chen, “When superhydrophobic coatings are icephobic: Role of surface topology,” *Surf Coat Technol*, vol. 358, pp. 207–214, 2019, doi: 10.1016/j.surfcoat.2018.11.039.

[40] S. Jung, M. Dorrestijn, D. Raps, A. Das, C. M. Megaridis, and D. Poulikakos, “Are superhydrophobic surfaces best for icephobicity?,” *Langmuir*, vol. 27, no. 6, pp. 3059–3066, 2011, doi: 10.1021/la104762g.

[41] K. Maghsoudi, E. Vazirinasab, G. Momen, and R. Jafari, “Icephobicity and durability assessment of superhydrophobic surfaces: The role of surface roughness and the ice adhesion measurement technique,” *J Mater Process Technol*, vol. 288, no. July 2020, p. 116883, 2021, doi: 10.1016/j.jmatprotec.2020.116883.

[42] M. Shamshiri, R. Jafari, and G. Momen, “Potential use of smart coatings for icephobic applicatioans: A review,” *Surf Coat Technol*, vol. 424, no. September, p. 127656, 2021, doi: 10.1016/j.surfcoat.2021.127656.

[43] K. Maghsoudi, E. Vazirinasab, G. Momen, and R. Jafari, “Advances in the Fabrication of Superhydrophobic Polymeric Surfaces by Polymer Molding Processes,” *Ind Eng Chem Res*, vol. 59, no. 20, pp. 9343–9363, 2020, doi: 10.1021/acs.iecr.0c00508.

[44] G. Barati Darband, M. Aliofkhazraei, S. Khorsand, S. Sokhanvar, and A. Kaboli, “Science and Engineering of Superhydrophobic Surfaces: Review of Corrosion Resistance, Chemical and Mechanical Stability,” *Arabian Journal of Chemistry*, vol. 13, no. 1, pp. 1763–1802, 2020, doi: 10.1016/j.arabjc.2018.01.013.

[45] H. A. M. Mustafa and D. A. Jameel, “Modeling and the main stages of spin coating process: A review,” *Journal of Applied Science and Technology Trends*, vol. 2, no. 03, pp. 91–95, 2021, doi: 10.38094/jastt203109.

[46] X. Gong and S. He, “Highly Durable Superhydrophobic Polydimethylsiloxane/Silica Nanocomposite Surfaces with Good Self-Cleaning Ability,” *ACS Omega*, vol. 5, no. 8, pp. 4100–4108, 2020, doi: 10.1021/acsomega.9b03775.

[47] S. Parvate, P. Dixit, and S. Chattopadhyay, "Superhydrophobic Surfaces: Insights from Theory and Experiment," *Journal of Physical Chemistry B*, vol. 124, no. 8, pp. 1323–1360, 2020, doi: 10.1021/acs.jpcb.9b08567.

[48] G. Lorenz and A. Kandelbauer, "Silicones," *Handbook of Thermoset Plastics*, pp. 555–575, 2014, doi: 10.1016/B978-1-4557-3107-7.00014-2.

[49] S. C. Shit and P. Shah, "A review on silicone rubber," *National Academy Science Letters*, vol. 36, no. 4, pp. 355–365, 2013, doi: 10.1007/s40009-013-0150-2.

[50] V. Danilov, C. Dölle, M. Ott, H. Wagner, and J. Meichsner, "Plasma treatment of polydimethylsiloxane thin films studied by infrared reflection absorption spectroscopy," *29th ICPIG*, no. June, p. 13, 2009.

[51] D. Fragiadakis, P. Pissis, and L. Bokobza, "Glass transition and molecular dynamics in poly(dimethylsiloxane)/silica nanocomposites," *Polymer (Guildf)*, vol. 46, no. 16, pp. 6001–6008, 2005, doi: 10.1016/j.polymer.2005.05.080.

[52] G. Wang *et al.*, "A Review on Fabrication Methods and Research Progress of Superhydrophobic Silicone Rubber Materials," *Adv Mater Interfaces*, vol. 8, no. 1, pp. 1–19, 2021, doi: 10.1002/admi.202001460.

[53] J. N. Wang *et al.*, "Wearable Superhydrophobic Elastomer Skin with Switchable Wettability," *Adv Funct Mater*, vol. 28, no. 23, pp. 1–8, 2018, doi: 10.1002/adfm.201800625.

[54] S. Hamouni, O. Arous, D. Abdessemed, G. Nezzal, and B. Van der Bruggen, "Alcohol and Alkane Organic Extraction Using Pervaporation Process," *Macromol Symp*, vol. 386, no. 1, Aug. 2019, doi: 10.1002/masy.201800247.

[55] E. P. Everaert, H. C. Van Der Mei, and H. J. Busscher, "Hydrophobic recovery of repeatedly plasma-treated silicone rubber. Part 2. A comparison of the hydrophobic recovery in air, water, or liquid nitrogen," *J Adhes Sci Technol*, vol. 10, no. 4, pp. 351–359, 1996, doi: 10.1163/156856196X00751.

[56] R. Zhang *et al.*, "Hydrophobicity improvement of contaminated HTV silicone rubber by atmospheric plasma jet treatment," *IEEE Transactions on Dielectrics and Electrical Insulation*, vol. 23, no. 1, pp. 377–384, 2016, doi: 10.1109/TDEI.2015.005117.

[57] J. Kim, M. K. Chaudhury, and M. J. Owen, "Hydrophobic recovery of polydimethylsiloxane elastomer exposed to partial electrical discharge," *J Colloid Interface Sci*, vol. 226, no. 2, pp. 231–236, 2000, doi: 10.1006/jcis.2000.6817.

[58] G. Momen and M. Farzaneh, "Survey of micro/nano filler use to improve silicone rubber for outdoor insulators," *Reviews on Advanced Materials Science*, vol. 27, no. 1, pp. 1–13, 2011.

[59] T. Senzai and S. Fujikawa, “Fast hydrophobicity recovery of the surface-hydrophilic poly(dimethylsiloxane) films caused by rechemisorption of dimethylsiloxane derivatives,” *Langmuir*, vol. 35, no. 30, pp. 9747–9752, 2019, doi: 10.1021/acs.langmuir.9b01448.

[60] E. Vazirinasab, R. Jafari, and G. Momen, “Application of superhydrophobic coatings as a corrosion barrier: A review,” *Surf Coat Technol*, vol. 341, no. November 2017, pp. 40–56, 2018, doi: 10.1016/j.surfcoat.2017.11.053.

[61] Y. Lin, H. Chen, G. Wang, and A. Liu, “Recent progress in preparation and anti-icing applications of superhydrophobic coatings,” *Coatings*, vol. 8, no. 6, 2018, doi: 10.3390/coatings8060208.

[62] E. Vazirinasab, G. Momen, and R. Jafari, “A non-fluorinated mechanochemically robust volumetric superhydrophobic nanocomposite,” *J Mater Sci Technol*, vol. 66, pp. 213–225, 2021, doi: 10.1016/j.jmst.2020.06.029.

[63] A. Allahdini, R. Jafari, and G. Momen, “Transparent non-fluorinated superhydrophobic coating with enhanced anti-icing performance,” *Prog Org Coat*, vol. 165, no. October 2021, p. 106758, 2022, doi: 10.1016/j.porgcoat.2022.106758.

[64] S. Roshan, A. A. Sarabi, R. Jafari, and G. Momen, “One-step fabrication of superhydrophobic nanocomposite with superior anticorrosion performance,” *Prog Org Coat*, vol. 169, no. April, p. 106918, 2022, doi: 10.1016/j.porgcoat.2022.106918.

[65] V. A. Ganesh, H. K. Raut, A. S. Nair, and S. Ramakrishna, “A review on self-cleaning coatings,” *J Mater Chem*, vol. 21, no. 41, pp. 16304–16322, 2011, doi: 10.1039/c1jm12523k.

[66] Z. Zuo, R. Liao, C. Guo, and X. Zhao, “Fabrication and anti-icing property of superhydrophobic coatings on insulator,” *Annual Report - Conference on Electrical Insulation and Dielectric Phenomena, CEIDP*, vol. 2015-Decem, pp. 161–164, 2015, doi: 10.1109/CEIDP.2015.7352052.

[67] X. Li and B. Bhushan, “A review of nanoindentation continuous stiffness measurement technique and its applications,” *Mater Charact*, vol. 48, no. 1, pp. 11–36, 2002, doi: 10.1016/S1044-5803(02)00192-4.

[68] J. Zhang and S. Seeger, “Superoleophobic coatings with ultralow sliding angles based on silicone nanofilaments,” *Angewandte Chemie - International Edition*, vol. 50, no. 29, pp. 6652–6656, 2011, doi: 10.1002/anie.201101008.

[69] J. Zimmermann, F. A. Reifler, U. Schrade, G. R. J. Artus, and S. Seeger, “Long term environmental durability of a superhydrophobic silicone nanofilament coating,” *Colloids Surf A Physicochem Eng Asp*, vol. 302, no. 1–3, pp. 234–240, 2007, doi: 10.1016/j.colsurfa.2007.02.033.

[70] L. Huang, L. Zhang, J. Song, X. Wang, and H. Liu, “Superhydrophobic Nickel-Electroplated Carbon Fibers for Versatile Oil/Water Separation with Excellent Reusability

and High Environmental Stability," *ACS Appl Mater Interfaces*, vol. 12, no. 21, pp. 24390–24402, 2020, doi: 10.1021/acsami.9b23476.

[71] K. Ellinas, A. Tserepi, and E. Gogolides, "Durable superhydrophobic and superamphiphobic polymeric surfaces and their applications: A review," *Adv Colloid Interface Sci*, 2017, doi: 10.1016/j.cis.2017.09.003.

[72] F. J. Wang, S. Lei, J. F. Ou, M. S. Xue, and W. Li, "Superhydrophobic surfaces with excellent mechanical durability and easy repairability," *Appl Surf Sci*, vol. 276, pp. 397–400, 2013, doi: 10.1016/j.apsusc.2013.03.104.

[73] C. H. Xue, Z. D. Zhang, J. Zhang, and S. T. Jia, "Lasting and self-healing superhydrophobic surfaces by coating of polystyrene/SiO2 nanoparticles and polydimethylsiloxane," *J Mater Chem A Mater*, vol. 2, no. 36, pp. 15001–15007, 2014, doi: 10.1039/c4ta02396j.

[74] Y. Li, S. Chen, M. Wu, and J. Sun, "All spraying processes for the fabrication of robust, self-healing, superhydrophobic coatings," *Advanced Materials*, vol. 26, no. 20, pp. 3344–3348, 2014, doi: 10.1002/adma.201306136.

[75] W. Zhang, D. Wang, Z. Sun, J. Song, and X. Deng, "Robust superhydrophobicity: Mechanisms and strategies," *Chem Soc Rev*, vol. 50, no. 6, pp. 4031–4061, 2021, doi: 10.1039/d0cs00751j.

[76] G. Wu, J. An, X. Z. Tang, Y. Xiang, and J. Yang, "A versatile approach towards multifunctional robust microcapsules with tunable, restorable, and solvent-proof superhydrophobicity for self-healing and self-cleaning coatings," *Adv Funct Mater*, vol. 24, no. 43, pp. 6751–6761, 2014, doi: 10.1002/adfm.201401473.

[77] K. Chen, Y. Wu, S. Zhou, and L. Wu, "Recent Development of Durable and Self-Healing Surfaces with Special Wettability," *Macromol Rapid Commun*, vol. 37, no. 6, pp. 463–485, 2016, doi: 10.1002/marc.201500591.

[78] D. Zhu, X. Lu, and Q. Lu, "Electrically conductive PEDOT coating with self-healing superhydrophobicity," *Langmuir*, vol. 30, no. 16, pp. 4671–4677, 2014, doi: 10.1021/la500603c.

[79] Q. Liu, X. Wang, B. Yu, F. Zhou, and Q. Xue, "Self-healing surface hydrophobicity by consecutive release of hydrophobic molecules from mesoporous silica," *Langmuir*, vol. 28, no. 13, pp. 5845–5849, 2012, doi: 10.1021/la300187q.

[80] M. Spaeth and W. Barthlott, "Lotus-effect®: Biomimetic super-hydrophobic surfaces an their application," *CIMTEC 2008 - Proceedings of the 3rd International Conference on Smart Materials, Structures and Systems - Smart Textiles*, vol. 60, pp. 38–46, 2008, doi: 10.4028/www.scientific.net/ast.60.38.

[81] C. Peng, Z. Chen, and M. K. Tiwari, "All-organic superhydrophobic coatings with mechanochemical robustness and liquid impalement resistance," *Nat Mater*, vol. 17, no. 4, pp. 355–360, 2018, doi: 10.1038/s41563-018-0044-2.

[82] Y. Wang, Y. Liu, J. Li, L. Chen, S. Huang, and X. Tian, "Fast self-healing superhydrophobic surfaces enabled by biomimetic wax regeneration," *Chemical Engineering Journal*, vol. 390, no. February, p. 124311, 2020, doi: 10.1016/j.cej.2020.124311.

[83] S. Chen, X. Li, Y. Li, and J. Sun, "Intumescent flame-retardant and self-Healing superhydrophobic coatings on cotton fabric," *ACS Nano*, vol. 9, no. 4, pp. 4070–4076, 2015, doi: 10.1021/acsnano.5b00121.

[84] Y. Cong, K. Chen, S. Zhou, and L. Wu, "Synthesis of pH and UV dual-responsive microcapsules with high loading capacity and their application in self-healing hydrophobic coatings," *J Mater Chem A Mater*, vol. 3, no. 37, pp. 19093–19099, 2015, doi: 10.1039/c5ta04986e.

[85] M. Liu, Y. Hou, J. Li, L. Tie, Y. Peng, and Z. Guo, "Inorganic adhesives for robust, self-healing, superhydrophobic surfaces," *J Mater Chem A Mater*, vol. 5, no. 36, pp. 19297–19305, 2017, doi: 10.1039/c7ta06001g.

[86] L. Qin, Y. Chu, X. Zhou, and Q. Pan, "Fast Healable Superhydrophobic Material," *ACS Appl Mater Interfaces*, vol. 11, no. 32, pp. 29388–29395, 2019, doi: 10.1021/acsami.9b07563.

[87] H. Zhou, H. Wang, H. Niu, Y. Zhao, Z. Xu, and T. Lin, "A Waterborne Coating System for Preparing Robust, Self-healing, Superamphiphobic Surfaces," *Adv Funct Mater*, vol. 27, no. 14, 2017, doi: 10.1002/adfm.201604261.

[88] Y. Li, L. Li, and J. Sun, "Bioinspired Self-Healing Superhydrophobic Coatings," *Angewandte Chemie*, vol. 122, no. 35, pp. 6265–6269, 2010, doi: 10.1002/ange.201001258.

[89] C. J. Brinker and G. W. Scherer, "Introduction," *Sol-Gel Science*, pp. xvi–18, 1990, doi: 10.1016/b978-0-08-057103-4.50006-4.

[90] S. K. Lahiri, P. Zhang, C. Zhang, and L. Liu, "Robust Fluorine-Free and Self-Healing Superhydrophobic Coatings by H 3 BO 3 Incorporation with SiO 2 -Alkyl-Silane@PDMS on Cotton Fabric," *ACS Appl Mater Interfaces*, vol. 11, no. 10, pp. 10262–10275, 2019, doi: 10.1021/acsami.8b20651.

[91] D. Weng, F. Xu, X. Li, Y. Li, and J. Sun, "Bioinspired photothermal conversion coatings with self-healing superhydrophobicity for efficient solar steam generation," *J Mater Chem A Mater*, vol. 6, no. 47, pp. 24441–24451, 2018, doi: 10.1039/c8ta08706g.

[92] K. Chen, J. Zhou, X. Che, R. Zhao, and Q. Gao, "One-step synthesis of core shell cellulose-silica/n-octadecane microcapsules and their application in waterborne self-healing multiple

protective fabric coatings," *J Colloid Interface Sci*, vol. 566, pp. 401–410, 2020, doi: 10.1016/j.jcis.2020.01.106.

[93] Q. Rao, K. Chen, and C. Wang, "Facile preparation of self-healing waterborne superhydrophobic coatings based on fluoroalkyl silane-loaded microcapsules," *RSC Adv*, vol. 6, no. 59, pp. 53949–53954, 2016, doi: 10.1039/c6ra09582h.

[94] Q. Rao, K. Chen, and C. Wang, "Facile preparation of self-healing waterborne superhydrophobic coatings based on fluoroalkyl silane-loaded microcapsules," *RSC Adv*, vol. 6, no. 59, pp. 53949–53954, 2016, doi: 10.1039/c6ra09582h.

[95] K. Chen, S. Zhou, S. Yang, and L. Wu, "Fabrication of all-water-based self-repairing superhydrophobic coatings based on UV-responsive microcapsules," *Adv Funct Mater*, vol. 25, no. 7, pp. 1035–1041, 2015, doi: 10.1002/adfm.201403496.

[96] A. Kumar, L. D. Stephenson, and J. N. Murray, "Self-healing coatings for steel," *Prog Org Coat*, vol. 55, no. 3, pp. 244–253, 2006, doi: 10.1016/j.porgcoat.2005.11.010.

[97] A. Ouarga *et al.*, "Towards smart self-healing coatings: Advances in micro/nano-encapsulation processes as carriers for anti-corrosion coatings development," *J Mol Liq*, vol. 354, p. 118862, 2022, doi: 10.1016/j.molliq.2022.118862.

[98] S. Xiang and W. Liu, "Self-Healing Superhydrophobic Surfaces: Healing Principles and Applications," *Adv Mater Interfaces*, vol. 2100247, 2021, doi: 10.1002/admi.202100247.

[99] U. Manna and D. M. Lynn, "Restoration of superhydrophobicity in crushed polymer films by treatment with water: Self-healing and recovery of damaged topographic features aided by an unlikely source," *Advanced Materials*, vol. 25, no. 36, pp. 5104–5108, 2013, doi: 10.1002/adma.201302217.

[100] B. Li *et al.*, "Planting carbon nanotubes onto supramolecular polymer matrices for waterproof non-contact self-healing," *Nanoscale*, vol. 11, no. 2, pp. 467–473, 2019, doi: 10.1039/c8nr07158f.

[101] N. Bai, Q. Li, H. Dong, C. Tan, P. Cai, and L. Xu, "A versatile approach for preparing self-recovering superhydrophobic coatings," *Chemical Engineering Journal*, vol. 293, pp. 75–81, 2016, doi: 10.1016/j.cej.2016.02.023.

[102] Z. Wang, L. Yuan, G. Liang, and A. Gu, "Mechanically durable and self-healing super-hydrophobic coating with hierarchically structured KH570 modified SiO2-decorated aligned carbon nanotube bundles," *Chemical Engineering Journal*, vol. 408, no. October 2020, p. 127263, 2021, doi: 10.1016/j.cej.2020.127263.

[103] A. Das, J. Deka, K. Raidongia, and U. Manna, "Robust and Self-Healable Bulk-Superhydrophobic Polymeric Coating," *Chemistry of Materials*, vol. 29, no. 20, pp. 8720–8728, 2017, doi: 10.1021/acs.chemmater.7b02880.

[104] M. Wu, Y. Li, N. An, and J. Sun, "Applied Voltage and Near-Infrared Light Enable Healing of Superhydrophobicity Loss Caused by Severe Scratches in Conductive Superhydrophobic Films," *Adv Funct Mater*, vol. 26, no. 37, pp. 6777–6784, 2016, doi: 10.1002/adfm.201601979.

[105] D. Zhang, Z. Cheng, and Y. Liu, "Smart Wetting Control on Shape Memory Polymer Surfaces," *Chemistry - A European Journal*, vol. 25, no. 16, pp. 3979–3992, 2019, doi: 10.1002/chem.201804192.

[106] T. Xie, "Recent advances in polymer shape memory," *Polymer (Guildf)*, vol. 52, no. 22, pp. 4985–5000, 2011, doi: 10.1016/j.polymer.2011.08.003.

[107] J. Hu, Y. Zhu, H. Huang, and J. Lu, "Recent advances in shape-memory polymers: Structure, mechanism, functionality, modeling and applications," *Prog Polym Sci*, vol. 37, no. 12, pp. 1720–1763, 2012, doi: 10.1016/j.progpolymsci.2012.06.001.

[108] X. J. Guo *et al.*, "Fabrication of robust superhydrophobic surfaces: Via aerosol-assisted CVD and thermo-triggered healing of superhydrophobicity by recovery of roughness structures," *J Mater Chem A Mater*, vol. 7, no. 29, pp. 17604–17612, 2019, doi: 10.1039/c9ta03264a.

[109] W. Wang, J. Salazar, H. Vahabi, A. Joshi-Imre, W. E. Voit, and A. K. Kota, "Metamorphic Superomniphobic Surfaces," *Advanced Materials*, vol. 29, no. 27, pp. 1–7, 2017, doi: 10.1002/adma.201700295.

[110] N. Bai, Q. Li, H. Dong, C. Tan, P. Cai, and L. Xu, "A versatile approach for preparing self-recovering superhydrophobic coatings," *Chemical Engineering Journal*, vol. 293, pp. 75–81, 2016, doi: 10.1016/j.cej.2016.02.023.

[111] H. Wang, H. Zhou, A. Gestos, J. Fang, and T. Lin, "Robust, superamphiphobic fabric with multiple self-healing ability against both physical and chemical damages," *ACS Appl Mater Interfaces*, vol. 5, no. 20, pp. 10221–10226, 2013, doi: 10.1021/am4029679.

[112] K. Chen, S. Zhou, and L. Wu, "Facile fabrication of self-repairing superhydrophobic coatings," *Chemical Communications*, vol. 50, no. 80, pp. 11891–11894, 2014, doi: 10.1039/c3cc49251f.

[113] X. Ding, S. Zhou, G. Gu, and L. Wu, "A facile and large-area fabrication method of superhydrophobic self-cleaning fluorinated polysiloxane/TiO2 nanocomposite coatings with long-term durability," *J Mater Chem*, vol. 21, no. 17, pp. 6161–6164, 2011, doi: 10.1039/c0jm04546b.

[114] Y. Li, L. Li, and J. Sun, "Bioinspired self-healing superhydrophobic coatings," *Angewandte Chemie - International Edition*, vol. 49, no. 35, pp. 6129–6133, 2010, doi: 10.1002/anie.201001258.

[115] S. Chen, X. Li, Y. Li, and J. Sun, “Intumescent Flame-Retardant and Self-Healing Superhydrophobic Coatings on Cotton Fabric,” vol. 22, p. 50, 2022, doi: 10.1021/acsnano.5b00121.

[116] S. Jia, Y. Lu, S. Luo, Y. Qing, Y. Wu, and I. P. Parkin, “Thermally-induced all-damage-healable superhydrophobic surface with photocatalytic performance from hierarchical BiOCl,” *Chemical Engineering Journal*, vol. 366, no. December 2018, pp. 439–448, 2019, doi: 10.1016/j.cej.2019.02.104.

[117] Y. Lee, E. A. You, and Y. G. Ha, “Facile one-step construction of covalently networked, self-healable, and transparent superhydrophobic composite films,” *Appl Surf Sci*, vol. 445, pp. 368–375, 2018, doi: 10.1016/j.apsusc.2018.03.201.

[118] B. Li and J. Zhang, “Polysiloxane/multiwalled carbon nanotubes nanocomposites and their applications as ultrastable, healable and superhydrophobic coatings,” *Carbon N Y*, vol. 93, pp. 648–658, 2015, doi: 10.1016/j.carbon.2015.05.103.

[119] M. Zeng *et al.*, “Hierarchical, Self-Healing and Superhydrophobic Zirconium Phosphate Hybrid Membrane Based on the Interfacial Crystal Growth of Lyotropic Two-Dimensional Nanoplatelets,” *ACS Appl Mater Interfaces*, vol. 10, no. 26, pp. 22793–22800, 2018, doi: 10.1021/acsami.8b03414.

[120] J. Zhang, J. Zhao, W. Qu, and Z. Wang, “Fabrication of superhydrophobic fabrics with outstanding self-healing performance in sunlight,” *Mater Chem Front*, vol. 3, no. 7, pp. 1341–1348, 2019, doi: 10.1039/c8qm00607e.

[121] S. Foorginezhad and M. M. Zerafat, “Fabrication of superhydrophobic coatings with self-cleaning properties on cotton fabric based on Octa vinyl polyhedral oligomeric silsesquioxane/polydimethylsiloxane (OV-POSS/PDMS) nanocomposite,” *J Colloid Interface Sci*, vol. 540, pp. 78–87, 2019, doi: 10.1016/j.jcis.2019.01.007.

[122] S. H. Phillips, T. S. Haddad, and S. J. Tomczak, “Developments in nanoscience: Polyhedral oligomeric silsesquioxane (POSS)-polymers,” *Curr Opin Solid State Mater Sci*, vol. 8, no. 1, pp. 21–29, 2004, doi: 10.1016/j.cossms.2004.03.002.

[123] J. Matisons, *Applications of Polyhedral Oligomeric Silsesquioxanes*.

[124] Y. Xue *et al.*, “Superhydrophobic electrospun POSS-PMMA copolymer fibres with highly ordered nanofibrillar and surface structures,” *Chemical Communications*, no. 42, pp. 6418–6420, 2009, doi: 10.1039/b911509a.

[125] I. Blanco, “The rediscovery of POSS: A molecule rather than a filler,” *Polymers (Basel)*, vol. 10, no. 8, 2018, doi: 10.3390/polym10080904.

[126] S. H. Dolatabadi, “Fabrication of Slippery Icephobic Coatings for application to High Voltage Insulator,” 2020.

[127] L. Zhu, J. Xue, Y. Wang, Q. Chen, J. Ding, and Q. Wang, “Ice-phobic Coatings Based on Silicon-Oil-Infused Polydimethylsiloxane,” 2013.

[128] G. Zhu *et al.*, “Preparation of gahnite (ZnAl2O4) superhydrophobic coating on aluminum alloy with self-healing and high stability properties,” *Colloids Surf A Physicochem Eng Asp*, vol. 634, no. November 2021, 2022, doi: 10.1016/j.colsurfa.2021.127977.

[129] X. Han, L. Ren, Y. Ma, X. Gong, and H. Wang, “A mussel-inspired self-repairing superhydrophobic coating with good anti-corrosion and photothermal properties,” *Carbon N Y*, 2022, doi: 10.1016/j.carbon.2022.05.056.

[130] H. Zhou, H. Wang, H. shao, T. Lin, H. Xu, and H. Niu, “Super-robust self-healing superhydrophobic coating with triboelectrification induced liquid self-repellency,” *Mater Des*, vol. 211, p. 110145, 2021, doi: 10.1016/j.matdes.2021.110145.

[131] X. Cao *et al.*, “A chemically robust and self-healing superhydrophobic polybenzoxazine coating without fluorocarbon resin modification: Fabrication and failure mechanism,” *Prog Org Coat*, vol. 163, no. September 2021, p. 106630, 2022, doi: 10.1016/j.porgcoat.2021.106630.

[132] Z. G. Bai, Y. Y. Bai, G. P. Zhang, S. Q. Wang, and B. Zhang, “A hydrogen bond based self-healing superhydrophobic octadecyltriethoxysilane−lignocellulose/silica coating,” *Prog Org Coat*, vol. 151, no. December 2020, p. 106104, 2021, doi: 10.1016/j.porgcoat.2020.106104.

[133] X. Li, B. Li, Y. Li, and J. Sun, “Nonfluorinated, transparent, and spontaneous self-healing superhydrophobic coatings enabled by supramolecular polymers,” *Chemical Engineering Journal*, vol. 404, no. July 2020, p. 126504, 2021, doi: 10.1016/j.cej.2020.126504.

[134] X. Wang *et al.*, “Self-healing superhydrophobic A-SiO2/N-TiO2@HDTMS coating with self-cleaning property,” *Appl Surf Sci*, vol. 567, no. July, p. 150808, 2021, doi: 10.1016/j.apsusc.2021.150808.

[135] Y. Shen *et al.*, “Multi-type nanoparticles in superhydrophobic PU-based coatings towards self-cleaning, self-healing and mechanochemical durability,” *Prog Org Coat*, vol. 159, no. July, p. 106451, 2021, doi: 10.1016/j.porgcoat.2021.106451.

[136] K. Zhang, F. Xu, and Y. Gao, “Superhydrophobic and oleophobic dual-function coating with durablity and self-healing property based on a waterborne solution,” *Appl Mater Today*, vol. 22, p. 100970, 2021, doi: 10.1016/j.apmt.2021.100970.

[137] R. Zhao, Y. Chen, G. Liu, Y. Jiang, and K. Chen, “Fabrication of self-healing waterbased superhydrophobic coatings from POSS modified silica nanoparticles,” *Mater Lett*, vol. 229, pp. 281–285, 2018, doi: 10.1016/j.matlet.2018.07.040.

[138] T. Lv, Z. Cheng, E. Zhang, H. Kang, Y. Liu, and L. Jiang, “Self-Restoration of Superhydrophobicity on Shape Memory Polymer Arrays with Both Crushed Microstructure

and Damaged Surface Chemistry," *Small*, vol. 13, no. 4, pp. 1–8, 2017, doi: 10.1002/smll.201503402.

[139] X. Y. Wang *et al.*, "Durable superhydrophobic coating based on inorganic/organic double-network polysiloxane and functionalized nanoparticles," *Colloids Surf A Physicochem Eng Asp*, vol. 578, no. June, p. 123550, 2019, doi: 10.1016/j.colsurfa.2019.06.016.

[140] R. Jafari, "Applications of Plasma Technology in Development of Superhydrophobic Surfaces : A Review," no. 418, 2013.

[141] A. Schütze, J. Y. Jeong, S. E. Babayan, J. Park, G. S. Selwyn, and R. F. Hicks, "The atmospheric-pressure plasma jet: A review and comparison to other plasma sources," *IEEE Transactions on Plasma Science*, vol. 26, no. 6, pp. 1685–1694, 1998, doi: 10.1109/27.747887.

[142] E. Vazirinasab, R. Jafari, and G. Momen, "Evaluation of atmospheric-pressure plasma parameters to achieve superhydrophobic and self-cleaning HTV silicone rubber surfaces via a single-step, eco-friendly approach," *Surf Coat Technol*, vol. 375, no. May, pp. 100–111, 2019, doi: 10.1016/j.surfcoat.2019.07.005.

[143] C. H. Bamford and J. C. Ward, "The effect of the high-frequency discharge on the surfaces of solids. I-The production of surface radicals on polymers," *Polymer (Guildf)*, vol. 2, no. C, pp. 277–293, 1961, doi: 10.1016/0032-3861(61)90031-3.

[144] E. Occhiello, M. Morra, P. Cinquina, and F. Garbassi, "Hydrophobic recovery of oxygen-plasma-treated polystyrene," *Polymer (Guildf)*, vol. 33, no. 14, pp. 3007–3015, 1992, doi: 10.1016/0032-3861(92)90088-E.

[145] U. Zulfiqar, M. Awais, S. Z. Hussain, I. Hussain, S. W. Husain, and T. Subhani, "Durable and self-healing superhydrophobic surfaces for building materials," *Mater Lett*, vol. 192, pp. 56–59, 2017, doi: 10.1016/j.matlet.2017.01.070.

[146] T. Dow Chemical Company, "SYLGARD™ 184 Silicone Elastomer Features & Benefits," 2017. [Online]. Available: www.consumer.dow.com

[147] E. I. Ag, "Aerosil ® R 202," p. 45127, 2011.

[148] "Enova® Aerogel IC3100 Particles." http://www.buyaerogel.com/product/enova-aerogel-ic3100/#:~:text=Enova® Aerogel IC3100 from,thin-film insulative coatings applications.

[149] "Trifluoropropyl POSS ®." p. 39401.

[150] T. Dow Chemical Company, "XIAMETER™ PMX-200 Silicone Fluid, 50-1,000 cSt," 2017.

[151] J. Park *et al.*, "Direct and accurate measurement of size dependent wetting behaviors for sessile water droplets," *Sci Rep*, vol. 5, no. June, pp. 1–13, 2015, doi: 10.1038/srep18150.

[152] “ATR – Theory and Applications.” [Online]. Available: www.piketech.com

[153] D. Mainali and L. Tang, “Positive and Nondestructive Identification of Acrylic-Based Coatings Using Partial Least Squares Discriminant Analysis with the Agilent 4300 Handheld FTIR.”

[154] G. Greczynski and L. Hultman, “A step-by-step guide to perform x-ray photoelectron spectroscopy,” *J Appl Phys*, vol. 132, no. 1, Jul. 2022, doi: 10.1063/5.0086359.

[155] D. Chen, M. D. Gelenter, M. Hong, R. E. Cohen, and G. H. McKinley, “Icephobic surfaces induced by interfacial nonfrozen water,” *ACS Appl Mater Interfaces*, vol. 9, no. 4, pp. 4202–4214, 2017, doi: 10.1021/acsami.6b13773.

[156] A. B. D. Cassie and S. Baxter, “Wetting of porous surfaces.,” *Transactions of the Faraday Society*, vol. 40, no. 5, pp. 546–551, 1944.

[157] H. Abdipour, M. Rezaei, and F. Abbasi, “Synthesis and characterization of high durable linseed oil-urea formaldehyde micro/nanocapsules and their self-healing behaviour in epoxy coating,” *Prog Org Coat*, vol. 124, no. August, pp. 200–212, 2018, doi: 10.1016/j.porgcoat.2018.08.019.

[158] S. M. Mirabedini, R. R. Farnood, M. Esfandeh, F. Zareanshahraki, and P. Rajabi, “Nanocomposite coatings comprising APS-treated linseed oil-embedded polyurea-formaldehyde microcapsules and nanoclay, part 2: Self-healing and corrosion resistance properties,” *Prog Org Coat*, vol. 142, no. February, p. 105592, 2020, doi: 10.1016/j.porgcoat.2020.105592.

[159] M. Samadzadeh, S. H. Boura, M. Peikari, A. Ashrafi, and M. Kasiriha, “Tung oil: An autonomous repairing agent for self-healing epoxy coatings,” *Prog Org Coat*, vol. 70, no. 4, pp. 383–387, 2011, doi: 10.1016/j.porgcoat.2010.08.017.

[160] M. Liravi, H. Pakzad, A. Moosavi, and A. Nouri-Borujerdi, “A comprehensive review on recent advances in superhydrophobic surfaces and their applications for drag reduction,” *Prog Org Coat*, vol. 140, no. August 2019, p. 105537, 2020, doi: 10.1016/j.porgcoat.2019.105537.

[161] S. P. Dalawai *et al.*, “Recent Advances in durability of superhydrophobic self-cleaning technology: A critical review,” *Prog Org Coat*, vol. 138, no. May 2019, p. 105381, 2020, doi: 10.1016/j.porgcoat.2019.105381.

[162] Y. Li, L. Li, and J. Sun, “Bioinspired self-healing superhydrophobic coatings,” *Angewandte Chemie - International Edition*, vol. 49, no. 35, pp. 6129–6133, 2010, doi: 10.1002/anie.201001258.

[163] X. Wang, X. Liu, F. Zhou, and W. Liu, “Self-healing superamphiphobicity,” *Chemical Communications*, vol. 47, no. 8, pp. 2324–2326, 2011, doi: 10.1039/c0cc04066e.

[164] C. H. Xue, X. Bai, and S. T. Jia, "Robust, Self-Healing Superhydrophobic Fabrics Prepared by One-Step Coating of PDMS and Octadecylamine," *Sci Rep*, vol. 6, no. May, pp. 1–11, 2016, doi: 10.1038/srep27262.

[165] G. Wu, J. An, X. Z. Tang, Y. Xiang, and J. Yang, "A versatile approach towards multifunctional robust microcapsules with tunable, restorable, and solvent-proof superhydrophobicity for self-healing and self-cleaning coatings," *Adv Funct Mater*, vol. 24, no. 43, pp. 6751–6761, 2014, doi: 10.1002/adfm.201401473.

[166] L. Qin, N. Chen, X. Zhou, and Q. Pan, "A superhydrophobic aerogel with robust self-healability," *J Mater Chem A Mater*, vol. 6, no. 10, pp. 4424–4431, 2018, doi: 10.1039/c8ta00323h.

[167] M. Lin and P. Chen, "Photographic study of bubble behavior in subcooled flow boiling using R-134a at low pressure range," *Annals of Nuclear Energy*, vol. 49. pp. 23–32, Nov. 2012. doi: 10.1016/j.anucene.2012.06.001.

[168] "Sz (Maximum Height) | Area Roughness Parameters."

[169] S. Sreekantan, A. X. Yong, N. Basiron, F. Ahmad, and F. De'nan, "Effect of Solvent on Superhydrophobicity Behavior of Tiles Coated with Epoxy/PDMS/SS," *Polymers (Basel)*, vol. 14, no. 12, 2022, doi: 10.3390/polym14122406.

[170] B. N. Sahoo, S. Nanda, J. A. Kozinski, and S. K. Mitra, "PDMS/camphor soot composite coating: towards a self-healing and a self-cleaning superhydrophobic surface," *RSC Adv*, vol. 7, no. 25, pp. 15027–15040, 2017, doi: 10.1039/c6ra28581c.

[171] C. H. Xue, Z. D. Zhang, J. Zhang, and S. T. Jia, "Lasting and self-healing superhydrophobic surfaces by coating of polystyrene/SiO2 nanoparticles and polydimethylsiloxane," *J Mater Chem A Mater*, vol. 2, no. 36, pp. 15001–15007, 2014, doi: 10.1039/c4ta02396j.

[172] D. W. Li, H. Y. Wang, Y. Liu, D. S. Wei, and Z. X. Zhao, "Large-scale fabrication of durable and robust super-hydrophobic spray coatings with excellent repairable and anti-corrosion performance," *Chemical Engineering Journal*, vol. 367, no. January, pp. 169–179, 2019, doi: 10.1016/j.cej.2019.02.093.

[173] H. Li *et al.*, "Durable superhydrophobic and oleophobic cotton fabric based on the grafting of fluorinated POSS through silane coupling and thiol-ene click reaction," *Colloids Surf A Physicochem Eng Asp*, vol. 630, no. September, p. 127566, 2021, doi: 10.1016/j.colsurfa.2021.127566.

[174] C. H. Xue, X. Bai, and S. T. Jia, "Robust, Self-Healing Superhydrophobic Fabrics Prepared by One-Step Coating of PDMS and Octadecylamine," *Sci Rep*, vol. 6, Jun. 2016, doi: 10.1038/srep27262.

[175] F. C. L. Ciolacu, N. R. Choudhury, N. Dutta, and E. Kosior, "Molecular level stabilization of poly(ethylene terephthalate) with nanostructured open cage trisilanolisobutyl-POSS," *Macromolecules*, vol. 40, no. 2, pp. 265–272, Jan. 2007, doi: 10.1021/ma061060d.

[176] T. Bharathidasan, S. V. Kumar, M. S. Bobji, R. P. S. Chakradhar, and B. J. Basu, "Effect of wettability and surface roughness on ice-adhesion strength of hydrophilic, hydrophobic and superhydrophobic surfaces," *Appl Surf Sci*, vol. 314, pp. 241–250, 2014, doi: 10.1016/j.apsusc.2014.06.101.

[177] M. Zou, S. Beckford, R. Wei, C. Ellis, G. Hatton, and M. A. Miller, "Effects of surface roughness and energy on ice adhesion strength," *Appl Surf Sci*, vol. 257, no. 8, pp. 3786–3792, 2011, doi: 10.1016/j.apsusc.2010.11.149.

[178] S. Heydarian, K. Maghsoudi, R. Jafari, H. Gauthier, and G. Momen, "Fabrication of liquid-infused textured surfaces (LITS): The effect of surface textures on anti-icing properties and durability," *Mater Today Commun*, vol. 32, no. February, p. 103935, 2022, doi: 10.1016/j.mtcomm.2022.103935.

[179] M. Shamshiri, R. Jafari, and G. Momen, "Icephobic properties of aqueous self-lubricating coatings containing PEG-PDMS copolymers," *Prog Org Coat*, vol. 161, no. May, p. 106466, 2021, doi: 10.1016/j.porgcoat.2021.106466.